University of Nottingham, School of Veterinary Medicine and Science

The role of MicroRNAs within extracellular vesicles in the creation of the pre-metastatic niche, for the development of prostate cancer metastasis to bone

Thesis submitted for the Master of Research Degree

Abigail Speakman - 4308561
April 2018

Abstract

In the UK in 2016, prostate cancer was the most commonly diagnosed cancer in men and it is the fifth most common cause of death due to cancer worldwide. 90% of these deaths are due to the development of metastatic lesions (most commonly in bone). The mechanisms which underpin the spread to bone remain to be determined. Communication of the primary tumour with the bone microenvironment may prepare the bone for metastasis through pre-metastatic niche formation. This project investigates this hypothesis through the determination of the role of extracellular-vesicle (EV) microRNA (miRNA) in the modulation of osteoblasts, the predominant cell type involved in osteoblastic prostate cancer bone metastasis.

MicroRNAs (miRNAs) are small, single stranded RNAs, and are hypothesised to play a role in primary tumour communication with distant sites through altered regulation of transcription and translation in recipient cells. EVs released from primary tumour cells are likely important vehicles for the transfer of miRNAs and other signalling molecules to osteoblasts cells in metastatic sites.

EVs originating from prostate cancer cell lines PC3, LNCaP and C4-2 and non-malignant prostate epithelial cell line PNT1A were used to investigate the transfer and subsequent function of miRNAs within an *in vitro* osteoblast cell line model (hOB).

The data demonstrated the selective packaging of miRNAs into EVs, indicated EV content does not reflect cellular expression. The transfer of labelled EV-miRNA demonstrates the efficiency of miRNA transfer is also dependent upon

the cell line from which the EVs originated. Furthermore, the data indicates other mechanisms of RNA regulation influence the resulting levels of EV-miRNAs within the recipient osteoblasts, but that EV-miRNAs are functional within recipient cells based on proof-of-principle evidence generated using Renilla-luciferase reporter assays. Finally, using global transcriptome analysis a number of biological pathways associated with osteoblast survival, differentiation and proliferation were found to be significantly modulated by prostate cancer (PC3) EVs compared to non-malignant controls (PNT1A).

This study confirmed the role of miRNAs transported by EVs as important mediators of alterations in osteoblast gene expression which could aid with pre-metastatic niche formation. Understanding the methods of communication between the primary tumour and distant sites is an important step towards the development of potential therapeutics. Blocking tumour communication with distant sites may reduce metastatic tumour formation and therefore have the potential to improve patient prognosis. Further investigation is needed to confirm whether the findings of this study similarly applicable *in vivo*.

Table of contents

Abstract i
Table of contents iii
Acknowledgments vi
Abbreviations vii
1 Chapter 1: Introduction 1
1.1 The prostate 1
1.2 Prostate cancer 2
1.2.1 Metastasis and the pre-metastatic niche 6
1.2.2 Management 8
1.2.3 Prognosis 11
1.2.4 Staging and Gleason Score 12
1.2.5 Circulating Prostate cancer markers 13
1.3 MicroRNAs 19
1.3.1 Biogenesis 20
1.3.2 MiRNA functions in cancer 21
1.3.3 MiRNA transfer between cells 32
1.4 Exosomes 36
1.4.1 Exosome marker proteins 37
1.4.2 MiRNAs within exosomes 41
1.4.3 MiRNAs as biomarkers 42
1.5 Study objectives 45
2 Chapter 2: Materials and Methods 47
2.1 Cell lines 47
2.2 Cell culture 47
2.3 Extracellular vesicle collection 48
2.4 Extracellular Vesicle isolation 51
2.5 Characterisation of EVs 51
2.5.1 Western blotting 51
2.5.2 Brownian motion analysis 54
2.6 RNA isolation 55
2.7 RNAseq analysis of microRNAs transferred via prostate cancer vesicles to osteoblasts 56
2.8 cDNA synthesis 58
2.9 MiRNA detection via PCR 58
2.9.1 Selection of primers 59

2.9.2 Normalisation 59
2.9.3 Standard curves 59
2.9.4 Analysis 60
2.10 Validation of the transfer of characterised miRNAs from prostate cancer cells to osteoblasts via vesicles. 60
2.11 Amplification of Reporter Plasmids 60
2.12 Restriction digest of psiCHECK-2 Plasmid 62
2.13 Design and Annealing of Oligos 64
2.14 Ligating the oligos and Plasmid 65
2.15 Transforming of E. coli with ligated plasmids 65
2.15.1 Sequencing of PsiCHECK-2 plasmid with miRNA oligo inserted DNA .. 66
2.16 Plasmid transfections – Optimisation 66
2.16.1 Neon Transfection System 67
2.16.2 TransIT-2020 Transfection reagent System and TransIT-X2 Dynamic Delivery System 68
2.17 Renilla Luciferase expression assay 68
2.18 Transfections with miR21-PsiCHECK-2 reporter 69
2.19 Investigation of the effect of adding EVs on renilla luciferase activity 70
2.20 Viability assay 71
2.21 Preparation of samples for RNA sequencing and Bioinformatic analysis ... 73
2.22 Analysis of RNA sequencing data 73
3 Chapter 3: Investigation of miRNAs contained within and transferred to recipient cells by Prostate cancer vesicles 76
3.1 Introduction 76
3.2 Results 76
3.2.1 Characterisation of EVs 76
3.2.1 RNAseq analysis of microRNAs transferred via prostate cancer vesicles to osteoblasts 82
3.2.2 Comparison of miRNA expression in cells and EVs 89
3.2.3 Validation of the transfer of characterised miRNAs from prostate cancer cell to osteoblasts via vesicles. 95
4 Chapter 4: Investigation of the effect of transferred miRNAs in recipient Osteoblasts 104
4.1 Introduction 104
4.2 Results 105
4.2.1 Design of luciferase reporter assays 105
4.2.2 Optimisation of Renilla luciferase luminescence assays 105

4.2.3 Viability experiment 109
5 Chapter 5: Bioinformatic analysis 114
5.1 Introduction 114
5.2 Results 114
5.2.1 Characterisation and filtration of RNAseq data 114
5.2.2 Gene enrichment analysis 116
5.2.3 KEGG pathway enrichment analysis 118
6 Chapter 6: Discussion 128
6.1 Investigation of miRNAs contained within and transferred to recipient cells by Prostate cancer vesicles 128
6.1.1 Characterisation of Extracellular Vesicles 128
6.1.2 RNAseq analysis of microRNAs transferred via prostate cancer vesicles to osteoblasts 129
6.1.3 Comparison of miRNA expression in cells and EVs 129
6.1.4 Validation of the transfer of characterised miRNAs from prostate cancer cell to osteoblasts via vesicles 132
6.2 Investigation of the effect of transferred miRNAs in recipient Osteoblasts 133
6.2.1 Investigation of the effect of adding EVs on renilla luciferase activity 133
6.2.2 Viability experiment 133
6.3 Bioinformatic analysis 135
6.3.1 Gene enrichment analysis 135
6.3.2 hOB cells treated with PNT1A EVs vs hOB cells treated with PC3 EVs KEGG pathway analysis 135
6.4 Conclusions 142
7 References 143
8 Appendix 163
8.1 Restriction digest results 163
8.2 Renilla luciferase luminescence assay results 164
8.2.1 hOB transfection optimisation results 164
8.2.2 Investigation of the effect of adding EVs on Renilla luciferase activity results 164
8.3 KEGG pathway analysis 167

Acknowledgments

Thanks to Dr Victoria James for the preparation of samples for RNAseq analysis (2.7) prior to the start of this investigation. Additional thanks for her continual support and advice throughout the project.

Thanks to Dr Tania Dottorini for the preparation of RNAseq data (2.7 and 2.22) and for help with its analysis.

Thanks to Catherine Probert for the treatment of cells prior to RNA extraction in the validation of the transfer of characterised miRNAs from prostate cancer cell to osteoblasts via vesicles experiment (2.10) and for her support and guidance on experimental technique at the beginning of the project.

Thanks finally to Cinzia Allegrucci for her support as a secondary supervisor.

Abbreviations

ADT	Androgen deprivation therapy
Ago	Argonaute protein
AR	Androgen receptor
BPH	Benign prostatic hyperplasia
BSA	Bovine serum albumin
CRCP	Castrate resistant prostate cancer
CTC	Circulating tumour cell
DHT	5α-dihydrotestosterone
DMEM	Dulbecco's Modified Eagle's medium
ECM	Extracellular matrix
EMT	Epithelial-to-mesenchymal transition
EpCAM	Epithelial cell adhesion molecule
ESCRT	Endosomal sorting complex required for transport
EV	Extracellular vesicle
FBS	Fetal Bovine serum
HDL	High density lipoprotein
HSP70	Heat shock protein 70

ICAM	Intercellular adhesion molecule
LH	Luteinising hormone
LHRH	Luteinising hormone releasing hormone
miRNA/miR	MicroRNA
MVB	Multi-vesicular body
PBS	Phosphate buffered saline
PBS-T	Phosphate buffered saline with tween
PSA	Prostate specific antigen
qRT-PCR	Quantitative real-time polymerase chain reaction
RISC	RNA-induced silencing complex
RNAseq	RNA sequencing
RP	Radical prostatectomy
SELDI-TOF MS	Surface-enhanced Laser Desorption Ionisation Time-of-Flight mass spectrometry

1 Chapter 1: Introduction

1.1 The prostate

The prostate is a small organ (approximately 3x4x2 cm (Moore *et al.*, 2018)) which surrounds the urethra on its exit from the bladder. The majority (approximately two thirds) of the prostate is made up of glandular tissue which is surrounded by a fibrous capsule containing nerve and vein plexuses (Moore *et al.*, 2018) and smooth muscle fibres (IQWiG - Institute for Quality and Efficiency in Health Care, 2016). McNeal (1981) analysed 500 prostates removed at autopsy and from the results divided the prostate into 4 anatomic regions (Figure 1.1) The peripheral zone contains 70% of all glandular tissue and has significantly different histological characteristics to the Central zone which contains 25% of glandular tissue. The transitional zone contains the remaining 5% of the glandular tissue (Fine and Mehra, 2015) and periurethral ducts (McNeal, 1981). The final region described by McNeal (1981) is the anterior fibromuscular stroma which is synonymous with the fibrous capsule described by Moore *et al.,* (2018).

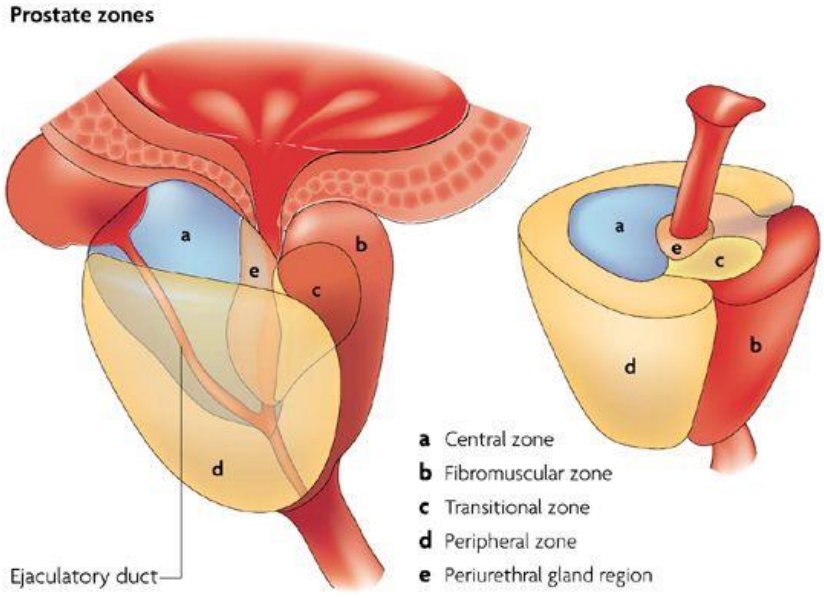


Figure 1.1 An image showing the zonal anatomy of the prostate.
((De Marzo et al., 2007) Used with permission licence no. 4377680414949)

The glandular portion of the prostate produces prostatic fluid which contains, important enzymes to activate sperm, citrate as a nutrient source and prostate specific antigen (PSA) (Marieb and Hoehn, 2015) which functions to reduce the viscosity of semen (Balk *et al.*, 2003). Prostatic fluid makes up between 20% (Moore *et al.*, 2018) and 33% (Marieb and Hoehn, 2015) of seminal fluid and its propulsion during ejaculation is aided by prostate gland muscle contraction (IQWiG - Institute for Quality and Efficiency in Health Care, 2016). The prostate also plays a role in the conversion of testosterone into dihydrotestosterone which has higher biologically activity and affinity for androgen receptors (AR) (Feldman and Feldman, 2001).

1.2 Prostate cancer

Prostate cancer is the most frequently newly diagnosed cancer of men in developed countries, with the third highest death rate of all cancers (Torre *et al.*, 2015). In the UK, in 2016, prostate cancer was the most commonly diagnosed cancer in males (Office for National Statistics, 2018). Worldwide, it is the fifth highest cause of death due to cancer and in 2012 over one million new cases were estimated to have been diagnosed (Torre *et al.*, 2015). Diagnoses increased after the introduction of PSA testing which enables earlier detection of disease. In the UK prostate cancer incidence has risen from 172.9 cases per 100,000 men in 2006 to 173.7 cases per 100,000 men in 2016, with a peak incidence of 192.1 cases per 100,000 men in 2013 (Office for National Statistics, 2018). During the same period the age standardised mortality rate has fallen from 52.7 deaths per 100,000 men in 2006 to 47.5 deaths per

100,000 men in 2016 (Office for National Statistics, 2018). However, these figures may have been affected by over-diagnosis often attributed to PSA testing (Etzioni *et al.*, 2002, Draisma *et al.*, 2009), where cancers that would not have presented clinically within the patient's lifetime are detected. This over-diagnosis can lead to unnecessary treatment which can have a serious impact on the patients' quality of life, as well as incurring unnecessary treatment costs (Korfage *et al.*, 2005, Draisma *et al.*, 2009).

Growth of early prostate cancer is androgen dependent whereby cells rely on 5α-dihydrotestosterone (DHT) (Russell and Kingsley, 2003) or testosterone to stimulate proliferation and inhibit apoptosis (Feldman and Feldman, 2001). This occurs through interaction with ARs; soluble proteins (Gao *et al.*, 2005) with three functional domains (Davey and Grossmann, 2016). The N-terminal regulates transcription (Davey and Grossmann, 2016). The DNA binding region is highly conserved and separates the N-terminal from the ligand binding domain (Davey and Grossmann, 2016). The gene for the AR is located on the X chromosome and codes for a protein 919 amino acids long, this gene is expressed in a range of tissues and has been commonly identified with mutations (Gao *et al.*, 2005). In the absence of androgen the AR is located in the cell cytoplasm but translocates to the nucleus following a conformational change when androgen binds (Davey and Grossmann, 2016). In the nucleus it binds to androgen response elements and co-regulators to alter transcriptional activity (Davey and Grossmann, 2016). The AR can also act more rapidly without binding directly to DNA through the activation of 2nd messenger pathways or sequestration of vital transcription factors (Davey and Grossmann,

2016).

Due to the heterogeneous nature of prostate cancer tumours there is a mixed population of cells which may or may not have mutations to the AR receptor. Androgen deprivation therapy (ADT)(1.2.2) creates selective pressure so that cells with mutations which enable androgen independent growth are selected for (Feldman and Feldman, 2001). Feldman and Feldman (2001) suggested that there are five mechanisms which enable cell survival and progression of cancer despite ADT. Briefly, these mechanisms are; the hypersensitivity mechanism, the promiscuous mechanism, the outlaw pathways mechanism, the bypass pathway mechanism and the 'lurker' cell mechanism. The hypersensitivity mechanism suggests that the cells adapt so that they are able to maintain proliferation through utilisation of the low levels of residual endogenous androgens. This may be through increased expression of the AR (Koivisto *et al.*, 1997), increased sensitivity of the AR (Gregory *et al.*, 2001) or increased activity of 5α-reductase (Makridakis *et al.*, 1997) to increase the production of DHT which has a higher affinity for the receptor. Visakorpi *et al.* (1995) found that there was great variability in the number of AR gene copies within cells from the same primary tumour but that an increased copy number was found in all cells from patients with androgen independent prostate cancer, suggesting that these cells had been positively selected for and proving that hypersensitivity of cells is a possible mechanism. The promiscuous mechanism involves mutation of the ligand binding region of the AR causing reduced receptor specificity (Buchanan *et al.*, 2001). This means the receptor is activated through the binding of non-androgen steroids and androgen

antagonists. The outlaw mechanism suggests that the AR can be activated through a ligand independent pathway (Culig *et al.*, 1994). The bypass pathway suggests that alternative pathways may be activated which entirely exclude the AR but similarly stimulate proliferation and prevent apoptosis. For example McDonnell *et al.* (1992) found increased expression of oncogenic *bcl-2*, which supresses apoptosis, in cells from androgen independent tumours. Finally the "lurker" cell mechanism hypothesises that a subpopulation of androgen independent cells was always present in the tumour and these cells are able to proliferate when competing cells are eliminated during ADT (Isaacs, 1999).

Through one of these mechanisms, or potentially a combination of these, tumour cells progress from androgen dependent to androgen independent, where cells react to androgens but do not require them for growth. The LNCaP cell line represents the early androgen dependent stage of cancer development, these cells express a mutated androgen receptor but are still sensitive to androgens (Russell and Kingsley, 2003). The LNCaP cell line was established from cells aspirated from a metastatic lymph node lesion from a 50 year old Caucasian man (Sobel and Sadar, 2005). The C4-2 cell line is a subline of LNCaP produced through co-injection of LNCaP cells and human osteosarcoma cell line MS into a castrated host. The C4-2 cells were harvested from the resultant tumour (Sobel and Sadar, 2005). C4-2 cells are able to metastasise to lymph nodes and bone if injected subcutaneously or orthotopically (Russell and Kingsley, 2003). C4-2 cells are similarly androgen responsive but express only low levels of ARs so are considered independent of androgens for their growth (Sobel and Sadar, 2005).

Cells can eventually become completely insensitive to ADT so that even second line deprivation therapy is ineffective (Davey and Grossmann, 2016), this is termed castrate resistance prostate cancer (CRPC). PC3 cells are an example of completely androgen independent, AR negative cells (Russell and Kingsley, 2003) and were established from a metastatic lesion of a 62 year old man (Kaighn *et al.*, 1979). This cell line represents very late prostate cancer and is unlikely to be representative of most patients.

1.2.1 Metastasis and the pre-metastatic niche

Prostate cancer metastases show significant tropism to bone (Croset *et al.*, 2015, Sikes *et al.*, 2004, Vela *et al.*, 2007), with Jacobs (1983) reporting bone lesions in over 80% of prostate cancer patients at autopsy. High blood flow to bone marrow is thought to at least partially account for the tropism to bone (Suva *et al.*, 2011). Expression of specific adhesion molecules on cancer cells is also thought to contribute as these promote adhesion to bone marrow endothelial cells (Hensel and Thalmann, 2016). The chemokine ligand 12 (CXCL12) interaction with chemokine receptor 4 (which is expressed on prostate cancer cells) is suggested to be one of the most important factors for regulating tropism to bone as CXCL12 is an mediator of bone marrow survival and expansion (Hensel and Thalmann, 2016). For successful metastasis tumour cells must undergo epithelial-to-mesenchymal transition (EMT)(Sethi *et al.*, 2011, Zhau *et al.*, 2008). This process involves phenotypic changes to reduce intracellular adhesions and increase the cells ability to migrate (Radisky, 2005). It enables cancer cells to enter circulation and be transported to distant sites (Montanari *et al.*, 2017).

The pre-metastatic niche refers to a site which has been prepared to increase the chances of successful colonisation by circulating tumour cells (Weilbaecher *et al.*, 2011). Tumour secreted factors are believed to be important for niche formation, these may be novel factors or tumour specific adaptations of factors already present in the niche microenvironment (Psaila and Lyden, 2009). Tumour secreted extracellular vesicles (EVs) have been shown to be important for the preparation of this niche and make survival possible for cells that would otherwise be destroyed (Hoshino *et al.*, 2015). The hematopoietic stem cell (HSC) niche within bone comprises of hematopoietic and mesenchymal cells, is responsible for HSC self-renewal, differentiation and proliferation (Boulais and Frenette, 2015) and plays an important part in bone marrow regulation. It is now thought that the HSC niche and the pre-metastatic niche targeted by prostate cancer cells are synonymous as circulating metastatic tumour cells compete with HSCs to colonise the same osteoblast regulated environments (Pedersen *et al.*, 2012). It is yet to be determined the contribution of EVs to the adaption of the HSC niche and the potential underpinning mechanisms.

1.2.2 Management

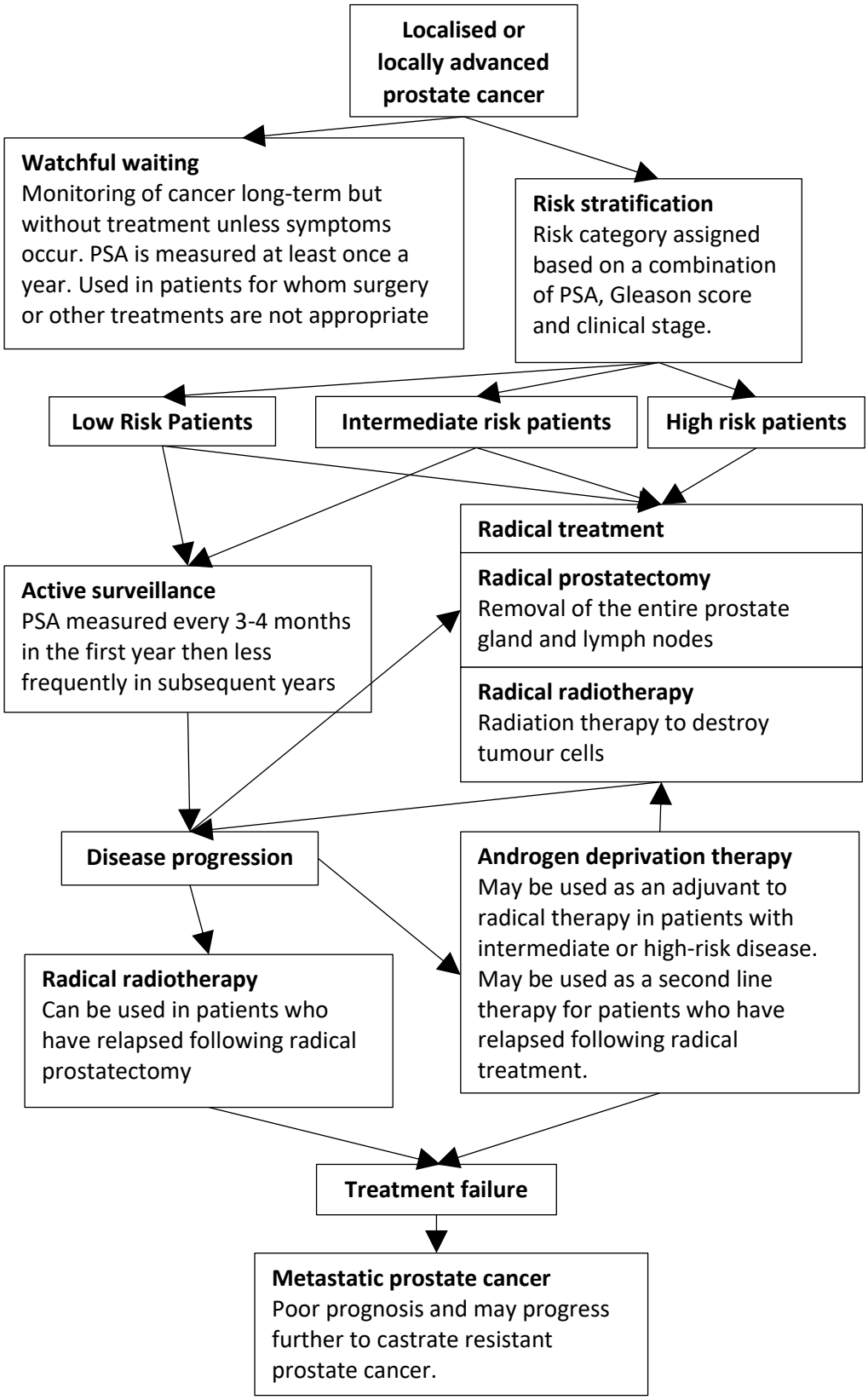


Figure 1.2 A flow chart showing the management options for localised prostate cancer once diagnosed through the use of PSA testing, digital rectal examination and biopsy for histological examination. Adapted from the NICE clinical guidelines; (National Collaborating Centre for Cancer, 2014).

Whilst still localised there are multiple treatment options for prostate cancer depending on risk of progression and the wishes of the patient (Figure 1.2). One potentially curative treatment is radical prostatectomy (RP) where the entire prostate gland and, if necessary, associated lymph nodes are surgically removed. RP is becoming an increasingly common surgery in Western countries (Bill-Axelson *et al.*, 2005). In England approximately 13% of patients diagnosed with prostate cancer will undergo radical prostatectomy (Public Health England, 2014). In 2013 this equated to 3,695 surgical procedures, the majority (77%) of which were conducted as the primary treatment with the aim to cure primary prostate cancer (BAUS, 2014). Although RP has been shown to reduce the risk of eventual distant metastases (Bill-Axelson *et al.*, 2005), Pound *et al.* (1999) found that approximately 5% of men who undergo radical surgery will still develop metastases within 15 years of surgery. Other studies have examined the risk of biochemical recurrence after RP; Huang *et al.* (2014) found that 24% of patients showed increased PSA indicating recurrence within 7 years. Pound *et al.* (1999) found that the median time to metastasis after biochemical recurrence observed was 8 years. Not all studies follow patients for a long enough period to see the development of clinical metastases, which means the incidence of development of metastases following RP may be higher than current estimates.

If patients are not considered good candidates for radical treatment or if cancer has already metastasised, androgen deprivation therapy (ADT) may be used to halt cancer growth and cause regression (Taplin *et al.*, 1995). Activation of the

androgen receptor on cancer cells can be prevented by removal of androgen supply or blockage of the receptor (National Collaborating Centre for Cancer, 2014). Surgical or medical castration can be used to reduce testosterone production (National Collaborating Centre for Cancer, 2014). Bilateral orchiectomy reduces the level of systemically circulating testosterone by 90-95% (Rove and Crawford, 2013) but is irreversible and makes intermittent therapy impossible. Medical castration can be achieved through the use of Luteinising Hormone-Releasing Hormone (LHRH) agonists or antagonists. LHRH agonists initially increase testosterone levels but continued stimulation results in reduced production of Luteinising hormone (LH) by the pituitary and a subsequent reduction in testosterone production (National Cancer Institute, 2014). LHRH antagonists prevent stimulation of the LHRH receptor in the pituitary gland (Stricker, 2001) and are reported to have a much more rapid action to reduce testosterone levels (Stricker, 2001, Crawford and Hou, 2009). Androgen synthesis inhibitors, such as abiraterone, prevent synthesis of testosterone by the adrenal glands or by prostate cancer cells themselves (National Cancer Institute, 2014). They achieve this through inhibition of CYP17, an enzyme vital for the conversion of cholesterol to testosterone (National Cancer Institute, 2014). Antiandrogens are androgen receptor antagonists which prevent activation of the AR through competitive inhibition of the binding site (National Collaborating Centre for Cancer, 2014). When medical or surgical castration is used concurrently with antiandrogens this is termed a combined androgen blockade (National Cancer Institute, 2014). ADT can be continuous or intermittent. There is evidence that patient quality of life

is improved when intermittent therapy is used (Hussain *et al.*, 2013, Calais da Silva *et al.*, 2009) but (Hussain et al., 2013) reported a 10% increase in the risk of death for patients treated intermittently, although it was noted that this difference was not statistically significant. Both methods are used to treat patients and the effect on overall disease progression and survival between treatment types is unclear. Although ADT can be very effective initially, after a median of 18-24 months it is no longer effective (So et al., 2005) and prostate cancer to progresses despite deprivation.

1.2.3 Prognosis

Prostate cancer which has metastasised is considered incurable (Watahiki *et al.*, 2011) and therefore the majority of deaths due to cancer are due to the development of these metastases. Deaths due to the primary tumour account for only 10% of deaths (Monteiro and Fodde, 2010), which means the ability to predict metastasis is important for accurate assessment of prognosis. The ability to stratify patients based on their risk of developing metastasis would enable more appropriate treatment selection. The initiation of adjuvant therapy in combination with RP can help to eradicate cells that have already spread (Weigelt *et al.*, 2005) and therefore reduce the risk of metastases occurring. Weigelt *et al.* (2005) looked at prediction of metastasis in breast cancer and noted that more than 80% of patients received adjuvant therapy despite only 40% of patients predicted to develop metastatic disease. The side effects of adjuvant therapy can be severe and so it would be highly beneficial to develop better predictors of metastatic disease at the time of diagnosis.

1.2.4 Staging and Gleason Score

All cancer types can be staged according to the TNM staging system. T stage describes the primary tumour, N describes the involvement of lymph nodes and M describes whether or not cancer has metastasised (AJCC, 2018). Staging provides an indicator of patient prognosis and aids management decision making. Prostate cancers are also given a Gleason score. This technique was established in 1966 (Gleason, 1966) and has been reviewed by the International Society of Urologic Pathology twice, most recently in 2014 (Chen and Zhou, 2016). Low-magnification microscopic assessment of biopsy samples is carried out and they are assigned scores between 1 and 5 based on the histological characteristics of cells (Gleason, 1966). The highest grade is then added to the most common grade to give the Gleason score, with a score of 6-10 indicating the presence of prostate cancer. Egevad *et al.* (2002) showed that in conservatively treated patients Gleason score can be of great prognostic value to predict disease specific death. This study grouped patients based on Gleason score (4-5, 6, 7 and 8-10) and found that there were significant differences in disease specific mean survival between groups with survival decreasing from 19.5 years (4-5 group) to only 4.7 years (8-10 group). However, the prognostic utility of the Gleason score system is limited by the difficulty associated with accurately determining the appropriate grade. Prostate tumours are highly heterogeneous and there may be multiple tumour foci within the same prostate (Ruijter *et al.*, 1996). Ruijter *et al.* (1996) examined 61 prostates removed via RP and identified 155 separate lesions, within which the histology was also variable. When comparing the RP samples to pre-

operative biopsy results this study found only 50% of samples had been correctly graded. In 10% of total cases the biopsy samples had been over-graded compared to the RP and the remaining 40% had been under-graded. In the early 2000s other studies report similar levels of agreement, ranging from 55% (Danneman *et al.*, 2017) to 45.5% (Egevad *et al.*, 2001). Danneman *et al.* (2017) showed an increase in agreement to 68% in the period of 2000-2012 and Egevad *et al.* (2001) showed that taking 7 or more biopsies increased agreement to 53.8% but despite this the accuracy of Gleason scoring is imperfect at best. In addition to this experienced personnel are needed for both sample collection and interpretation to ensure accuracy of the results, which may be lacking in some countries or regions. Patients whose lesions are under-graded are at risk of not receiving the most appropriate treatment and therefore a more sensitive method of detection would be highly beneficial to enable better determination of patient prognosis.

1.2.5 Circulating Prostate cancer markers

MiRNAs are the main circulating markers covered by this review (see 1.3) but other markers have also been studied.

1.2.5.1 Circulating Tumour cells

As a tumour is proliferating, cells at the peripheries may detach and enter the blood stream (Williams, 2013). These cells can cause the development of metastases given the correct conditions at a distant site. However, Liotta *et al.* (1976) found that more than $0.5x10^3$ fibrosarcoma cells needed to be injected into the bloodstream to produce metastases in immune competent mice. Fidler (1970) investigated where cells were distributed after entering the

bloodstream and found that only 1.5% of melanoma cells injected intravenously were still viable 24 hours later. Potentially due to this rapid cell death the levels of circulating tumour cells (CTCs) in the blood of cancer patients is very low; with up to only 50 cells per 7.5ml of blood (Williams, 2013), however this varies depending on the individual and the cancer type. Because of their low level, enrichment of CTCs is needed before detection is possible. There are a number of methods for this (reviewed by Pantel and Alix-Panabières (2010)) which either separate CTCs based on their buoyancy and size (Vona *et al.*, 2000) or using immunomagnetic enrichment targeting EpCAM (Mavroudis, 2010), which is expressed on the surface of most but not all CTCs (Pantel and Alix-Panabières, 2010). The method approved for *in vitro* diagnostics by the Food and Drug Administration (USA) is the CellSearch CTC Test (Janssen Diagnostics, 2013, USA). This system has been validated for use in patients with breast, colorectal and metastatic prostate cancer (Mavroudis, 2010, Riethdorf *et al.*, 2007, Miller *et al.*, 2010). CellSearch is an automated system which uses magnetic beads coated with EpCAM antibody to separate the CTCs, followed by staining with fluorescently labelled cytokeratins; CK8, CK18 and CK19 (Mavroudis, 2010), which enables CTCs to be counted. Vone *et al.* (2000) demonstrated, in a technique known as ISET, that epithelial CTCs can be separated based on their size using a filtering membrane. Farace *et al.* (2011) compared the effectiveness of these two methods to detect CTCs from patients with metastatic breast, prostate or non-small cell lung carcinoma and found that the best method depended on the cancer type. CTC counts for patients with breast cancer were increased using the CellSearch protocol

compared to the ISET protocol. However for patients with prostate or lung cancer they found that ISET was a better detection method. This may be related to the downregulation of EpCAM associated with EMT which limits the detection of CTCs via the CellSearch method (Pantel and Alix-Panabières, 2010).

Scher *et al.* (2009) looked at the CTC counts of patients with metastatic CRPC and used these values to group them into those with predicted favourable (4≥ CTCs per 7.5ml of blood) or unfavourable (5≤ CTCs per 7.5ml of blood) prognosis. To predict the risk of death the authors found that a combination of baseline CTC, CTC fold change and baseline lactate dehydrogenase was the best discriminator. However, this study used the CellSearch system and therefore CTC counts may have been underestimated. Cristofanilli *et al.* (2004) and Cohen *et al.* (2008) similarly categorised patients with metastatic breast cancer and metastatic colorectal cancer based on CTC per 7.5ml of blood before beginning treatment. These studies had similar results, showing that a higher CTC count predicted lower overall survival and reduced progression free survival. Although their detection can be challenging, the consensus between the results of different studies across cancer types suggests that CTCs can be a very useful method of predicting patient prognosis and the likelihood of successful treatment.

1.2.5.2 Proteins

Prostate specific antigen (PSA) is a protein commonly used diagnostically in prostate cancer, however its low specificity (when 4ng/ml is used as the threshold for further investigation the test has a specificity of only 40% (Jain et

al., 2002)), and tendency to increase in benign conditions (Jain et al., 2002), makes it less than ideal. Because of the genetic changes occurring during cancer there is scope for major changes to the proteome of these cells which means analysis of the proteins in the bloodstream could provide a useful prognostic indicator. Adam *et al.* (2002) obtained proteomic data from the serum of patients with prostate cancer, Benign Prostatic Hyperplasia (BPH) or from healthy males through the use of Surface-enhanced Laser Desorption Ionisation Time-of-Flight mass spectrometry (SELDI-TOF MS). Because no single protein peak consistently differentiated healthy individuals and patients this study used the data from a test set of sera from already diagnosed patients to create a decision tree classification algorithm. This algorithm was shown to correctly diagnose prostate cancer 96% of the time with a sensitivity of 83% and a specificity of 97% when prostate cancer patients were differentiated from healthy males or those with BPH. Petricoin *et al.* (2002) also used SELDI-TOF MS and used a training set of data to teach an artificial intelligence analysis system to create the algorithm. Using this algorithm they were able to successfully diagnose 95% of patients with prostate cancer and identified 78% of patients with benign conditions. Using SELDI-TOF MS only gives the mass to charge ratio (m/z) of the protein so Malik *et al.* (2005) used liquid chromatography and gel electrophoresis to identify the proteins creating the MS peaks. Apolopoprotein A-II was identified as a protein consistently upregulated in prostate cancer (Malik *et al.*, 2005) and was shown to be able to detect prostate cancer in patients whose PSA was below 4.0ng/ml. These studies suggest that patterns of proteins can be a useful tool for identification

of patients with prostate cancer alongside traditional PSA testing.

Protein expression in cells has been found to be significantly different between patients with localised and metastatic prostate cancer (Pang *et al.*, 2010), with many proteins upregulated in cells from metastatic tumours. Six of the 58 differently expressed proteins identified by Pang *et al.* (2010) were able to be functionally linked to metastasis. This study found e-FABP5 was significantly upregulated in the prostate tissue and serum of patients with metastatic disease but did not investigate serum levels of any other proteins.

1.2.5.3 Circulating nucleic acids

Cell free nucleic acids are normally rapidly degraded in serum but in some malignancies, including cancer, they may be elevated. The mechanism for this is still under debate: Schwarzenbach *et al.* (2011) hypothesised that the DNA is released into the blood after the phagocytosis of cancer cells by macrophages. Swarup and Rajeswari (2007) suggested that DNA is passively released during tumour necrosis or cell apoptosis. In addition to increased release from cancerous tissues the increased level of cell free DNA (cfDNA) may reflect a reduction of activity of degradative enzymes DNase I and II, which has been noted during cancer (Swarup and Rajeswari, 2007). Schwarzenbach *et al.* (2009) took blood samples from patients with localised or metastatic prostate cancer and quantified the amount of cfDNA. They found that patients with metastatic disease had significantly higher levels of cfDNA compared to those with localised disease and the levels correlated to the extent that the authors hypothesised that cfDNA level could be used to monitor metastatic progression. However, Ellinger *et al.* (2011) stated that the majority of cfDNA

is produced by healthy cells so measuring expression level may not be the best method to diagnose or stage prostate cancer. Goessl *et al.* (2001) looked at epigenetic changes occurring in the DNA of prostate cancer tumours, specifically the level of promotor hypermethylation of the glutathione S transferase P1 (*GSTP1*) gene. This change causes loss of gene expression and has not been detected in normal prostate tissue or in the DNA of those with BPH. DNA was extracted from tissue, nucleated blood cells, ejaculate, urine sediment and serum or plasma, collected from patients with BHP or prostate cancer. In all sample types, except urine sediment, detection of *GSTP1* promotor hypermethylation had 100% specificity to distinguish between prostate cancer and BPH patients with sensitivity varying from 30% (nucleated blood cells) to 90% (tissue). Plasma or serum samples were able to detect prostate cancer 72% of the time but the sensitivity increased to 93% for patients with advanced, metastatic disease suggesting it could be particularly useful to identify patients with advanced disease. The loss of heterozygosity at specific genome satellites has also been investigates as a marker of cancer but these were only found to be able to accurately detect prostate cancer in combination with methylation assays (Sunami *et al.*, 2009).

RNAs are necessary for the production of proteins to cause cell proliferation and metastasis in cancer. 5T4 is a transmembrane glycoprotein which is upregulated in many epithelial cancers and is associated with increased metastatic potential (Kopreski *et al.*, 2001). Using blood samples collected from metastatic breast and advanced non-small cell lung cancer patients Kopreski *et al.* (2001) investigated whether 5T4 mRNA could be detected in the serum.

Although 5T4 was only detected in 8/19 serum samples this was significantly higher than the detection rate in samples from healthy volunteers (3/25) which indicates that further investigation of this mRNA in circulation may be warranted.

1.3 MicroRNAs

MicroRNAs (miRNAs/miR-) are small, single-stranded, noncoding, RNA molecules which regulate protein expression (Goto et al., 2015a). The genes from which miRNA precursors are transcribed are often located at 'fragile sites' which frequently undergo deletion, amplification or translocation (Calin *et al.*, 2004) during cancer development, which combined with epigenetic changes, means miRNA expression can be significantly altered in cancer. This makes them an important focus of research aiming to improve cancer diagnostics and treatment. MiRNAs can act as oncogenes or tumour suppressor genes depending on the cancer type and status of the surrounding cells (Cortez *et al.*, 2011). For example Nam *et al.* (2008) studied the miRNA expression profile of serous ovarian carcinomas and found that *miR-125b* was downregulated in cancerous tissue samples compared to samples from patients with benign uterine disease. In this tissue type *miR-125b* acted as a tumour suppressor as it was associated with reduced cell proliferation. In comparison Ozen *et al.* (2008) found that miR-125b was upregulated in prostate cancer tissue, compared to samples from benign prostate tissue. This study also found miR-125b was associated with genes for control of translation which are upregulated in prostate cancer suggesting an oncogenic function. Le *et al.* (2009) found that miR-125b is a negative regulator of the p53 pathway for

apoptosis in humans. P53 is an important tumour suppressor who's loss of function could explain the findings of Ozen *et al.* (2008).

1.3.1 Biogenesis

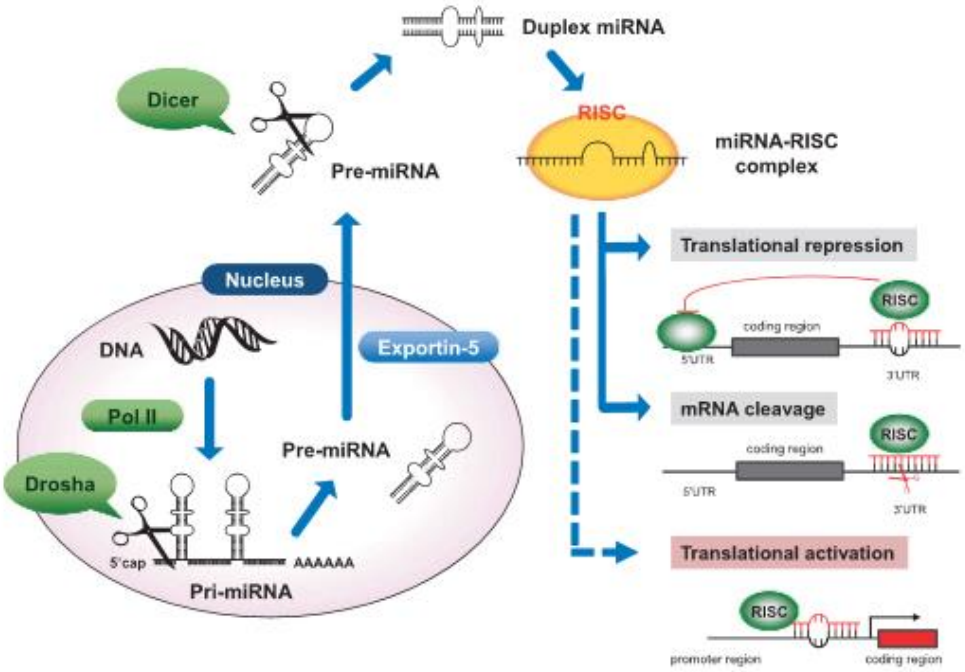


Figure 1.3 MiRNA Biogenesis (Goto et al., 2015b) (Used with permission. License number 4377010606519)

RNA polymerases (II or III) transcribe the precursor of miRNAs, which are cleaved into hairpin intermediates by Drosha RNase III endonuclease (Suzuki *et al.*, 2009). After transport into the cytoplasm the pre-miRNA is cleaved again by Dicer RNase III endonuclease into double stranded molecules of 19-22 nucleotides in length (Goto et al., 2015a). This molecule contains a duplex of miRNA and miRNA* also known as the 3p and 5p strands. The miRNAs bind to a protein from the Argonaute (Ago) family to form an RNA-induced silencing complex (RISC) which enables the action of the mature single stranded miRNA (Goto et al., 2015a)(Figure 1.3). Ago proteins bind to the miRNAs' phosphodiester backbone, so are not limited to miRNAs with specific base sequences, and this conformation enables efficient recognition of the target

sequence (Pratt and MacRae, 2009). Imperfect complementarity of the mature RNA to regions of mRNAs causes translational repression of the target proteins (Croce, 2009). Perfect matching of the 3' region with mRNAs causes mRNA degradation but miRNAs can also bind to the promotor regions of genes resulting in increased transcription (Goto et al., 2015a). MiRNAs have the potential to interact with multiple genes and affect transcription and translation in ways that are not yet fully understood.

1.3.2 MiRNA functions in cancer

1.3.2.1 Oncogenic effects of miRNAs in tissue

miR-409-3p/-5p (miR-409) was investigated for its effect on EMT, an important process for metastasis (Josson *et al.*, 2014). Using qRT-PCR analysis this study found that miR-409 was significantly upregulated in the prostate cancer cell lines which metastasises to bone in comparison to the non-metastatic line. They found that miR-409 was similarly upregulated in embryonic stem cells which undergo EMT as part of normal development. To confirm the oncogenic properties of miR-409, mice were injected with non-cancerous, miR-409 expressing cells, or control cells. Cells were injected into the mice's prostates and they were monitored for tumour development. Of the mice injected with cells expressing miR-409 60% developed tumours whilst none of the control mice were affected. Finally, to confirm its role in metastasis miR-409 knockdown cancer cells and control cancer cells were injected via the intra-cardiac route into mice. Those which received the miR-409 knockdown cells showed no development of metastases 15 weeks post-injection whilst 100% of those injected with control cells developed bone lesions. Despite this increase

in miR-409 expression in tissues Nguyen *et al.* (2013) found that miR-409-3p was downregulated in the serum of patients with metastatic prostate cancer in comparison to patients with low risk prostate cancer, which could be explained by selective expression of miRNAs. However Nguyen *et al.* (2013) also found no significant changes of expression across the normal and prostate cancer tissue samples that they tested which contradicts the finding of Josson *et al.* (2014). Josson *et al.* (2014) used androgen independent prostate cancer cell lines (*in vitro*) in their study whereas Nguyen *et al.* (2013) used samples taken from patients who were showing progression after androgen deprivation therapy (*in vivo*).

MiR-182 is highly upregulated in prostate cancer tumour tissue compared to non-tumour tissue, collected from patients with prostate cancer (Ambs et al., 2008). MiR-182 is proposed to be an important oncogene in prostate cancer development (Hirata et al., 2013). Hirata *et al.* (2013) used an inhibitor of miR-182 to prevent expression in PC3 cells, this resulted in significantly decreased cell proliferation and invasion compared to non-inhibited cells. When a miR-182 precursor was transfected into a normal prostate cell line the authors observed significantly increased cell proliferation and migration 48 hours later in comparison to the non-transfected cells. These findings indicate that increased miR-182 plays a role in stimulating the development of metastatic properties but further studies are needed to corroborate these findings.

Watahiki *et al.* (2011) studied the expression of miRNAs within cells and their relationship to prostate cancer metastasis using metastatic and non-metastatic

prostate cancer cell lines. This study used the metastatic line generated by Wang *et al.* (2005) (LTl-313H) and its non-metastatic equivalent (LTL-313B). These cells were xenografted into SCID mice. Unlike commonly used cell lines such as LNCaP and PC3 these cell lines have not adapted to *in vitro* growth and still have a normal tumour stroma which may be important for cancer pathogenesis (Wang *et al.,* 2005). MiRNA was extracted from cells and sequenced by the Genome Sciences Centre at the British Columbia Cancer Agency to produce miRNA libraries. They considered the miRNAs to be differentially expressed when there was at least a 2-fold difference between normalised counts. In total they found 104 miRNAs to be differently expressed between the libraries. When only changes of 5-fold or above were considered they found upregulation of 23 and downregulation of 24 miRNAs which seems to suggest that the miRNA are split evenly between having tumour suppressive and oncogenic effects. Whilst this study did not corroborate the findings of Josson *et al.* (2014) as they did not find increased expression of miR-409 their findings correlate with several other studies (Table 1.1).

Expression change found by Watahiki *et al.* (2011)	**MiRNA differentially expressed.**	**Supporting studies**
Increased expression in samples from patients with metastatic disease	miR-9*, miR-379	Brase *et al.* (2011); Compared serum samples of patients with localised and metastatic disease.
	miR-9*, miR-18b, miR-126, miR-200a miR-136, miR-let-7d, miR-27a, miR-27b, miR30a, miR-99a, miR-142-5p, miR-151-3p	Watahiki *et al.* (2013); Compared plasma samples collected from patients with localised and metastatic CRPC.
	miR-125	Mitchell *et al.* (2008)*; Compared serum samples from healthy controls and patients with metastatic disease.
	miR-379	Gururajan *et al.*(2014);

		Compared C4-2 and LNCaP cell lines and found miR-379 to be associated with EMT.
	miR-451, miR-106a	Moltzahn *et al.*(2011); Compared tissue expression across healthy, low risk, intermediate risk and high risk patient samples.
Decreased Expression in samples from patients with metastatic disease	miR-191, miR-145	Leite *et al.*(2013) Compared tissue expression across localised, high risk and metastatic patient samples
	miR-24	Moltzahn *et al.*(2011); Compared tissue expression across healthy, low risk, intermediate risk and high risk patient samples.
	miR-101	Hudson *et al.* (2013)†;

		Analysis of data set including information on non-cancerous tissue, localised primary tumours and distant metastases.
	miR-16, miR-363, miR-106b, miR-205	Watahiki *et al.* (2013); Compared plasma samples collected from patients with localised and metastatic castrate resistant disease.
	miR-145	Leite *et al.* (2011b) Compared tissue expression across healthy, localised and metastatic patient samples.

Table 1.1 A table showing the studies which support the findings of Watahiki *et al.* (2011). *Did not ascertain whether miR-125 expression was greater in metastatic prostate cancer in comparison to localised disease so miR-125 may only be effective at differentiating normal patients from those with prostate cancer. † Found miR-101 expression to be decreased in localised and metastatic disease compared to healthy samples so may not be useful to differentiate metastatic disease.

This study's method of miRNA detection enabled the identification of novel miRNAs in addition to measurement of previously noted miRNAs and produced a much broader signature of results, which are not replicated in their entirety in any of the other studies. The results of this study are likely to more closely represent the expression within tumours within humans as the samples were taken from tumours growing within an organism rather than cells grown purely *in vitro.* However, this study included comparison of only one cell line and its non-metastatic equivalent, so it cannot be assumed that their finding would be the same for all stages of metastasis or all patients. A wider study using similar methodology would be highly beneficial to confirm the findings.

1.3.2.2 Oncogenic effects of miRNAs in plasma

Brase *et al.* (2011) prospectively studied the plasma miRNA signature of patients with different prostate cancer stages who had not been treated using androgen deprivation or cytotoxic therapy. On analysis of the samples they found that in total, patients with metastatic disease had a much higher serum level of cell free miRNA in comparison to those with primary disease. In their screening study they found that 5 miRNAs were upregulated in patients with metastatic disease; miR-375, miR-9*, miR-141, miR-200b and miR-516-3p. These miRNAs were further validated using a larger cohort and the study found that miR-375 was the best marker for differentiation between metastatic and localised prostate cancer. MiR-141 expression was also found to be increased in patients with higher risk disease (defined as those with a Gleason score greater than or equal to 8). Nguyen *et al.* (2013) similarly compared plasma miRNA signatures in patients with localised and metastatic disease but patients

with metastatic disease had been treated with androgen deprivation therapy leading to the development of metastatic CRPC. Despite the difference in the selection of patients, this study also found that miR-375 and miR-141 were increased in metastatic disease. Bryant *et al.* (2012) found no significant difference in the expression of miR-375 when serum samples from health controls and patients with prostate cancer were compared but did find a greater than 10-fold increase when metastatic and localised cancers were compared. These findings suggest that the change in expression of miR-375 only occurs when the cancer becomes metastatic which would make it a useful biomarker for diagnosis and prediction.

Of the studies identified in this review, miR-141 is the most commonly reported miRNA associated with metastasis. In addition to being reported by Brase *et al.* (2011) and Nguyen *et al.* (2013) five other studies were found which reported an increase of miR-141 in the sera of patients with metastatic disease. Mitchell *et al.* (2008) compared age-matched healthy controls with 25 patients with metastatic disease and selected six miRNAs (miR-100, miR-125b, mir-141, miR-143, miR-205 and miR-296) which they predicted, based on previous literature, would be detectable in the serum of patients with metastasis but not in the sera of healthy individuals. MiR-205 was outside of the detection limit on both groups but all other miRNA showed increased expression in the metastatic group with miR-141 showing the greatest (46-fold) increase in expression. This study found a correlation between miR-141 and PSA level and calculated that serum levels could be used to detect metastatic cancer with 60% sensitivity and 100% specificity. Using receiver operating characteristic curves Watahiki *et al.*

(2013) found miR-141 was similarly of sensitive (56%) and specific (96%) when used to distinguish between metastatic CRPC and localised disease. Similarly to the finding of Bryant *et al.* (2012) for miR-375, Agaoglu *et al.* (2011) found no significant difference in the expression of miR-141 between the control and prostate cancer groups but did find that it was the best miRNA tested to distinguish between metastatic and localised disease. Despite having an AUC of 76%, miR-141 was not found to be a better discriminator than PSA concentration. This suggests the PSA may be useful to detect potentially metastatic disease even if it is not highly specific for screening purposes however further studies would be needed to confirm this finding and it is unlikely to be a better diagnostic tool than bone scanning. Zhang *et al.* (2013) looked specifically at miR-141 and its relationship to bone metastasis. This study found that patients with bone metastases expressed much higher serum levels of miR-141 than those with localised disease. Further to this, they discovered a correlation between the amount of miR-141 expressed and the number of metastases detected using a bone scan. Identification of bone metastases on a bone scan requires expertise for both image capture and interpretation. This study highlights the potential of miR-141 to detect metastatic disease earlier than would be possible with bone scans and without the requirement of the same level of expertise. It also suggests that miR-141 could be used as a marker to determine the extent of metastases, which would be a useful tool to evaluate prognosis. None of these studies have determined whether miR-141 is itself oncogenic, the results do not indicate causal relationship and it cannot be determined whether increased levels are causing

the metastases to develop or whether increased miR-141 occurs subsequently to metastasis development due to increased cell volume to express it. Additional pre-clinical studies are needed to determine whether knockdown of miR-141 could be a potential therapeutic strategy, in addition to being a metastatic marker.

MiR-21 is a commonly cited as an important marker for cancer (Zhang *et al*., 2011, Agaoglu *et al*., 2011, Li et al., 2012, Goto *et al*., 2015b). A review by Goto *et al.* (2015a) found that within eight published prostate cancer miRNA signatures, obtained from clinical tissue miR-21 and miR-182 were consistently upregulated. Li *et al.* (2012) found that miR-21 had prognostic utility to predict the risk of biochemical recurrence in patients treated via radical prostatectomy. MiR-21 levels in tissue samples was found to be correlated to pathological stage, lymph node metastasis, capsular invasion and reduced recurrence free survival interval. Its utility as a marker for metastasis was investigated by Agaoglu *et al.* (2011) who compared serum expression between patients with localised, locally advanced and metastatic disease. MiR-21 expression was significantly higher in patients with metastatic disease compared to those with localised disease. When ROC curves were used to distinguish patients from healthy control samples miR-21 had an AUC of 88% indicating it may be a useful screening test and could also aid with determining prognosis.

1.3.2.3 Tumour suppressive effects of miRNAs

HEF1 is the gene responsible for the production of oncogenic proteins which promote EMT and bone invasion by prostate cancer cells (Guo *et al.*, 2013).

Expression of *HEF1* is increased in metastatic prostate cancer cells which have reduced miR-145 expression and transfection of cells with miR-145 causes a decrease in *HEF1* expression (Guo *et al.,* 2013). Guo *et al.* (2013) suggested that *HEF1* can have a feedback effect on the expression of miR-145 but is also regulated by it as miR-145 can bind to the 3'-UTR of *HEF1* to affect translation. Leite *et al.* (2011b), Leite *et al.* (2013) and Peng *et al.* (2011) found that miR-145 expression was significantly higher in tissue samples from localised prostate cancer than in samples from metastatic cancer. Watahiki *et al.* (2011) also found decreased expression of miR-145 in metastatic cell lines but there was a less than 5 fold change. These studies seem to agree with the findings of Guo *et al.* (2013) that miR-145 expression must be decreased to enable cells to undergo EMT and become invasive enabling the cancer to become metastatic. MiR-145 appears to act as a tumour suppressor but its effects are overcome when the cancer has progressed to metastasis.

A similar pattern to that of miR-145 has also been observed for miR-143. Peng *et al.* (2011) found that expression of miR-143 was significantly downregulated in tissue samples from patients with metastatic disease in comparison to localised prostate cancer. Leite *et al.* (2013) also found that miR-143 decreased as the prostate cancer samples tested became increasingly aggressive. Conversely Mitchell *et al.* (2008) found that when the serum from patients with metastatic prostate cancer was compared to healthy controls the expression of miR-143 was significantly increased.

Comparing the results of these studies is difficult due to variation in

methodology used for samples preparation, RNA isolation and detection. Mitchell *et al.* (2008) showed that plasma and serum levels should be equivalent so this enables studies which used these to be compared, but studies that used tissue samples may have prepared samples differently resulting in changes in isolated RNA. Some studies used specific primers to look for miRNAs that they thought were likely to be differentially expressed (e.g. (Peng et al., 2011) and (Mitchell et al., 2008)) which means they did not report variation of expression of as many miRNAs as were reported by studies which used unbiased methods such as microarrays or sequencing as their detection method (Watahiki *et al.*, 2011). Normalisation of RT-qPCR Ct values against a housekeeping gene is very important to enable accurate comparison of expression. A number of studies (Josson *et al.*, 2014, Nguyen *et al.*, 2013) used the small nuclear RNA U6 (RNU6) as their normalisation gene despite the findings of Lamba *et al.* (2014) and Ratert *et al.* (2012), who found that RNU6 is an unstable marker which can result in inaccurate normalisation. The use of different, and potentially unstable housekeeping genes may have therefore affected the results and the comparability between studies.

1.3.3 MiRNA transfer between cells

MiRNAs have an intracellular effect but may also be released from the cell via extracellular vesicles (EVs; including microvesicles (1.3.3.1) and exosomes (1.4)) and apoptotic bodies (1.3.3.1) or bound to high density lipoproteins (HDLs) or proteins (1.3.3.2). This enables them to have an intercellular effect. Exosomes (1.4) are a major vehicle for miRNA transport.

1.3.3.1 Microvesicles and apoptotic bodies

In addition to exosomes miRNAs can be found contained in circulation within microvesicles and apoptotic bodies (Sohel, 2016). These vesicles, also membrane bound but shed directly from the plasma membrane, are larger than exosomes and are released early (microvesicles) or late (apoptotic bodies) in the apoptotic process (Sohel, 2016).

Microvesicles are of a less uniform size (50-1000nm in diameter (Lee *et al*., 2012)) and more variable membrane composition than exosomes and have no consistent characteristic markers (Lee *et al.*, 2012) due to their formation directly from the plasma membrane. Microvesicles can transfer miRNAs into cells and may provide a mechanism for the introduction of therapeutics into cells (Ratajczak *et al.*, 2012). Bryant *et al.* (2012) investigated the miRNA profiles of microvesicles isolated from the plasma of healthy controls and patients with prostate cancer and found significant upregulation of 11 miRNAs in the microvesicles derived from prostate cancer patients' plasma. The miRNA profiles were also found to be able to differentiate between metastatic and localised disease. This study shows that disease state does have an effect on the miRNAs within microvesicles but whether these miRNAs could be transferred into other cells was not investigated.

Apoptotic bodies have been shown to convey paracrine signals to other cell types (Zernecke *et al.*, 2009) and the same study confirmed the transfer of miRNAs via apoptotic bodies to recipient vascular cells. Aihara *et al.* (1994) reported a positive correlation between the number of apoptotic bodies in the tissues of patients with prostate cancer and Gleason score and hypothesised

that increased cell death is associated with more malignant tumours. However this study did not consider the potential for the apoptotic bodies to be a contributing factor to increased Gleason score and therefore did investigate their contents. Because of their size, which is similar to that of cell debris, many protocols investigating circulating miRNAs exclude apoptotic bodies (Turchinovich *et al.*, 2012) and so their role in miRNA transfer may be underappreciated.

The author could not find any studies which suggested that apoptotic bodies or microvesicles are responsible for the transfer of miRNAs to or from prostate cancer cells.

1.3.3.2 High Density Lipoproteins (HDLs) and protein binding

MiRNAs not contained within vesicles may bind to high density lipoproteins (HDLs) or to protein complexes which enable them to travel in the blood (Sohel, 2016) and avoid enzymatic degradation.

Vickers *et al.* (2011) isolated HDLs from human plasma and used a microarray to investigate whether miRNAs were present. They found that the total levels of miRNA were increased in patients with familial hypercholesterolemia and that the number of miRNAs present also increased. This study also found that when cells were treated with an HDL-miR-375 complex the intracellular expression of miR-375 was increased 11.8 fold. Luciferase reported assays were conducted which found that when cells were treated with the HDL-miRNA complex there was a significant decrease in Renilla-luciferase activity. This shows that HDLs can transmit functional miRNAs between cells.

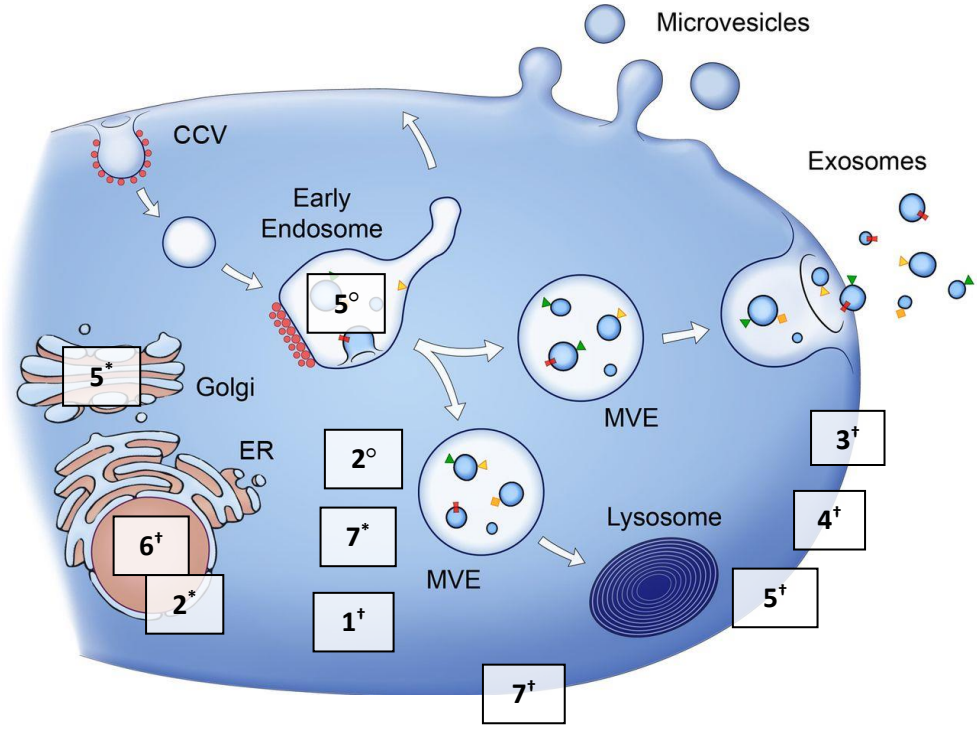
MiRNAs are also found bound to Argonaute2 (Ago2) in circulation (Turchinovich *et al.*, 2011, Arroyo *et al.*, 2011). Arroyo *et al.* (2011) found that the proportion of miRNA in a serum sample contained within vesicles varied depending on which miRNA was assayed. This study used immunoprecipitation of Ago2 to confirm that miRNAs are associated with Ago2 in circulation but noted that the efficiency of the immunoprecipitation was below 60% so the figures generated were likely to be an underestimate of the actual proportion of miRNAs complexed to Ago2. This study found that for two of the miRNAs studied around 20% of total circulating miRNAs were present in these complexes. Let-7a was not found in plasma in this form so the authors proposed that although Ago2 complexes are an important carrier of some miRNAs in circulation others are exclusively associated with membrane bound vesicles. Turchinovich *et al.* (2011) similarly studied Ago2-miRNA complexes and found that these complexes make up a much larger proportion of circulating miRNA than those contained within exosomes. Similarly to the findings of Arroyo *et al.* (2011) they identified 22 miRNAs which were exclusively isolated from the EV fraction of the plasma but also found 69 miRNAs which were only present in the supernatant bound to Ago2. These studies did not assess whether these miRNAs could be delivered to other cell types and affect translation and transcription in these recipient cells. Yoo *et al.* (2010) found that cellular Ago2 is more commonly found in cells from prostate cancer compared to normal prostate tissue but did not investigate circulating Ago2. Cancer specific studies are needed to assess whether Ago2-bound miRNAs can play a part in alteration of transcription and preparation of the

metastatic niche.

1.4 Exosomes

Exosomes are membrane bound vesicles of 50-90nm in diameter, which are found in almost all biological fluids (Sohel, 2016). Multiple exosomes form via inward budding of an endosome within the cell to form a multivesicular body (MVB) (Kowal *et al.*, 2014)(Figure 1.4). The exosomes are then secreted into the extracellular fluid when the MVB fuses with the plasma membrane (Kowal *et al.*, 2014). Because of their endosomal origins, certain proteins associated with membrane binding and fusion are enriched in exosomes (Simons and Raposo, 2009). These can be used as markers to identify and isolate exosomes.

1.4.1 Exosome marker proteins



1 Alix **2** Annexin V **3** CD9 **4** EpCAM 5 Flotillin-1 **6** HSP70 **7** ICAM

† Based on information from the Human Protein Atlas (Uhlén *et al.*, 2005) and Uniprot Database (The UniProt Consortium, 2017).

* Based on information from the Human Protein Atlas (Uhlén *et al.*, 2005)

○ Based in information from the Uniprot Database (The UniProt Consortium, 2017)

Figure 1.4 A figure showing the biogenesis of different vesicle types and localisation of exosome associated proteins in a normal cell. (Used with permission (Raposo and Stoorvogel, 2013). License no. 4377041018944)

Programmed Cell Death 6 Interacting Protein (Alix) recruits the Endosomal Sorting Complex Required for Transport (ESCRT) to enable inward budding of the membrane into the endosomal lumen (Akers *et al.*, 2013). This makes it vital for the formation of MVBs and therefore is commonly found in exosomes from multiple cell types (Simons and Raposo, 2009). Alix is also involved in cell apoptosis (Schorey and Bhatnagar, 2008).

Annexin V is part of the annexin protein group. These are Ca^{2+} dependent phospholipid binding proteins which regulate cell membrane organisation (Gerke and Moss, 2002). The conformation of these proteins enables them to

bind reversibly to membranes as they only interact with the peripheries of phospholipids (Rescher and Gerke, 2004). They act as scaffold proteins which enables them to regulate interactions between the cytoplasm and the cytoplasmic surface of cellular membranes (Rescher and Gerke, 2004). They enable the membrane to act as a platform for assembly of cytoskeletal components, such as actin (Rescher and Gerke, 2004). This regulation of the cytoskeleton (Schorey and Bhatnagar, 2008) is indirectly important for the formation of exosomes as it enables transport of MVBs to the cell surface. Annexins are also important for membrane binding which enables fusion of intracellular compartments (Théry *et al.*, 2002) and therefore the release of exosomes. Because they are needed for exosome formation Annexins can be found in almost all exosome types irrespective of their cell of origin (Simons and Raposo, 2009), the specific annexin present may however be dependent on cell type.

Tetraspannin-29 (CD9) is part of the tetraspanin glycoprotein family which can have a positive or negative affect on the activation of associated molecules (Zöller, 2008). CD9 is localised to the plasma membrane of cells (Uhlen *et al.*, 2017). Tetraspanins are abundant in exosomes with CD63, CD81 and CD82 also common (Schorey and Bhatnagar, 2008). CD9 is important for the regulation of cell morphology, motility and signalling (Hemler, 2005) as it can interact with many other proteins (Théry *et al.*, 2002). An increase in CD9 expression has been associated with prostate cancer (Uhlén *et al.*, 2005) and metastatic gastrointestinal cancer (Murayama *et al.*, 2004).

Epithelial Cell Adhesion Molecule (EpCAM) is an epithelial cell transmembrane glycoprotein whose expression was found to be related to the level of epithelial cell proliferation (Went *et al.*, 2004). As its name suggests it is important for cell adhesion, but in addition to this it is suggested to be important for cell signalling, migration, proliferation and differentiation (Trzpis *et al.*, 2007). It is associated with epithelial carcinoma due to its high expression on rapidly proliferating tumours (Trzpis *et al.*, 2007) and (Went et al., 2004) found that EpCAM expression was increased in poorly differentiated cells and in CRPC compared to low grade carcinomas.

Heat Shock Protein 70 (HSP70) is a protein involved in antigen presentation in combination with MHC I and II (Schorey and Bhatnagar, 2008) and is ubiquitous in exosomes (Théry *et al.*, 2002). It acts as a chaperone proteins for the AR within the cytoplasm in the absence of androgen (Davey and Grossmann, 2016). These proteins have important housekeeping functions including folding newly synthesised proteins, refolding misfolded proteins and membrane translocation of secretory proteins and those produced in organelles (Mayer and Bukau, 2005). They are also important in protecting cells against heat stress (Mayer and Bukau, 2005). HSP70 expression is decreased in prostate cancer tissues compared to healthy prostate tissue (Uhlen *et al.*, 2017) though its expression in normal and cancer-derived exosomes has not be explored.

Intra-Cellular Adhesion molecule (ICAM or CD54) is a cell specific transmembrane protein (Théry *et al.*, 2002). This protein binds to integrins (NCBI, 2017) and is important to stabilise intercellular interactions to enable

cell signalling. It is commonly found on exosomes derived from antigen presenting cells due to co-stimulatory functions (Lotvall and Valadi, 2007). ICAM-1 has been shown to be conserved across exosomes derived from B cells and dendritic cells (Théry *et al.*, 2002) and it is likely that based on their increased expression in endothelial cells and other leucocytes (NCBI, 2017) that they would also be present in exosomes from these cells.

The role of Flotilin-1 is not definitively known (Langhorst *et al.*, 2005) but it is suggested to be involved in vesicle trafficking and regulation of cell morphology (NCBI, 2018). Flotilin is known to be involved with membrane transport and fusion (Simons and Raposo, 2009) making it important for exosome biogenesis. Flotilin and Alix are commonly enriched in exosomes (Simons and Raposo, 2009) but their expression in prostate cancer tissue was the same or lower than in normal prostate tissue (Uhlen *et al.*, 2017).

1.4.2 MiRNAs within exosomes

Containment within exosomes makes the miRNAs resistant to degradation by RNases (Sohel, 2016) and they can be subjected to room temperature incubation or freeze thaw cycles without miRNA levels being altered (Mitchell *et al.*, 2008).

Melo *et al.* (2014) compared miRNA expression in exosomes released from breast cancer cells and those released from normal cells. They found that despite the parent cancer cells containing lower levels of the miRNAs compared to normal cells, the expression of miRNAs was increased in cancer derived exosomes. Further to this, they found that the total level of miRNAs increased in exosomes derived from patients with metastatic disease compared to localised breast cancer. When exosomes were cultured this study observed an increase in miRNA expression and found that cancer exosomes contain pre-miRNAs which are then processed into mature miRNAs using RISC proteins which are also contained within the exosomes. When exosomes from normal cells were assessed in the same way they were not found to contain the RISC proteins. Hessvik *et al.* (2012) conducted a similar study using prostate cancer and normal prostate cell lines. Exosomes were isolated from the culture media of these cells and microarrays were used to identify the miRNAs present. They found 31 miRNAs expressed only in exosomes, 49 which were only expressed in the cells and 333 which were expressed in both cells and exosomes. The findings of Sohel (2016) and Melo *et al.* (2014) confirm that, as suggested by Hessvik *et al.* (2012) miRNAs are selectively packaged into exosomes. In addition to this exosomes from cancer cells can be enriched with miRNAs after

exosomes budding occurs (Melo *et al.*, 2014) meaning their extracellular concentration may be very different to the cellular concentration.

Multiple studies have shown that exosomes provide a vehicle for the transfer of miRNAs to other cells where they are able to alter translational function (e.g. (Pegtel *et al.*, 2010), (Valadi *et al*., 2007), (Melo *et al.,* 2014)).

1.4.3 MiRNAs as biomarkers

The reports of overdiagnosis leading to potentially unnecessary, invasive treatment and reports of disease recurrence despite treatment highlight the need for more sensitive detection methods, which can distinguish between patients with indolent disease and those at risk of developing advanced prostate cancer. Whilst PSA testing is minimally invasive, as it only requires a patient to supply a blood sample, it cannot accurately determine patient prognosis. Currently it is used as a screening tool and if the result is suggestive of disease other, more invasive, methods are used to confirm a diagnosis. Prostate biopsy followed by histological examination can provide useful information about tumour stage and grade, but the results may not be representative of the state of the entire prostate gland due to the nature of sampling. None of the currently available methods are ideal in terms of diagnostic accuracy or their ability to predict prognosis.

Despite variations in experimental design, the studies identified in this review seem to indicate that there is a significant difference in expression of certain miRNAs once cancer has become metastatic. Whilst detection of these changes could be useful for the detection of metastasis without the need for invasive

biopsies it would be even more useful if an miRNA signature could be used at the time of initial diagnosis to stratify the risk of the patient of developing advanced or metastatic disease. Weigelt *et al.* (2005) suggested that breast cancer with metastatic capacity may have acquired mutations at early stage of tumorigenesis which enabled distinction of cancers that would remain localised and cancers that would metastasise based on their gene profiles early in pathogenesis. Ramaswamy *et al.* (2003) studied gene expression of metastatic adenocarcinomas from 12 different sites and compared these to their primary counterparts. This study found there were 128 genes which could distinguish between metastatic and primary cancer and hypothesised that some primary tumours had the gene expression profile associated with metastasis and so are primed to metastasise whilst others are not. To test this hypothesis, hierarchical clustering was used on large gene-expression data sets from patients with primary lung adenocarcinoma and identified two distinct clusters of genes in primary tumours which correlated with development or lack of development of metastasis. When this methodology was applied to other tumour types, the study found consistent upregulation of eight and downregulation of nine genes across all samples and suggested that there was a generic gene-expression profile for metastasis in all solid tumours. MiRNAs can affect the expression of multiple genes so the finding that gene expression changes sufficiently in early tumorigenesis to enable differentiation of tumour types suggests that there may be similar changes in miRNA expression. Most of the studies considered in this review look at the miRNA signature once metastasis has developed and therefore do not report the miRNA signature at

the time of diagnosis. Prospective studies where serum or tissue samples are analysed for the miRNA signature at the time of diagnosis might be key in determining whether they can be used to predict risk of metastasis very early on.

Vonderscher (2008) discussed the properties of an ideal biomarker for kidney toxicity. The findings of this workshop can be applied to biomarkers of other disease processes; Table 1.2.

Characteristic;	**Evidence that miRNAs meet this criteria;**
High Sensitivity and specificity	Mitchell *et al.* (2008) and Watahiki *et al.* (2013) found that miRNAs could be used to differentiate between localised and metastatic prostate cancer with near perfect specificity however their sensitivity was less ideal (56-60%). These findings suggest that miRNAs may not be an ideal biomarker for initial detection but that they can provide more information about cancer type after identification.
Easy to measure	Plasma samples can be easily collected for analysis and were shown to have diagnostic potential by multiple studies discussed in this review. If surgical intervention is indicated based on miRNA levels in plasma then biopsies can be taken during removal to provide additional information about the risk of metastasis and prognosis.

Expression should correlate to severity	The expression of miRNAs within tissues or plasma changes depending on disease progression. Increased expression occurs in patients with metastatic disease compared to localised disease. Zhang *et al.* (2013) found that miR-141 expression increased as the number of metastases increased, showing that miRNAs can be used to determine severity. However not all miRNAs followed this pattern as some are expressed only at certain stages of disease or expression decreases so whether there is a correlation depends on the miRNA assessed.
The marker should be analytically stable	Subjecting samples to freeze thaw samples or leaving samples at room temperature does not affect later analysis (Mitchell *et al.*, 2008) which means miRNA can be collected from patients and transported without the risk of affecting the results or stored to enable subsequent comparison.

Table 1.2 The ideal characteristics of a biomarker as set out by (Vonderscher, 2008) and a summary of the evidence to support whether miRNAs fulfil these characteristics.

1.5 Study objectives

- To determine whether miRNAs can be isolated from EVs derived from prostate cancer cells.
- To determine whether EV miRNAs can be transferred into recipient cells.

- To determine whether transferred miRNAs have an effect on target gene expression in recipient cells
- To determine what changes occur in recipient cells in response to treatment with cancer derived EVs containing miRNAs.

2 Chapter 2: Materials and Methods

2.1 Cell lines

PC3 cells were purchased from the European Collection of Authenticated Cell Cultures (ECACC).

Human adult Osteoblasts (hOB) were kindly supplied by the laboratory of Professor Susan Anderson, University of Nottingham. This cells line was derived from adult femoral head trabecular bone and cultured as described (Anderson *et al.*, 1998).

LNCaP and C4-2 cells were provided in collaboration by Nigel Mongan and were cultured as described by (Kashyap et al., 2013).

PNT1A were also kindly provided in collaboration by Nigel Mongan. These cells are immortalised prostate epithelium cells from a normal 35-year-old male and obtained from ECACC.

HEK293 cells were purchased from the ECACC. These cells are derived from a normal embryonic human kidney.

2.2 Cell culture

PC3 and hOB cells were cultured in Dulbecco's Modified Eagle's medium (DMEM) with high glucose, L-glutamine, $NaHCO_3$, sodium pyruvate and phenol red, produced by Sigma (#D6429, Sigma-Aldrich, UK). C4-2, LNCaP and PNT1A cells were cultured in RPMI-1640 media with $NaHCO_3$, L-glutamine and phenol red, produced by Sigma (#R8758, Sigma-Aldrich, UK). Both types of media were supplemented with 10% Fetal Bovine Serum (FBS) (#F6178, Sigma-Aldrich, USA) and 1% Pen Strep (#P4333, Sigma-Aldrich, UK). All cells were cultured in T75 flasks and incubated at 37°C in 5% CO_2. Cells were routinely passaged prior to

growth exceeding approximately 80% confluency. To subculture, medium was removed, and the cells washed with 4ml 1X Phosphate buffered saline (PBS) (#D8662, Sigma Aldrich, UK), prior to the addition of 2ml of trypsin EDTA (#T4049, Sigma Aldrich, UK) and incubation for 2-5 minutes at 37°C. 8ml of culture media (containing 10% FBS) was added to neutralise the trypsin and the cells pelleted by centrifugation at 500rpm for 5 minutes. The pelleted cells were resuspended in 10ml of media and transferred to new T75 flasks.

2.3 Extracellular vesicle collection

The number of cells used varied between experiments to provide similar yields of EVs (Table 2.1), total cell counts were conducted using a haemocytometer (#AC1000, Hawksley, UK). Cells were incubated for approximately 16 hours overnight at 37°C, 5% CO_2, following this incubation cells were washed in 1X PBS and the media changed to one containing 1% Pen Strep and 10% exosome-depleted serum (#A25904DG, Gibco, USA) (for volume see Table 2.1). Cells were incubated for a further 24 or 48 hours (detailed in Table 2.1) at 37°C, 5% CO_2 prior to vesicle isolation.

Experiment	Cell type	Plate size	Number of cells	Volume of exosome depleted media added	Hours incubated after addition of exosome depleted media
Validation of the transfer of characterised miRNAs from prostate cancer cell to osteoblasts via vesicles (2.10 and 3.2.3)	PC3 hOB HEK293	$15cm^2$	$5x10^6$	13ml	24
	hOB	$10cm^2$	$5x10^5$	9ml	
Comparison of expression of miRNAs between cells and EVs (3.2.2)	PC3 PNT1A C4-2 LNCaP	$15cm^2$	$5x10^6$	13ml	24

Characterisation of EVs (2.5 and 3.2.1)	PC3 PNT1A C4-2 LNCaP hOB	$10cm^2$	$3.5x10^6$	9ml	48
RNA sequencing (2.7, 2.21, 3.2 and 5.2)	PC3 PNT1A	$15cm^2$	$5x10^6$	13ml	24
	hOB	$15cm^2$ and $10cm^2$	$5x10^6$ and $5x10^5$	13ml and 9ml	

Table 2.1 A table showing the number of cells used in different experiments

2.4 Extracellular Vesicle isolation

After incubation the supernatant was collected from the cells and centrifuged at 500rpm for five minutes at room temperature (approximately 21°C). The supernatant was processed using the exoEasy Maxi Kit (#76064, Qiagen, Germany), following the manufacturer's instructions. Briefly, one volume of buffer XBP was added to the sample and mixed by inversion of the tube. The sample was applied to an exoEasy in 16ml aliquots and centrifuged at 500 xg for 1 minute at room temperature. 10ml of buffer XWP was added to the column and centrifuged at 2800 xg for 5 minutes. EVs were eluted in 400µl of elution buffer XE by incubating for 1 minute at room temperature and centrifugation at 500xg for 5 minutes. Finally, Buffer XE was reapplied to the column and incubated for a further 1 minute followed by centrifugation at 2800 xg for 5 minutes. EVs were transferred to a 1.5ml microcentrifuge tube and stored at -20°C until needed.

2.5 Characterisation of EVs

To characterise the types of extracellular vesicle present in the resulting elution (2.4) they were analysed using western blotting and Brownian motion analysis.

2.5.1 Western blotting

To determine the presence of vesicles, western blotting was used to detect the presence of protein markers concordant with endosomal biogenesis (HSP70, CD9, CD54, EpCAM, Annexin V and flotillin-1) and to test for contamination by other cellular components (Golgin subfamily A member 2 (GM130) protein was used as a control for this). EV samples were concentrated using Amicon Ultra 0.5 Centrifugal filter devices (#UFC500308, Merck-Millipore, Ireland). Briefly, 400µl of EV sample was added to device and the device was capped and then

centrifuged at 14,000 xg for 20 minutes at room temperature. The device was then placed upside-down into a clean 1.5ml microcentrifuge tube and the tube was centrifuged at 1,000 xg for one minute at room temperature to recover the concentrated sample. The concentration of the samples was determined using the Qubit Protein Assay Kit (#Q33211, ThermoFisher, UK) and the Qubit 2.0 instrument (ThermoFisher, UK).

Equal amounts of protein (approximately 40,000ng) were mixed with 4X Laemmli buffer (#1610747, Biorad, UK) and 12µl of each sample electrophoresed on a 10% or 4-20% gradient SDS-PAGE gel at 200V for 40 minutes in 1X-Tris-glycine-SDS buffer (#1610732, Biorad, UK). Only one replicate was used for each sample. Standard protein markers were created by combining 2µl of Bio-Rad All Blue protein standard (#1610373, Bio-Rad, UK) with 3µl of MagicMark XP Western Protein standard (#LC5602, Invitrogen, USA). However, due to poor visualisation of the protein markers the amount of MagicMark XP was increased to 5µl in later experiments. Proteins were transferred onto nitrocellulose membrane (#1620112, Bio-Rad, Germany) using the semi-dry Trans-Blot Turbo Transfer System (#1704150, Bio-Rad, UK) for 7 minutes at 25V constant in 1X Tris-Glycine buffer (#1610734, Biorad, UK) with 10% v/v methanol. Following protein transfer, membranes were blocked in 5% Bovine serum albumin (BSA) (#BP1605100, Fisher, USA) in 1X Phosphate buffered saline with tween (PBS-T: 3.2 mM Na2HPO4, 0.5 mM KH2PO4, 1.3 mM KCl, 135 mM NaCl, 0.05% Tween20, pH 7.4) and incubated at room temperature with agitation (25rpm) for 60 minutes. Membranes were incubated with primary antibodies HSP70, CD9, CD54 and EpCAM primary

antibodies (Exosomal Marker Antibody Sampler Kit #74220, Cell Signalling Technology, USA) diluted 1:1000 in 3ml of 5% BSA v/v in 1X PBS-T at 4°C for approximately 16 hours with continuous agitation.

Following incubation with primary antibodies, the membranes were washed 4 times in 1x PBS-T with agitation (45 rpm) for 10 minutes per wash and subsequently incubated with HRP-linked anti-rabbit secondary antibody (#74220, Cell Signalling Technology, USA) diluted at 1:50,000 in a 3% solution of skimmed milk powder in 1X PBS-T. Membranes were incubated with agitation (25 rpm) for 60 minutes at room temperature followed by a repeat of the previous wash steps (4X 10 minutes in 1X PBS-T with agitation at 45 rpm). Antibody-bound proteins were visualised by incubating the membranes with 600µl of SuperSignal West Femto Maximum sensitivity substrate kit (#34095, Thermo Fisher Scientific, USA) for 5 minutes and room temperature and imaged using the ChemiDoc MP Imaging System (#17001402, Bio-Rad, UK) using the default chemiluminscenece setting.

On occasion membranes were reprobed for additional protein markers, where this was the case the membranes were stripped by incubation in Restore Western Blotting Stripping Buffer (#21059, Thermo Fisher Scientific, USA) for 10 minutes at room temperature. Following the stripping step, membranes were washed 3 times in PBS-T for 5 minutes per wash with agitation (25 rpm) and then blocked and used for subsequent protein detection as previously described. On occasion stripping of membranes for 10 minutes proved to be insufficient in removing bound primary antibody. Therefore, the incubation in

stripping buffer was extended to 20 minutes, all other steps remained the same.

2.5.2 Brownian motion analysis

To determine whether the EVs contained particles within the size range attributed to exosomes, EVs isolated from hOB, PC3, C4-2, LNCaP and PNT1A cells were subjected to Brownian motion analysis. This analysis was conducted by Dr Victoria James. Briefly, the ZetaView instrument (Particalmetrix) (Mehdiani et al., 2015) was used to determine vesicle size and number. The instrument was aligned using 200 nm sized polystyrene particles (Particle metrix) diluted to a concentration of 600 ± 100 particles per ml in HPLC purified water prior to readings being taken. Vesicle samples at 100µg/ml total protein concentration were diluted 1 in 1000 in PBS and 1ml of suspension was analysed using the following settings (sensitivity 85, shutter speed 70, minimum brightness 25, maximum area 500, minimum size 20, framerate 30, tracelength 15, video quality medium). Three readings were taken at 11 different positions within the cell and each sample was tested in triplicate. Average (median) particle size and particle concentration were determined.

2.6 RNA isolation

RNA was isolated from EVs and cells using the miRNeasy kit (#217004, Qiagen, Germany), following the manufacturers protocol. Briefly, 700µl of QIAzol lysis reagent (#79306, Qiagen, USA) was added to the cells or eluted EVs and the sample was homogenised by pipetting up and down. Additionally, cells were scraped from the culture surface and transferred to a 1.5ml microcentrifuge tube. Samples were incubated at room temperature for 5 minutes before the addition of 140µl of chloroform. Samples were vortexed for 15 seconds, incubated at room temperature for 2-3 minutes, and subsequently centrifuged at 12,000 xg for 15 minutes at 4°C. The resulting aqueous phase was transferred to a new tube and 1.5 volumes of 100% ethanol was added and mixed by pipetting. Samples were transferred to the miRNeasy spin column in 700µl aliquots and centrifuged at 8000 xg for 15 seconds at room temperature. Columns were washed with 700µl of buffer RWT and centrifuged at 8000 xg for 15 seconds at room temperature, followed by 500µl of buffer RPE and centrifugation as before. A final volume of 500µl buffer RPE was added to each column and centrifugation was carried out at 8000xg for 2 minutes at room temperature. The column was transferred to a new collection tube and 30µl of RNase-free water was added directly to the column membrane to elute the RNA using centrifugation at 8000 xg for 1 minute. RNA was quantified using the NanoDrop 8000 Spectrophotometer (#ND-8000-GL, Thermo Scientific, UK) and stored at -80°C.

2.7 RNAseq analysis of microRNAs transferred via prostate cancer vesicles to osteoblasts

This experiment was conducted by Dr Victoria James prior to the author beginning the project.

Two 15cm^2 plates of PC3 and hOB cells and two 10cm^2 plates of hOB were seeded (Table 2.1). The cells were incubated overnight and then the media was replaced with exosome depleted media (as previously described in section 2.3), with the addition of 1µl/ml of 5-ethynyl Uridine (5EU) label (#C10365, Invitrogen, USA). The cells were then incubated overnight, and EVs isolated as described in 2.4.

After isolation 10µl of the EVs was mixed with the same volume of 5X lysis buffer (#E1941, Promega, USA) and frozen overnight before being quantified using the Qubit protein quantification protocol.

A further 150µl of the EVs was diluted with 10ml of DMEM media (containing 10% exosome depleted serum) and added to a 10cm^2 plates of hOB cells, and treated cells were incubated overnight at 37°C, 5% CO_2.

The RNA was isolated from the remaining isolated EVs (~240µl) and following incubation total RNA was extracted from the hOB cells following the protocol described in 2.6. From the total RNA sample, any EU-labelled RNA was isolated using the Click-iT nascent RNA capture kit (#C10365, Invitrogen, USA). Briefly, 25µl of Click-iT EU buffer, 4µl of $CuSO_4$, 1.25µl Biotin Azide, 17µl EU RNA (at a concentration to ensure 20,000ng of RNA was added) and 12.5µl of Click-iT reaction buffer additive 1 were vortexed and then incubated for 3 minutes. 1.5µl of Click-iT reaction buffer additive 2 was added and the sample incubated

for 30 minutes at room temperature with vortexing at five minute intervals. 10µl of ultrapure glycogen (diluted 1 in 10), 50µl 7.5M ammonium acetate and 700µl of chilled 100% ethanol were added and mixed by inversion. The sample was incubated for approximately 16 hours at -80°C.

Samples were centrifuged at 13000 xg for 20 minutes at 4°C. The pelleted RNA was washed with 700µl of 70% ethanol and centrifuged at 13000 xg for five minutes at 4°C. The ethanol was removed and the pellet left to dry at room temperature for ten minutes before being resuspended in 35µl of RNase free water. To prepare the Dynabeads MyOne Streptavidin T1, 15µl of beads per sample were washed three times with 25µl of Click-iT reaction wash buffer 2. Washed beads were resuspended in the original starting volume (15µl) of Click-iT reaction wash buffer 2.

To bind 5-EU labelled RNA, 19µl of RNA were combined with 20µl of 2X Click-iT RNA binding buffer and 1µl of RNase OUT inhibitor and incubated at 68-70°C for five minutes. Following the incubation, 15µl of washed Dynabeads and 445µl of wash buffer 2 were added to each binding reaction. Reactions were incubated at room temperature for 30 minutes with continuous rotation. After 30 minutes, beads were immobilised and subject to five washes in 250µl wash buffer one followed by five washes with 250µl wash buffer 2. The beads were resuspended in 15µl of wash buffer 2 and used directly in the cDNA synthesis protocol described in 2.7.

RNA sequencing (RNAseq) was performed by Barts Genome Centre (Queen Mary University, London) as follows. Samples were prepared using the Truseq

RNA and small RNA libraries (#RS-122-2101 and #RS-200-0012, Illumina, USA) and sequenced using the NextSeq 500 (Illumina, USA) High Output Run (150 cycles) for two biological replicates. Cutadapt (Martin, 2011), SHRiMP (Rumble *et al.*, 2009), SAMtools (Li *et al.*, 2009) and edgeR (Robinson *et al.*, 2010) were used respectively for trimming, mapping, generating raw counts and differential expression analysis.

2.8 cDNA synthesis

cDNA was synthesised using the MystiCq microRNA cDNA Synthesis Mix (#MIRRT-25RXN, Sigma, USA). Briefly, the maximal amount of RNA -7µl – was added to 2µl Poly (A) tailing buffer (x5) and 1µl Poly (A) Polymerase (5,000 units/ml) and reactions incubated at 37°C for 30 minutes then at 70°C for 5 minutes. To each reaction, 1µl of reverse transcriptase was and reactions incubated at 42°C for 20 minutes then at 85°C for five minutes. cDNA was stored at -20°C.

2.9 MiRNA detection via PCR

Quantitative real-time PCR (qRT-PCR) to detect the levels of miRNAs in EVs and in cells was conducted using the MystiCq microRNA SYBR Green qPCR ReadyMix (#MIRRM03, Sigma, USA). In 96 well qPCR plates 5µl SBYR green ReadyMix was combined with 0.2µl Assay specific primer, 0.2µl Universal primer (10 mg/mL) (#MIRUP, Sigma, USA), 1µl of cDNA (product of 2.8) and 3.6µl Nuclease free water.

Reactions were analysed using a LightCycler 480 II (#05015278001, Roche Life Science, UK) and a programme consisting of an initial denaturation of 95°C for 2 minutes then 40 cycles of 95°C 5 seconds, 60°C 15 seconds and 70°C for 15

seconds.

2.9.1 Selection of primers

MiRNAs were selected through bioinformatic analysis and the following miRNA assays were selected for study; miR-21-5p (10 mg/mL, MIRAP00047, Sigma Aldrich, UK), miR-100-5p (10 mg/mL, MIRAP00118, Sigma Aldrich, UK), miR-3182 (10 mg/mL, MIRAP00912, Sigma Aldrich, UK) and miR-4448 (10 mg/mL, MIRAP01067, Sigma Aldrich, UK).

In addition to these four, miR-101-3p (10 mg/mL, MIRAP00120, Sigma Aldrich, UK) and miR-223-5p (10 mg/mL, MIRAP00282, Sigma Aldrich, UK) were identified as potentially useful endogenous controls. However, on analysis miR-101 was precluded as a control as it presented with a cancer-specific levels within EVs.

2.9.2 Normalisation

SNORD 43 (10 mg/mL, MIRCP00004, Sigma Aldrich, UK) and SNORD 48 (10 mg/mL, MIRCP00007, Sigma Aldrich, UK) were identified through a literature search as being stably expressed in all cells and EVs and so were selected for use as endogenous controls (SNORD 43; (Leite *et al.*, 2011a, Leite *et al.*, 2011b, Sanders *et al.*, 2012, Leite *et al.*, 2013), SNORD 48; (Sauer *et al.*, 2014, Sanders *et al.*, 2012)). The geometric mean of the triplicates of both of these small RNAs were used in the analysis of the data to enable comparison of miRNA levels across cell types or in EVs.

2.9.3 Standard curves

Standard curves for each miRNA assay were created using 1 in 4 serial dilutions of total PC3 cDNA. Following determination of the PCR efficiencies, the $\Delta\Delta$CT

method (Livak and Schmittgen, 2001) was chosen for subsequent analysis.

2.9.4 Analysis

Data was exported into Excel (Microsoft, 2016) and $\Delta\Delta$CT analysis was used to calculate the change of miRNAs level between different cell types, EVs and between cells and EVs.

The analysis software GraphPad Prism 7.01 (GraphPad Software, 2017) was used to conduct unpaired, non-parametric t test analysis to look for significant differences in results. This software was also used to generate graphs from the data.

2.10 Validation of the transfer of characterised miRNAs from prostate cancer cells to osteoblasts via vesicles.

The preparation of EV samples was completed by Catherine Probert. Two 15cm^2 plates of PC3, HEK293, PNT1A and hOB cells and four 10cm^2 plates of hOB were seeded (Table 2.1). The miRNAs were labelled with EU label as previously described (2.7). EVs from each of the 15cm^2 plates were isolated and half used to treat hOB cells whilst the RNA was extracted from the other half (2.6). Following a 24 hour incubation the total RNA was extracted from the hOB cells and the EU labelled RNA was extracted as previously described (2.7).

MicroRNAs within EVs and labelled miRNAs within cells were quantified by RT-qPCR as described in 2.9 using assays for miR-21, miR-100, miR-3182, miR-4448 and mir-101 and using SNORD 43 and 48 as endogenous controls.

2.11 Amplification of Reporter Plasmids

Transformed DH5-α *E. coli* cells containing different reporter plasmids were cultured to amplify the plasmid DNA. The plasmids amplified were pmiR Renilla

luciferase vector only (RL-VO) (#AM5795, ThermoFisher) or containing the 3'UTR of *RAVER* (RL-RAVER), PGL4 Renilla Luciferase (PGL4-RL) (#TM259, Promega), PGL3 Firefly (PGL3-FF) and Psicheck-2 (#C8021, Promega, UK). The DH5-α strain is genetically modified to make it non-pathogenic and the plasmids all confer resistance to ampicillin.

For plasmid amplification, 20µl of *E. coli* suspension was streaked onto agar plates containing ampicillin to select for the transformed bacteria only. The plates were incubated at 37°C for approximately 16hours, following which colonies were picked and inoculated into 10ml of nutrient broth (#70122, Sigma Aldrich, UK) with 0.1% v/v ampicillin. Cultures were incubated in a shaking incubator at 37°C overnight. Following the incubation, the *E. coli* were pelleted by centrifugation at 300rpm for 5 minutes. The plasmid DNA was extracted using the PureYield Plasmid Miniprep system (#A1223, Promega, USA). Briefly, the E. coli pellet was resuspended in 600µl of RNase free water and 100µl of Cell Lysis Buffer and incubated at room temperature for two minutes. 350µl of ice-cold Neutralisation Solution was added to stop the reaction prior to centrifuging the samples at 14,000xg for 3 minutes at room temperature (all subsequent centrifugation steps were carried out at 14,000xg at room temperature unless otherwise stated). The supernatant was transferred to a PureYield Minicolumn and centrifuged for 15 seconds, followed by the addition of 200µl of Endotoxin removal wash and a further 15 second centrifugation step. 400µl of column wash solution was added and the tube centrifuged for 30 seconds. The minicolumn was then transferred to a new collection tube and 30µl of nuclease free water was added to the

membrane. The column was incubated at room temperature for one minute and then centrifuged for 15 seconds to elute the plasmid DNA. The DNA was quantified using the NanoDrop 8000 and stored at -20°.

2.12 Restriction digest of psiCHECK-2 Plasmid

The psiCHECK-2 vector plasmid (#C8021, Promega, UK) was selected for use because it contains both Renilla and Firefly luciferase reporter genes to enable endogenous normalisation.

To enable the insertion of miRNA specific oligos into the psiCHECK-2 plasmid, 1µg of plasmid was digested using 1µl each of restriction endonucleases Xho1 (#R0146S, NEB, USA) and Pme1 (#R0560S, NEB, USA), 5µl of 10X CutSmart Buffer (#B7204S, NEB, USA) and RNase free water to a final volume of 50µl. Reactions were incubated at 37°C for two hours.

10µl of digested product mixed with 2µl of Gel Loading Dye (#B7024, NEB, USA) were visualised on a 1% agarose gel containing 0.003% Nancy-520 (#01494, Sigma-Aldrich, USA) electrophoresis at 120V for 30 minutes in 1X Tris-Acetic acid-EDTA (TAE) buffer (40 mM Tris-acetate/1 mM EDTA). Gels were visualised using the ChemiDoc MP Imaging System (#17001402, Bio-Rad, UK) and 10µl of a 1KB DNA standard (#G5711, Promega, USA) used to determine band sizes. Bands corresponding to the digested plasmid (appendix Figure 8.1) were excised and the plasmid DNA isolated using the Wizard SV Gel and PCR Clean-Up system (#A9281, Promega, USA). Briefly, excised bands were weighed and incubated in 1µl of Membrane binding solution per mg of gel at 55°C for 10 minutes. Following dissolution of the gel, the sample was transferred to a

Minicolumn and incubated for 1 minute and then centrifuged for 1 minute (all centrifuge steps were carried out at 16,000xg at room temperature). The column was washed once with 700µl of membrane was solution and centrifuged for 1 minute, and then washed with 500µl of membrane solution wash and centrifuged for 5 minutes. The minicolumn was transferred to a 1.5ml and 50µl of nuclease free water was added and incubated for 1 minute at room temperature. The tube was centrifuged for 1 minute to elute the DNA. DNA was quantified using the NanoDrop 8000 and stored at -20°C.

2.13 Design and Annealing of Oligos

Oligos were designed for miR-21, miR-100 and miR-101 based on the microRNA sequence obtained from the miRBase database (Griffiths-Jones, 2004). Perfect (complete match of the seed sequence) and bulged oligos (created by mis-matching 2 bases within the seed sequence) were designed and the restriction site sequences for Xho1 and PmeI were added to the 5' and 3' ends of the oligo, respectively (detailed in Table 2.2).

		Forward	Reverse
miR-100	Perfect	5'tcgagCACAAGTTCGGATCTACGGGTTgttt3'	5'aaacAACCCGTAGATCCGAACTTGTGc3'
	Bulged	5'tcgagCACAAGTTCGG**TG**CTACGGGTTggggCACAAGTTCGG**TG**CTACGGGTTgggggCACAAGTTCGG**TG**CTACGGGTTgttt 3'	5'aaacAACCCGTAG**CA**CCGAACTTGTGccccAACCCGTAG**CA**CCGAACTTGTGccccAACCCGTAG**CA**CCGAACTTGTGc 3'
miR-101	Perfect	5' tcgagTTCAGTTATC**AC**AGTACTGTAgttt 3'	5' aaacTACAGTACT**GT**GATAACTGAAc 3'
	Bulged	5'tcgagTTCAGTTATC**TG**AGTACTGTAggggTTCAGTTATC**TG**AGTACTGTAggggTTCAGTTATC**TG**AGTACTGTAgttt 3'	5'aaacTACAGTACT**CA**GATAACTGAAccccTACAGTACT**CA**GATAACTGAAccccTACAGTACT**CA**GATAACTGAAc 3'
miR-21	Perfect	5'tcgagTCAACATCAGTCTGATAAGCTAgttt3'	5'aaacTAGCTTATCAGACTGATGTTGAc3'
	Bulged	5'tcgagTCAACATCAGAAGATAAGCTAggggTCAACATCAGAAGATAAGCTAggggTCAACATCAGAAGATAAGCTAgttt3'	5'aaacTAGCTTATCTTCTGATGTTGAccccTAGCTTATCTTCTGATGTTGAccccTAGCTTATCTTCTGATGTTGAc3'

Table 2.2 A table showing the sequences of the oligos designed based on miR-21, -100, and -101.

Oligos were diluted to a concentration of 100µM using Multicore 10x buffer (#R999A, Promega, USA), oligos were further diluted to a final concentration of 10µM in nuclease free water. 25µl of each of the oligo pair (bulged or perfect) were combined and annealed by incubating at 95°C for 5 minutes and then allowed to cool to room temperature.

2.14 Ligating the oligos and Plasmid

For the ligation reaction 2µl T4 DNA ligase buffer (#B0202S, NEB, USA), 8µl 33ng digested plasmid (product of 2.12), 1µl Annealed miR-21 Oligos (product of 2.13), 1µl T4 DNA ligase (#M02020S, NEB, USA) and 8µl RNase free water were combined and incubated for 16 hours at 16°C. The enzyme was inactivated through incubation at 65°C for 10 minutes. The tubes were cooled on ice for 10 minutes then stored at -20°C. The resulting reporter has been named miR21-PsiCHECK-2.

2.15 Transforming of E. coli with ligated plasmids

To amplify the ligated plasmids, *E. coli* were transformed as follows: 1µl of each of the ligated plasmids was added to 50µl of DH5-α *E. coli* cells (#C2987H, NEB, USA). 50µl of *E. coli* only and a control plasmid (#N3041A, NEB, USA) were used as positive and negative controls for the transformation. *E. coli* were incubated on ice for 30 minutes and then heat shocked for 45 seconds at 42°C using a water bath. They were then rapidly returned to ice for two minutes, following which 1ml of nutrient broth was added and the *E. coli* were incubated at 37°C for one hour. Following the incubation, 200µl of the *E. coli* suspension was spread onto 0.01% w/v ampicillin agar plates. Plates were incubated for 16 hours at 37°C

Following the incubation, colonies were picked and inoculated into 5ml of nutrient broth containing 0.1% v/v ampicillin. Cultures were incubated overnight at 37°C in a shaking incubator to enable aeration. 800µl of the Incubated cultures were mixed with 300µl of 50% v/v glycerol in nuclease free water and stored at -80°C as a stock for future use. The remaining culture was centrifuged at 3000rpm for 5 minutes to pellet the *E. coli* and the plasmid DNA extracted as previously described in 2.11.

2.15.1 Sequencing of PsiCHECK-2 plasmid with miRNA oligo inserted DNA

To confirm the insertion of the annealed oligos, 10µl of plasmid DNA at a concentration of 100ng/µl was supplied to Source Bioscience along with a custom designed primer at 10nM concentration for Sanger sequencing. The resulting sequence histograms were analysed using FinchTV (GeoSpiza, 2016).

2.16 Plasmid transfections – Optimisation

To determine an optimal transfection technique, electroporation via the Neon System (#MPK5000, Invitrogen, UK) and lipid-mediated transfection using TransIT-2020 Transfection reagent (#MIR5400, Mirus, USA) and the TransIT-X2 Dynamic Delivery System (#MIR6000, Mirus, USA) were compared. For this optimisation, RL-RAVER and RL-VO plasmids at a ratio of 1:50 (firefly:renilla) were used.

2.16.1 Neon Transfection System

This system uses the Neon Pipette (#MPP100, Invitrogen, UK) and Pipette station (#MPS100, Invitrogen, UK) to electroporate cells to enable introduction of the plasmids. Briefly, PC3 cells were passaged (as described previously) 48 hours before electroporation. Prior to performing the electroporation, reagents were warmed to 37°C in a water bath. Trypsinised cells were washed in PBS and resuspended in DMEM media to give a concentration of 1.0 $x10^7$ cells/ml. The solution was pipetted up and down to obtain a single cells suspension. Two wells of a 24 well plate were prepared with 0.5ml of DMEM media with 10% FBS but no antibiotics.

The Neon Pipette Station was prepared by adding 3ml of Electrolytic Buffer to the Neon tube and slotting this into the station and the protocol set as 1250V, with pulse width of 30ms and a single pulse. To a 1.5ml tube 0.5µg of plasmid DNA was added followed by 1µl of Nuclease free water and then 7.5µl of the cell suspension (equivalent to 0.75 $x10^5$ cells per well). The mix was drawn up into a 10µl Neon pipette tip and fitted into the pipette station. The cells were pulsed and then ejected into the pre-prepared 24-well plate. Cells were incubated for 48 hours at 37°C, 5% CO_2 before assaying for luciferase expression.

2.16.2 TransIT-2020 Transfection reagent System and TransIT-X2 Dynamic Delivery System

For these lipid-mediated transfection systems, PC3 cells were seeded into a 24 well plate at $0.95x10^5$ cells/well with 0.5ml DMEM media per well. Cells were incubated overnight at 37°C, 5% CO_2.

Twenty-four hours later, TransIT-2020 and TransIT-X2 reagents were warmed to room temperature and vortexed to mix. OptiMEM reduced serum media (#31985062, Gibco, USA) was warmed to 37°C in a water bath. 0.5µg of plasmid DNA (equivalent to that used with the Neon electroporation protocol) was mixed with 50µl of OptiMEM and 1.5µl of the appropriate TransIT reagent. Reactions were incubated at room temperature for 20 minutes to enable a transfection complex to form and then added dropwise to the cells in the 24-well plate, the plate was rocked to distribute the complex and cells were incubated for 48 hours.

2.17 Renilla Luciferase expression assay

The transfected cells were assayed using the Dual-Luciferase Reporter Assay system (#E1910, Promega, USA). Cells were washed in 1X PBS, then lysed in 100µl of 1x Passive lysis buffer (#E1910, Promega, UK) and incubated at room temperature for 15 minutes with constant agitation. 25µl of Luciferase Assay substrate II was predispensed into 1.5ml Eppendorf tubes, lysed cells were pipetted to obtain a single cell suspension and 5µl of the suspension was mixed with the Luciferase Assay substrate II by pipetting. The GloMax 20/20 Luminometer (#E5311, Promega, USA) was set up using the Promega Dual Glo protocol and was used to measure the luminescence. After the first measurement (measuring firefly luminescence) 25µl of pre-prepared Stop &

Glo reagent was added to the tube and mixed by pipetting. The tube was returned to the machine and the second measurement taken (measuring Renilla luminescence). For the optimisation experiment only 2 replicates were used for each transfection type.

Renilla luciferase expression was normalised to the firefly luciferase values.

2.18 Transfections with miR21-PsiCHECK-2 reporter

The optimisation experiments indicated that the TransIT-X2 system was the best method for transfection and so this was used to transfect PC3 cells with miR21-psiCHECK-2 reporter. Cells were transfected with 0.5µg miR21-psiCHECK-2 following the protocol described in 2.16.2 using the undigested PsiCHECK-2 plasmid (amplification described in 2.11) as the control. The luciferase assay was conducted as described in 2.17 but only 1µl of lysed cells was added to the reaction due to the luminescence being above the detectable range when 5µl was used.

2.19 Investigation of the effect of adding EVs on renilla luciferase activity

For each cell type (PC3, LNCaP, C4-2, PNT1A and hOB) 3.5 x10^6 cells were seeded onto each of two 10cm^2 plates. EVs were collected following the protocol described in 2.3 from one 10cm^2 plate, whilst the other was used to collect total conditioned media. The conditioned media was concentrated using Pierce Protein Concentrator PES, 100K MWCO columns (#88532, Thermo Scientific, UK).

Both the isolated EVs and the concentrated conditioned media were quantified using the Qubit protein quantification protocol.

HOB cells were seeded and transfected with 0.5µg plasmid DNA as previously described with either the PsiCHECK-2 only plasmid as a vector only control or the miR21-psiCHECK-2 reporter. Five hours post-transfection, either EVs or concentrated media were added at 100ug of protein per well.

The luminescence was assayed as previously described 2.17.

This experiment was repeated with two biological replicates and each were assayed with two technical replicates.

2.20 Viability assay

When the cells were microscopically examined before being assayed using the Promega Dual Glo protocol, an increase in the number of detached cells in the wells treated with EVs, was observed, this indicated a potential reduction in viability. To investigate whether this was coincidental or a significant difference, an additional experiment was designed to compare the viability of cells which had been transfected and treated with EVs or elution buffer to those which had not been transfected and treated. Trypan Blue 0.4% solution (#15250061, Gibco, USA) was used to count only viable cells.

First, to determine the effect of the transfection complex alone, controls which were not transfected and which were treated with the transfection reagent but without DNA were compared to transfection with miR21-psiCHECK-2. The viability of cells treated with only the transfection complex was not found to be significantly different to the viability of cells which were not transfected so only the non-transfected cells were compared to the miR21-psiCHECK-2 transfected cells.

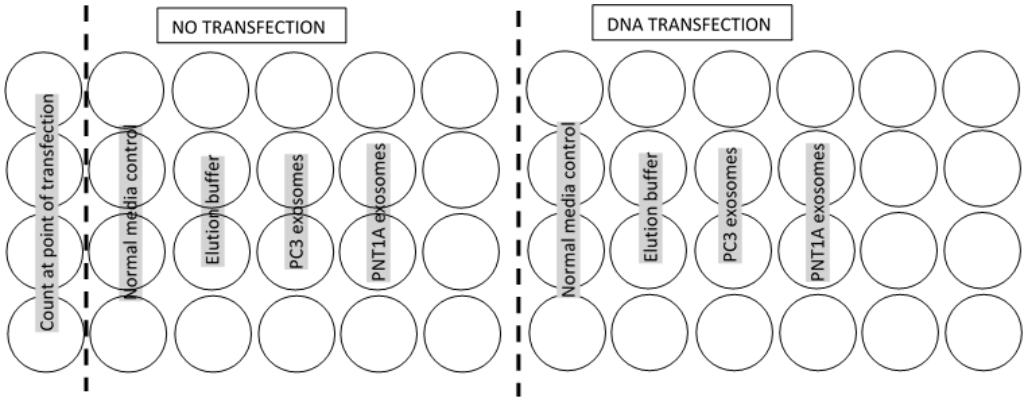


Figure 2.1 A plan showing the treatment of hOB cells in two 24-well plates for the viability repeat experiment.

Briefly, 0.95 x10^5 viable cells were seeded per well into two 24-well plates as shown in Figure 2.1. Cells were cultured overnight. Cells were either

transfected (as previously) with 0.5µg plasmid DNA containing the miR21-psiCHECK-2 reporter or treated with an equal volume of media. At this time cell counts were conducted on the first four wells (as described below) to give the number of viable cells at the time of transfection. Four hours later cells were treated with normal media, elution buffer, PC3 EVs or PNT1A EVs at 100ug of protein per well according to Figure 2.1. EV samples were diluted appropriately with nuclease free water so that the same volume was added to each well.

The next day the media was removed from the wells and they were rinsed with 1x PBS. Cells were trypsinised with 100µl of Trypsin EDTA then this was neutralised with 500µl of DMEM. The suspended cells were centrifuged at 1800rpm for four minutes. The supernatant was removed and the cells were resuspended in 0.5ml of PBS. In a new tube 100µl of suspended cells was mixed with the same volume of trypan blue. A cell count was conducted using the haemocytometer. Separate counts of viable and blue stained (dead) cells were kept so that percentage cell viability could be calculated. For each treatment group there were 4 biological replicates and 2 technical replicates from each biological replicate.

GraphPad Prism was used to create graphs of the data and perform statistical analysis. 2-way ANOVA analysis was used to look for differences in viability between transfection type and treatment type.

2.21 Preparation of samples for RNA sequencing and Bioinformatic analysis

EVs were isolated from PC3, PNT1A and hOB cells as previously described (2.3, 2.4). The protein concentration of these EVs was determined using the qubit protocol. Half of the remaining preparation was combined with 10ml of exosome depleted media, added to established hOB cells and incubated for 24hours. The RNA was extracted from both the EVs and the treated hOB cells (2.6) and RNA sequencing was performed by Barts Genome Centre (Queen Mary University, London) as follows. Samples were prepared using the Truseq RNA and small RNA libraries (#RS-122-2101 and #RS-200-0012, Illumina, USA) and sequenced using the NextSeq 500 (Illumina, USA) High Output Run (150 cycles) for three biological replicates.

2.22 Analysis of RNA sequencing data

The preparation of this sequencing data for analysis was conducted by Dr Tania Dottorini.

For each replicate the sequencing produced four data sets because the sample was split across four lanes for sequencing. Each data set contained the forward and reverse sequences and these had to be separately concatenated with the other 3 sequences from each replicate. This generated a complete forward and reverse sequence for each replicate.

The analysis pipeline was different for this set of RNAseq data due to there being three replicates compared to the two in the previous experiment (2.7) and because more up to date software became available after the first analysis was conducted. Skewer (Jiang *et al.*, 2014) was used to remove the sections of

sequence associated with the primers required for sequencing. Kallisto (Bray *et al.*, 2016) quantified the abundances of transcripts using pseudoalignment with targets and Sleuth (Pimentel *et al.*, 2017) was used to compare the enrichment of transcripts between treatment groups. Strict selection criteria were used so that only transcripts with a q-value of 0.01 or less were included in the output.

Three data sets showing comparative expression of transcripts were produced using sleuth;

- hOB cells treated with PNT1A EVs (HP) (Control) vs hOB cells treated with PC3 EVs (HP3) (treated)
- hOB cells only (H) (control) vs hOB cells treated with PNT1A EVs (HP) (treated)
- hOB cells only (H) (control) vs hOB cells treated with PC3 EVs (HP3) (treated)

The output from Sleuth was converted to an excel file to enable the author to filter the results. They were then ordered based on their $\log_2$ fold change and any with fold change between -2 and 2 were removed. Each of the three data sets was then subdivided into up- or downregulated of the transcripts of the treated group.

NIPA functional analysis was then conducted to determine whether the identified genes showed enrichment within KEGG pathways (Kanehisa *et al.*, 2016). This was done using version 0.6.3 of a script written by Professor Richard Emes. A P-value cut off of 0.05 was used to ensure only significant results were generated.

3 Chapter 3: Investigation of miRNAs contained within and transferred to recipient cells by Prostate cancer vesicles

3.1 Introduction

The current literature suggests that extracellular miRNAs may play an important part in the formation of the pre-metastatic niche and the progression of prostate cancer through their transportation to other cells by cancer vesicles (Hessvik *et al.*, 2012, Melo *et al.*, 2014, Takahashi *et al.*, 2017). This has led to the formation of the following hypotheses:

- MiRNAs can be isolated from extracellular vesicles
- MiRNAs can be transferred between cells

3.2 Results

3.2.1 Characterisation of EVs

We intended to investigate the role of miRNAs contained within vesicle preparations that correspond to the size of exosomes and are enriched for markers concordant with exosome biogenesis. However, although isolated using a propriety exosome isolation kit (#76064, Qiagen, Germany), it is unlikely that other vesicles were not also present in the resultant preparations. This is currently a caveat of all small-vesicle studies due to the absence of vesicle-type specific markers. Western blot analysis was used to determine whether EVs of endosomal origin are enriched in these preparations through the detection of marker proteins related to their biogenesis. Brownian motion analysis was also used to confirm that the isolated vesicles were within the expected range of diameter for EVs.

3.2.1.1 Western Blotting analysis

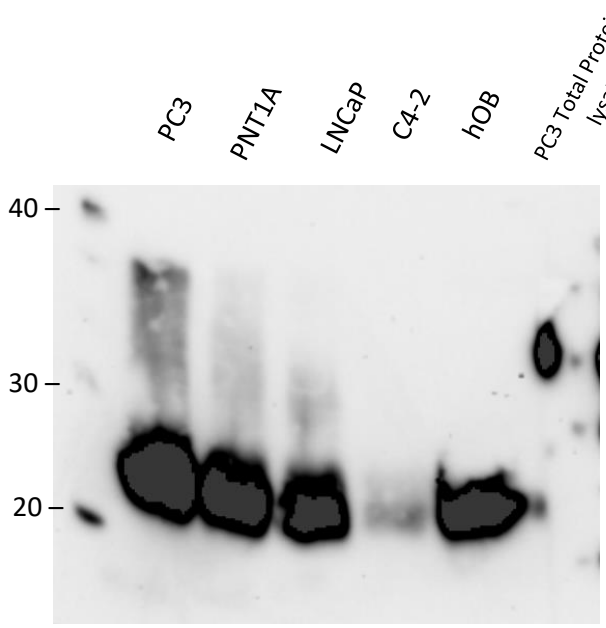


Figure 3.1. Characterisation of vesicle preparations by determining the expression of membrane proteins. The presence of transmembrane protein CD9 was determined by Western blot in vesicles isolated from prostate cancer cell lines PC3, LNCaP, and C4-2, and non-cancer cell lines PNT1A and hOB. A comparison to total protein lysates prepared from prostate cancer PC3 cells was used as a non-vesicle control. Representative of 2 replicates.

The expression of cell surface protein CD9 was analysed by western blot and was shown to be present in the vesicle preparations from all the cell lines, although only a low level was seen in the C4-2 sample (Figure 3.1). Whilst CD9 is expressed on the surface of cells, it is enriched in the membrane of EVs. Therefore, the lack of detectable CD9 in the PC3 total protein lysate lane (of equivalent protein concentration) demonstrates the enrichment of this marker in the vesicle fractions, concordant with the enrichment of EVs in these preparations. In addition to CD9, although not considered to be exclusive to EVs we determined the presence of other vesicle membrane proteins EpCAM, Annexin, CD54 and flotillin (Figure 3.2), heat shock protein HSP70, and as a negative control the presence of golgi protein GM130 (Figure 3.3).

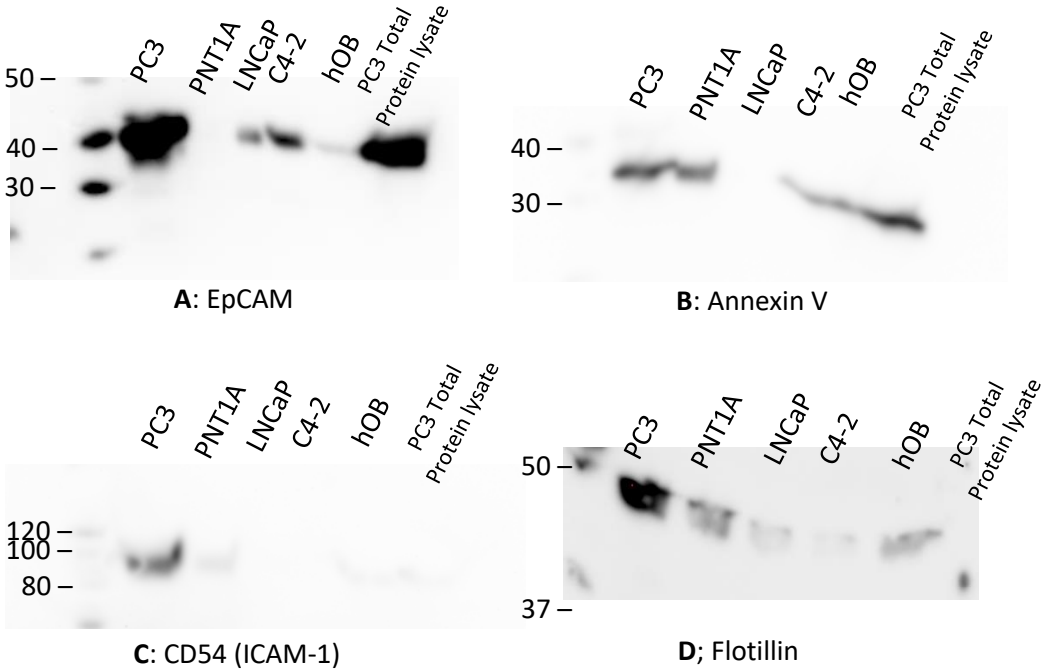


Figure 3.2 Characterisation of vesicle preparations by determining the expression of membrane proteins. The expression of proteins EpCAM (A), Annexin V (B), CD54 (C) and Flotillin (D) were determined by Western blot in vesicles isolated from prostate cancer cell lines PC3, LNCaP, and C4-2, and non-cancer cell lines PNT1A and hOB. A comparison to total protein lysates prepared from prostate cancer PC3 cells was used as a non-vesicle control. Representative of 2 replicates.

Expression of EpCAM (Figure 3.2A) was detected in all EV preparations except those isolated from PNT1A, and expression was lower in the EV fraction isolated from hOB cells when compared to the prostate cancer cell lines. As EpCAM is upregulated in cells undergoing increased proliferation (Went *et al.*, 2004), the high level of expression in vesicles isolated from prostate cancer cells is as expected when compared to slower growing stromal cells. The lower expression in hOB EVs may also relate to the non-epithelial origin of the cell lines, as in healthy tissues EpCAM expression is limited to epithelial cells (Trzpis *et al.*, 2007).

Annexin V is important during the biogenesis of EVs (Théry *et al.*, 2002) and represents the translocation of phosphatidylserine to the outer membrane.

Annexin V is not uniquely a marker of EVs and can be found on other vesicle types including apoptotic bodies. As with the other markers used in this analysis, their relevance to EVs has been determined using non-neoplastic cell types (Futter and White, 2007, Théry *et al*., 2002). Annexin V was found in all EV preparations, with the exception of LNCaP, as well as the total cell lysate control (Figure 3.2B). It is unclear why LNCaP EV preparations would not possess Annexin V, but as the same preparation contains CD9 (an established marker of EVs) this sample was likely to still be enriched in EVs.

HSP70 was not detected in any of the EV preparations from any of the cell types assessed. This is understandable considering expression has been observed to decrease in prostate cancer cells (Uhlen *et al.*, 2017) and is not thought to be highly expressed in non-antigen presenting cells which do not interact with MHC I and II (Schorey and Bhatnagar, 2008). Therefore, the lack of expression in hOB and PNT1A cells is not surprising. However, at the current time we cannot rule out the lack of detection was not a result of the antibody used.

CD54 is a commonly found protein on EVs from haematopoietic cells (Zhang and Grizzle, 2014) and is expressed on a range of epithelial cell types (NCBI, 2017). CD54 was detected in the EVs isolated from the PC3 cell line, as well as PNT1A and hOB (Figure 3.2C), albeit the level was lower in these latter two cell lines. Rokhlin and Cohen (1996) reported that PC3 cells release soluble CD54, but LNCaP cells do not. Cell-specific mechanisms of CD54 release could account for the different expression between the EVs isolated from these cell types. Since it is a subline of LNCaP, C4-2 is likely to show the same expression pattern.

Flotillin was detected in the EVs preparations (Figure 3.2D) from all the cell types (though weakly in C4-2 EVs) which reflects its vital role in membrane fusion, which enables EV formation.

Finally, as a negative control we tested for the expression of golgi apparatus protein GM130 (Uhlen *et al.*, 2017). GM130 expression was not detected in any of the EV preparations, confirming the lack of total cell lysate contamination (Figure 3.3).



Figure 3.3 Characterisation of vesicle preparations by determining the expression of membrane proteins. The expression of golgi apparatus protein GM130 was determined by Western blot in vesicles isolated from prostate cancer cell lines PC3, LNCaP, and C4-2, and non-cancer cell lines PNT1A and hOB. A comparison to total protein lysates prepared from prostate cancer PC3 cells was used as a non-vesicle control. Representative

3.2.1.2 Brownian motion analysis

EVs were characterised by electrophoresis and Brownian motion analysis using laser scattering microscopy (ZetaView, ParticleMetrix) (Figure 3.4). These data demonstrate the range of vesicle sizes detected and the particles per ml detected. The predominant vesicle population in our preparations is >100nm, suggesting we are purifying a mixed vesicle population. However, the size range of exosomes, and other vesicles, can be variable and dependent upon the cell types and other stimuli. We are yet to fully understand how culture conditions influences vesicle characteristics.

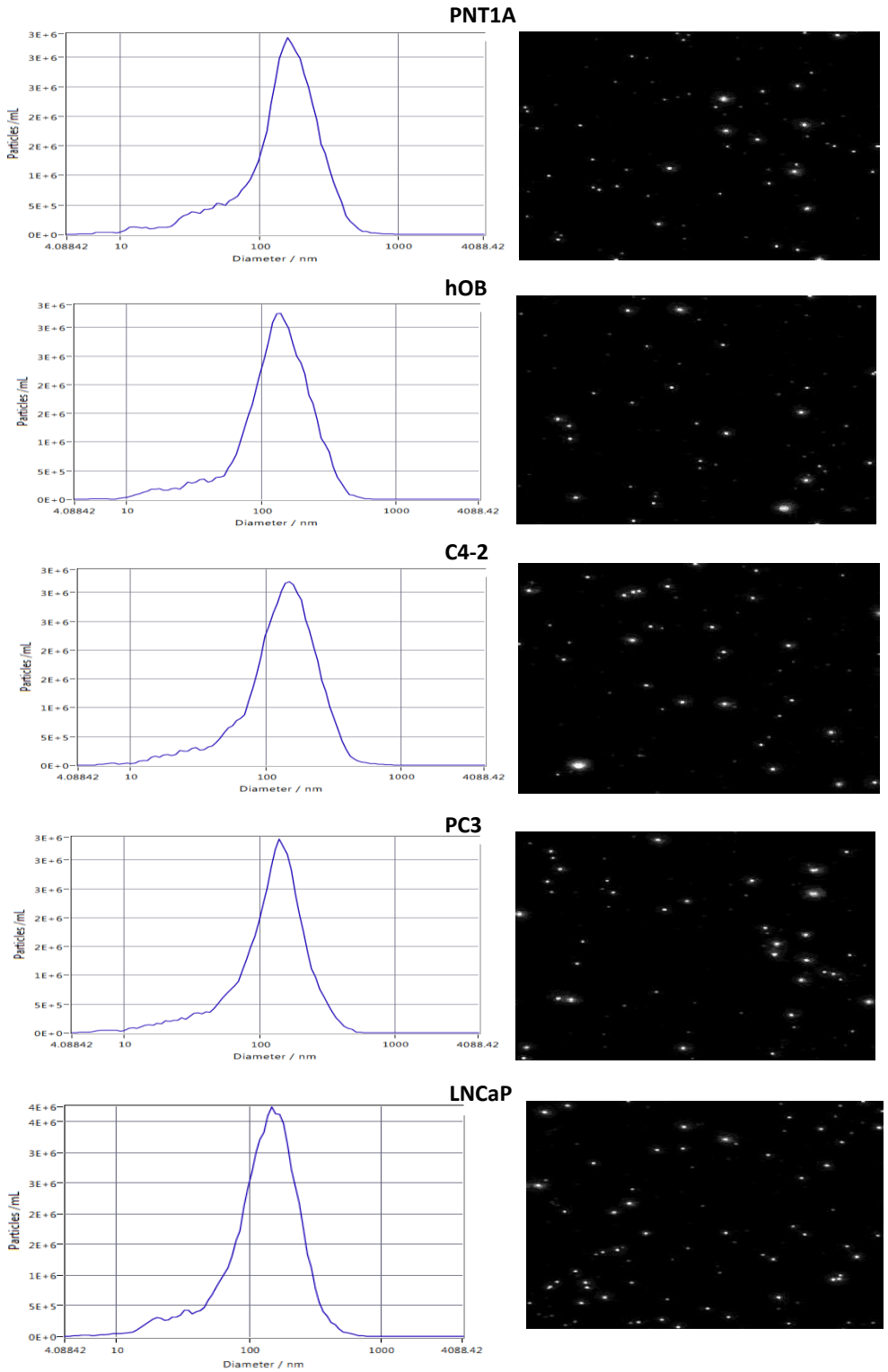


Figure 3.4 Electrophoresis and Brownian motion video analysis combined with laser scattering microscopy were used to determine the average concentration of EV particles isolated per assay setup and the average size (peak) compared between cell lines. Example traces and still frames of the video tracking analysis conducted per cell line are shown. N=3

ns = not significant, *** P<0.0001 (One-way ANOVA and Holm-Sidak correction)

3.2.1 RNAseq analysis of microRNAs transferred via prostate cancer vesicles to osteoblasts

To determine if miRNAs can be transferred from prostate cancer vesicles to osteoblasts we identified miRNAs found within EVs prepared from PC3 cells. Using an RNA tracking technique, based on labelling prostate cancer cell RNA with 5EU label, we determined if prostate cancer cell derived RNAs could be detected in osteoblasts treated with prostate cancer vesicles.

Analysis of the 5EU-labelled RNAs originating from PC3 prostate cancer cells, determined 16 miRNAs were detected in the osteoblasts treated with 5-EU labelled PC3 vesicles. When compared with the miRNAs present in PC3 vesicles, 13 of the 16 miRNAs were detected (3.3% of the miRNA EV cargo) between the isolated 5EU-RNA and PC3 EV populations Figure 3.5.

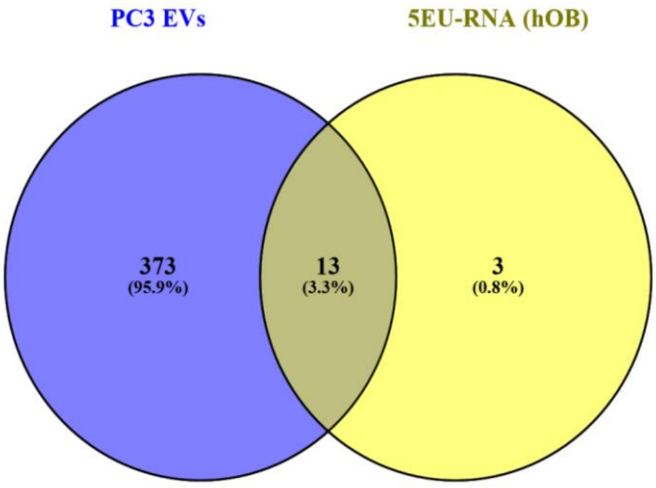


Figure 3.5 Comparison of the miRNAs detected in extracellular vesicles (EVs) isolated from PC3 cells and those detectable in recipient hOB cells following transfer from EVs. Venn diagrams created using Venny 2.1.0 (Oliveros, 2007-2015)

Three miRNAs were significantly enriched (see Table 3.1) in the 5EU-isolation but not detectable in the PC3 EVs indicating a background level of false-positive enrichment at 18.75% of the captured RNA population or equivalent to 0.8% of the EV RNA cargo population. The 13 in common miRNAs are detailed in Table 3.1.

MiRNAs significantly enriched uniquely in hOB cells		**miRNAs significantly enriched in the 5EU-labelled RNA population and also present in PC3 EVs**	
miRNA	**P-value**	**miRNA**	**P-value**
hsa-miR-1-3p	$2.33x10^{-26}$	hsa-let-7f-5p	0.46497
hsa-miR-199a-3p	$4.36x10^{-39}$	hsa-let-7g-5p	0.835838
hsa-miR-199b-3p	$5.13x10^{-39}$	hsa-miR-100-5p	0.000606
		hsa-miR-101-3p	$7.36x10^{-5}$
		hsa-miR-182-5p	0.00451
		hsa-miR-191-5p	$5.97\ x10^{-5}$
		hsa-miR-21-5p	$2.12\ x10^{-6}$
		hsa-miR-23a-3p	$2.59\ x10^{-5}$
		hsa-miR-3135b	$1.48\ x10^{-9}$
		hsa-miR-3182	$2.42\ x10^{-6}$
		hsa-miR-4448	$1.02\ x10^{-6}$
		hsa-miR-4791	0.003987
		hsa-miR-542-3p	0.853179

Table 3.1 A summary of miRNAs detected in the 5EU-labelled RNA population isolated from hOB cells treated with PC3 EVs.

FunRich (Pathan *et al.*, 2017) was used to look at the genes targeted by these 13 transferred miRNAs and to investigate their potential functions. FunRich uses the HPRD (Keshava Prasad *et al*., 2009), Entrez gene (Maglott *et al*., 2005) and UniProt (UniProt Consortium, 2010) gene ontology databases. Using the 'find targets' function generated 1900 potential gene targets. The cellular component, which describes the location of action of gene products, indicated that most of the products of genes targeted were found in the nucleus and cytoplasm (Figure 3.6). Although the P-value for this was not significant this analysis also showed that 24.59% of gene products were localised to the plasma membrane.

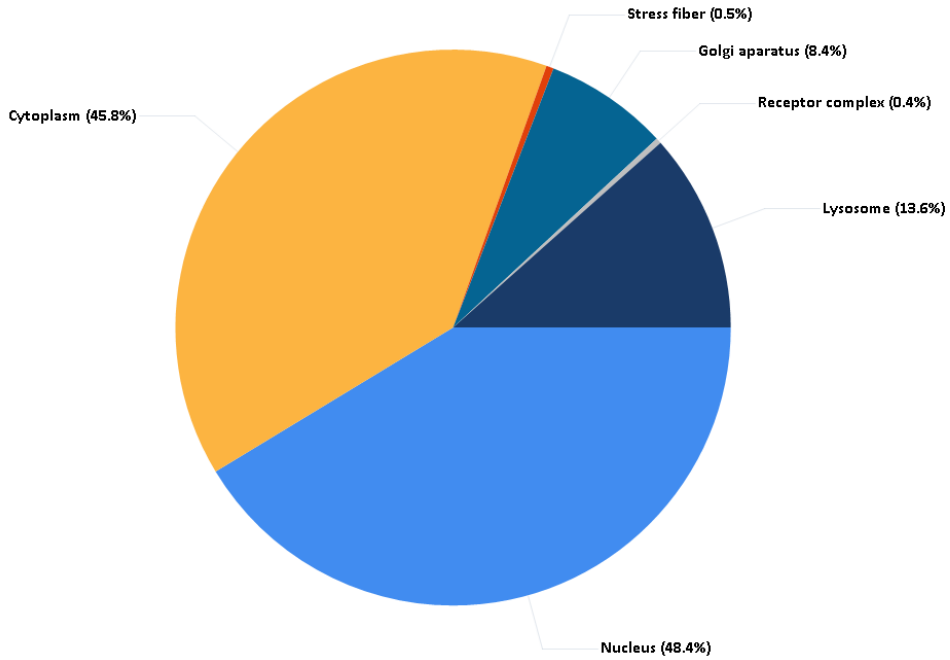


Figure 3.6 A pie chart showing the cellular component of the genes targeted by the 13 transferred miRNAs (Table 3.1). This shows the 7 areas where the genes are predicted to most commonly act; nucleus (P= 8.89x10-10), cytoplasm (P= 2.69x10-6), Golgi apparatus (P= 0.058), stress fibres (P= 0.088), receptor complex (P= 0.370 and Lysosomes (P=0.668). The percentages indicate the percentage of genes which are found to act at this location.

The molecular functions of the target genes were also analysed using FunRich; (Figure 3.8). The genes were found to most commonly affect transcription,

translation, protein synthesis, energy metabolism and cell signalling.

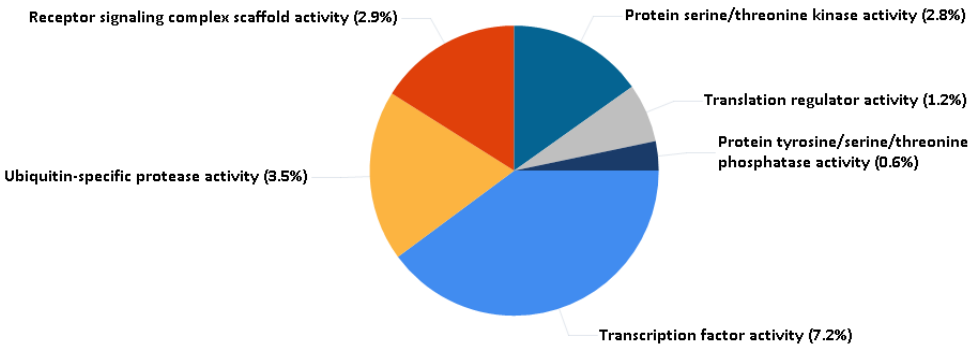


Figure 3.8. A pie chart showing the molecular functions targeted by the genes targeted by the 13 5EU labelled, transferred miRNAs (Table 3.1). The percentages indicate the percentage of genes associated with this function. The most commonly affected functions are; Transcription factor activity ($P=1.09x10^{-7}$), Ubiquitin-specific protease activity ($P=3.36x10^{-5}$), Translation regulator activity ($P=4.74x10^{-4}$), Protein serine/threonine kinase activity ($P= 2.12x10^{-4}$) and Receptor signalling complex scaffold activity ($P= 1.84x10^{-4}$).

Analysis of the biological processes (Figure 3.7) demonstrates an enrichment of targets involved in the transport and regulation of nucleic acid metabolism, a finding which supports the potential for transferred miRNAs to impact upon gene regulation by modifying nucleic acid availability. In addition to nucleic acid metabolism, signal transduction and cell communication are also highlighted as being enriched for target genes (Figure 3.7). Together these data support the contribution of EV miRNAs in potentially regulating the gene expression

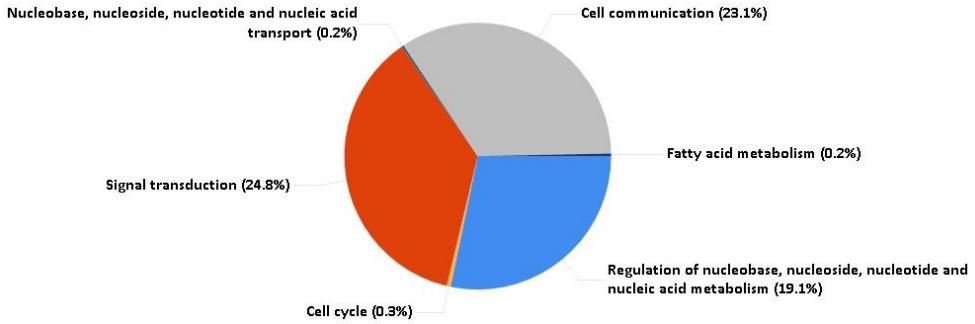


Figure 3.7 A pie chart showing the biological processes associated with the genes targeted by the 13 transferred miRNAs (Table 3.1). The 6 most commonly associated processes are; Regulation of nucleobase, nucleoside, nucleotide and nucleic acid metabolism ($P= 8.46x10^{-6}$), Signal transduction ($P= 4.04x10^{-4}$), Cell communication ($P= 0.0021$), Cell cycle ($P= 0.0201$), Nucleobase, nucleoside, nucleotide and nucleic acid transport ($P= 0.272$) and Fatty acid metabolism ($P= 0.0276$). The percentages indicate the percentage of genes associated with this function.

and cellular communication of recipient osteoblasts (hOB).

This data was compared with miRNAs previously reported to be upregulated in metastatic or localised prostate cancer compared to normal tissues by Bryant *et al.* (2012) and Watahiki *et al.* (2011). Very few miRNAs were found to be in common across these studies (Figure 3.9).

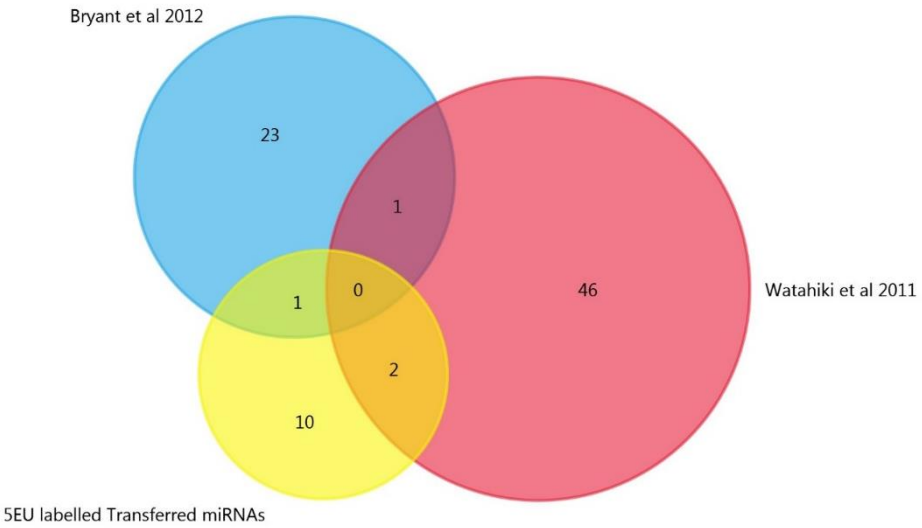


Figure 3.9 A Venn diagram showing the interaction between the miRNAs identified through our experiment and those previously cited in literature. (Bryant *et al.*, 2012, Watahiki *et al.*, 2011). Generated using FunRich.

However, when the gene targets of these miRNAs were investigated and similarly compared (Figure 3.10), 5.36% of the genes were common to all three studies. Further to this, 86.68% of the genes targeted by the 5EU labelled transferred miRNAs were also targets of at least one miRNA cited in the other

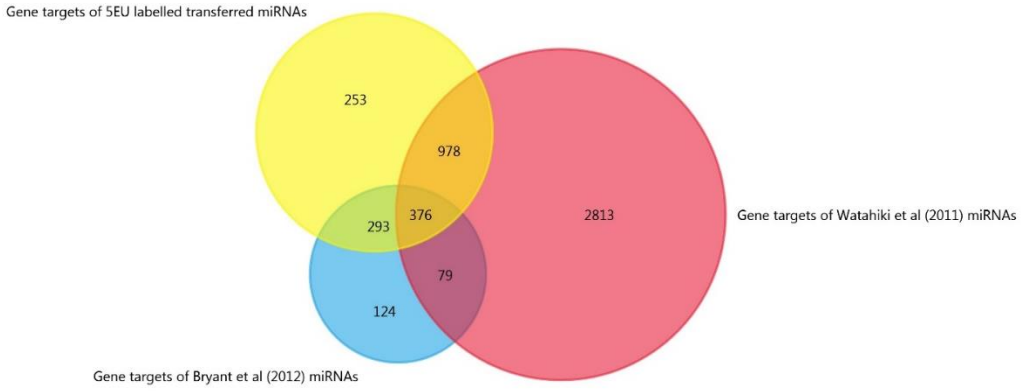


Figure 3.10 A Venn diagram showing a comparison of the genes targeted by the miRNAs identified as being associated with prostate cancer.

studies.

Investigation of the molecular functions of the genes associated with the miRNAs from the cited studies shows similarities between commonly affected functions (Figure 3.11). For all gene sets transcription factor activity was the most commonly enriched function with around 7% of genes from each set affecting this function (5EU- transferred miRNAs 7.2%, P= 1.09×10^{-7}. (Bryant et al., 2012) 7.6%, P= 6.25×10^{-5}. (Watahiki et al., 2011) 7.2%, P= 2.15×10^{-15}). Ubiquitin-specific protease activity (USPA) and Protein serine/threonine kinase activity (PSTKA) were commonly affected by both the 5EU -transferred miRNAs (USPA: 3.5%, P=3.36×10^{-5}. PSTKA: 2.8%, P= 0.00021) and the miRNAs identified by (Watahiki et al., 2011) (USPA: 3.3%, P= 6.24×10^{-9}. PSTKA: 2.6%, P= 3.43×10^{-7}). Receptor signalling complex scaffold activity was a function affected by both 5EU- transferred miRNAs (2.9%, P= 0.00018) and (Bryant et al., 2012)'s miRNAs (3.5%, P=0.070). Further to these similarities, when the top 20 most affected molecular functions from each miRNA set was compared 70% of functions affected by the 5EU- transferred miRNAs were also affected by at least one other data set.

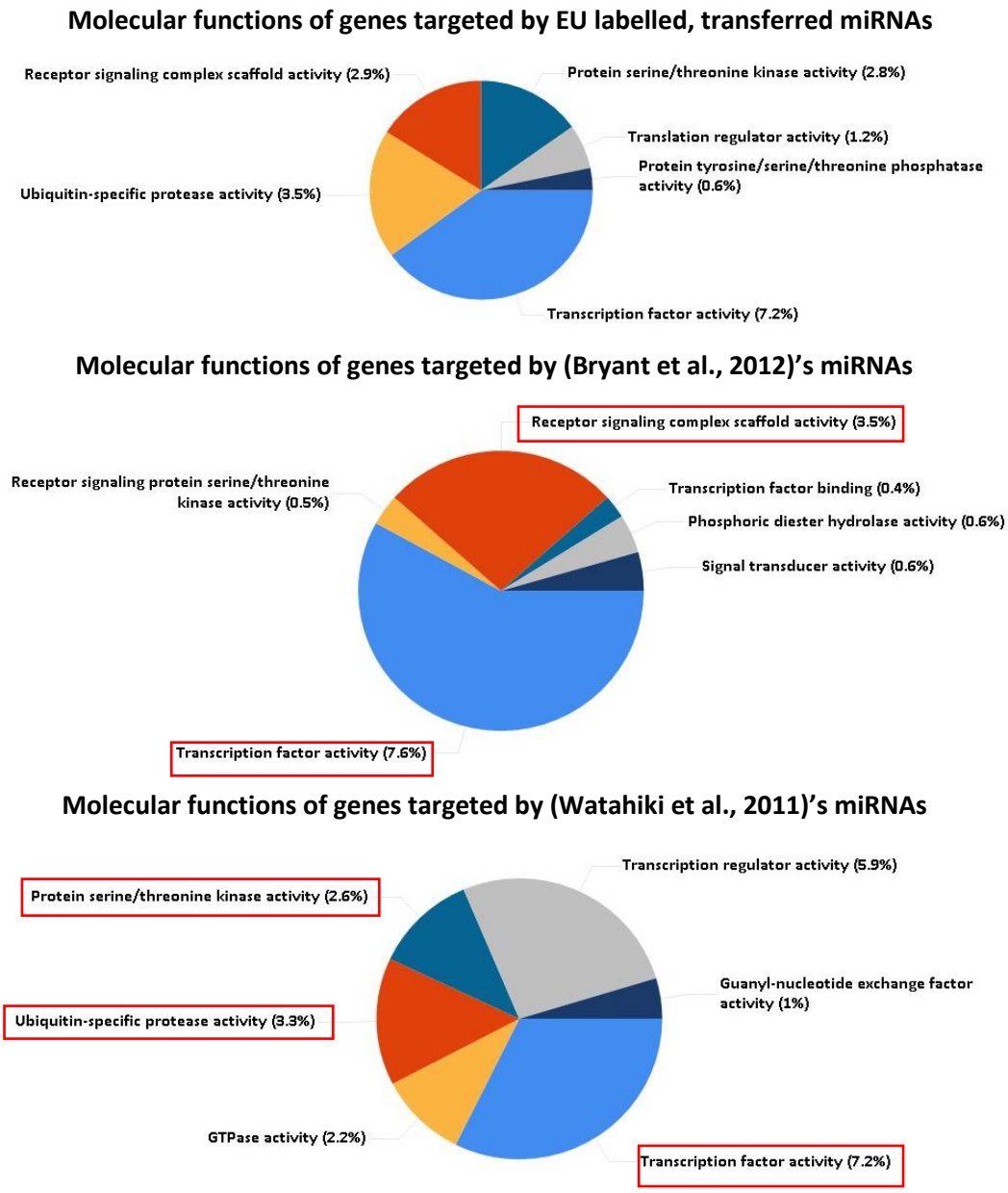


Figure 3.11 A figure showing the comparison of the molecular functions between the results from this study and the cited studies. The red outline highlights those functions which are the same as those most common in the 5EU labelled pie.

3.2.2 Comparison of miRNA expression in cells and EVs

Based on the results of the RNAseq analysis of miRNAs transferred from prostate cancer cells to osteoblast via vesicles, we undertook to characterise the expression of a subset of these miRNAs in other prostate cancer cell lines and the EVs they produce. We selected to look at the expression of miR-21, mir-100, miR-4448 and miR-101 by quantitative PCR in both the cells and the resulting EVs from prostate cancer cell lines PC3, LNCaP, C4-2 and non-cancer prostate epithelial cell line PNT1A.

Ct values greater than or equal to 35 meant that this analysis was not possible for miR-223 and miR-3182 and these were subsequently removed from the

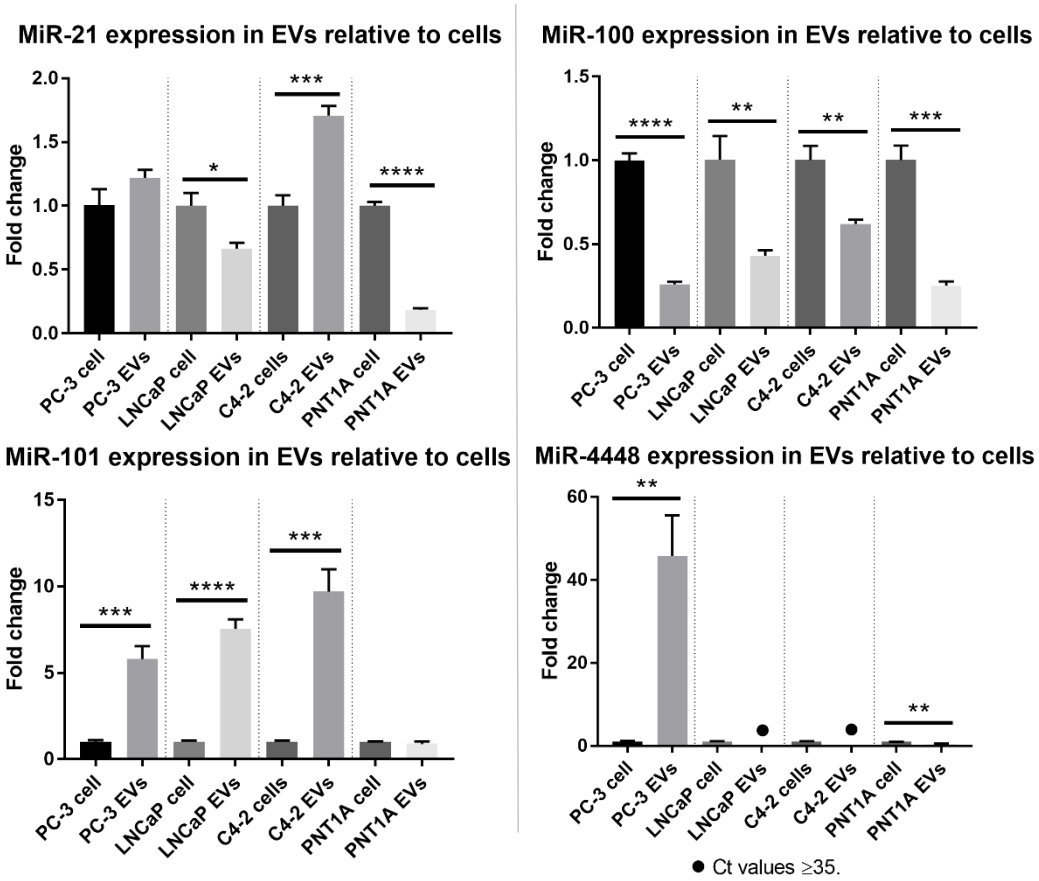


Figure 3.12 Graphs showing the difference in expression of miRNAs miR-21, miR-100, miR-4448 and miR-101 between cells and EVs. Bars indicate which values were compared through unpaired, non-parametric t-tests.

* P < 0.05 ** P < 0.005 *** P < 0.0005 **** P < 0.0001

N=3

analysis.

To investigate the selective packaging of miRNAs into EVs, their expression in cells and in EVs originating in the same cells type was compared (Figure 3.12).

Expression of miR-21 was found to be significantly different (LNCaP P=0.0055, C4-2 P= 0.0004 and PNT1A P<0.0001) between cells and EVs for all cell types except PC3. MiR-100 expression was found to be significantly decreased (PC3 P<0.0001, LNCaP P=0.0023, C4-2 P= 0.0017 and PNT1A P= 0.0001) in EVs compared to cells for all cell types. Expression of miR-101 was found to be significantly increased (PC3 P= 0.0004, LNCaP P< 0.0001 and C4-2 P= 0.0003) in EVs compared to their cells of origin for all cell types except PNT1A. MiR-4448 expression was significantly increased (P= 0.0014) in PC3 EVs compared to PC3 cells but was significantly decreased (P= 0.0040) in PNT1A EVs compared to PNT1A cells. The Ct values of ≥35 for LNCaP and C4-2 EVs make this analysis unreliable for these cell types. The expression of miRNAs varies depending of the cell type, the data supports the selective inclusion/enrichment of some miRNAs into EVs when compared to the overall abundance within the cell.

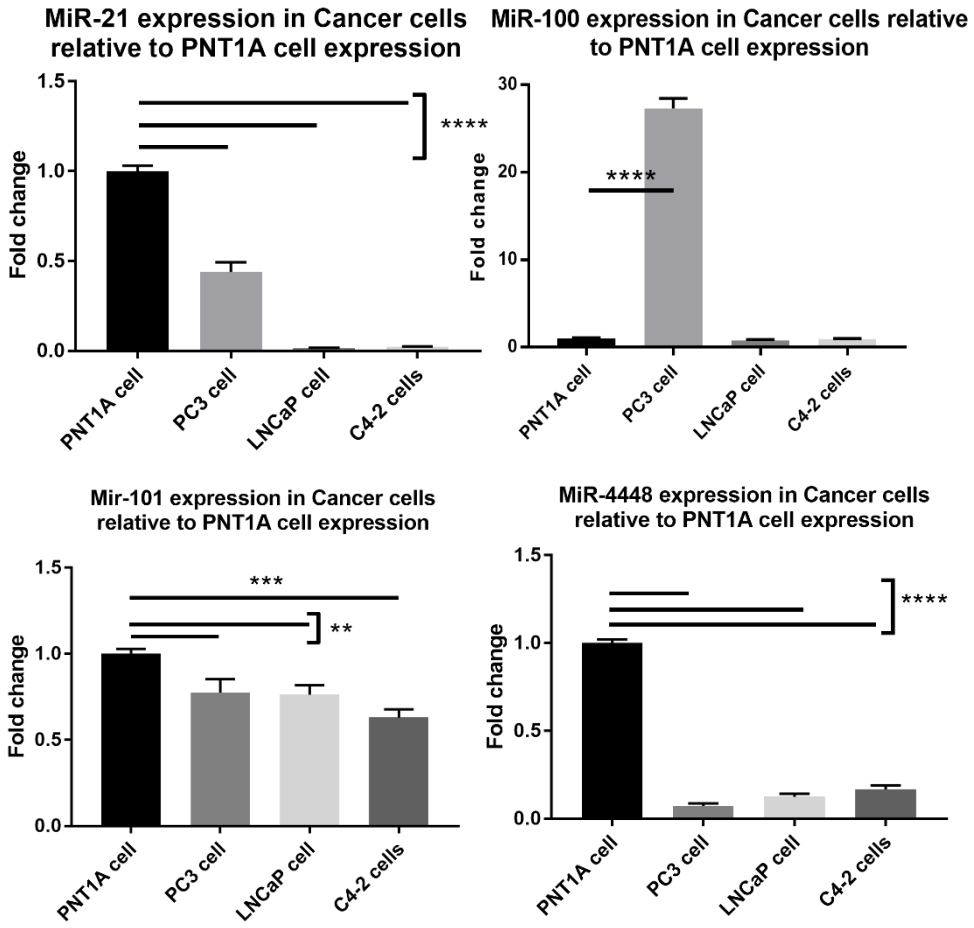


Figure 3.13 Showing the difference in expression of miRNAs (miR-21, miR-100, miR-101 and miR-4448) in cancer cells relative to the expression in PNT1A cells. Bars indicate which values were compared through unpaired, non-parametric t-tests.

* P < 0.05 ** P < 0.005 *** P < 0.0005 **** P < 0.0001

N=3

To investigate whether certain miRNAs are commonly upregulated in cancer cells, expression in PC3, LNCaP and C4-2 cells was compared to PNT1A cells (Figure 3.13). Expression of miR-21 was significantly lower ($P< 0.0001$ for all cell types) in all cancer cells in comparison to the PNT1A cell. MiR-100 expression was significantly increased ($P< 0.0001$) in PC3 cells but was not significantly different in LNCaP or C4-2 cells. MiR-101 expression was significantly decreased (PC3 $P= 0.0095$, LNCaP $P= 0.0029$ and C4-2 $P= 0.0003$) in all cell types. MiR-4448 expression was significantly decreased ($P< 0.0001$ for all cell types) in all cell types compared to PNT1A cells. MiR-100 expression in PC3 cells was the only instance in which the expression was higher in a cancer cell compared to the PNT1A cell. However, the previous analysis indicated that expression in EVs can be considerably different than cellular expression so the expression of miRNAs within EVs originating from cancer cells was compared to expression in PNT1A EVs.

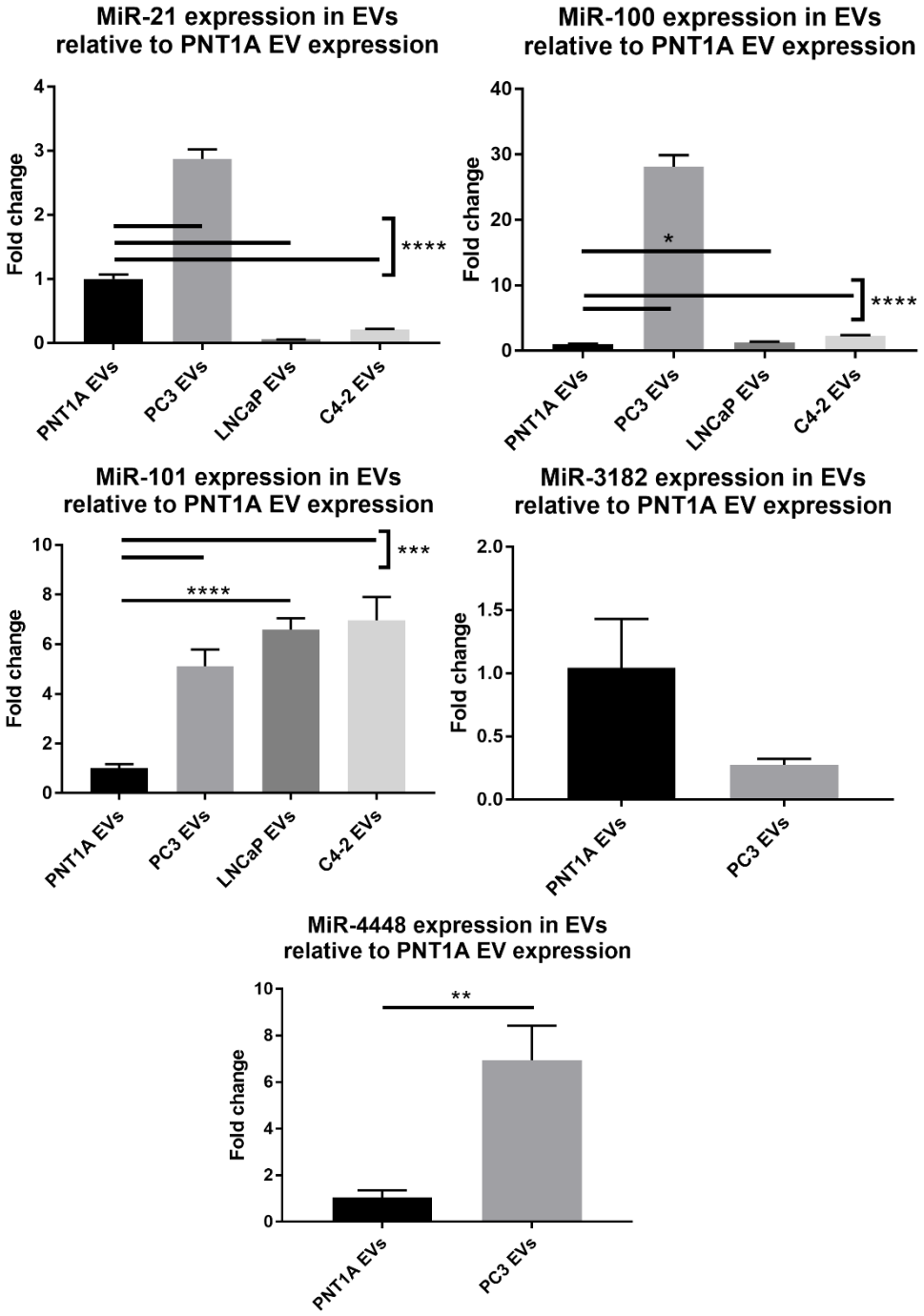


Figure 3.14 Showing the difference in expression of miRNAs (miR-21, miR-100, miR-101, miR-3182 and miR-4448) in cancer EVs relative to the expression in PNT1A EVs. Bars indicate which values were compared through unpaired, non-parametric t-tests. * P < 0.05 ** P < 0.005 *** P < 0.0005 **** P < 0.0001 ` N=3

The expression of miRNAs in cancer cell EVs was investigated, relative to the expression in PNT1A EVs (Figure 3.14)

Expression of miR-21, miR-100, miR-101 and miR-4448 was significantly increased (miR-21 and miR-100 $P< 0.0001$, miR-101 $P= 0.0005$ and miR-4448 $P=0.0025$) in PC3 EVs compared to the expression in PNT1A EVs. Expression of miR-21 was significantly decreased (LNCaP and C4-2 $P< 0.0001$) in LNCaP and C4-2 EVs compared to the PNT1A EVs. Expression of miR-100 and miR-101 in LNCaP and C4-2 EVs were significantly increased compared to the level in PNT1A EVs (miR-100: LNCaP $P= 0.0172$, C4-2 $P< 0.0001$. miR-101: LNCaP $P< 0.0001$, C4-2 $P= 0.0004$). Ct values were greater than or equal to 35 for the expression of miR-3182 and miR-4448 in LNCaP and C4-2 EVs. There was no significant difference in expression of miR-3182 between PC3 and PNT1A EVs. Despite expression being significantly lower in the cancer cells compared to the PNT1A cells (excluding miR-100 expression in PC3 cells), miR-21 and miR-4448 were both found to have higher expression in PC3 EVs compared to the PNT1A control and expression of miR-100 and miR-101 was significantly increased in all cancer EVs, consistent with the selective packaging or miRNAs into cancer vesicles.

3.2.3 Validation of the transfer of characterised miRNAs from prostate cancer cell to osteoblasts via vesicles.

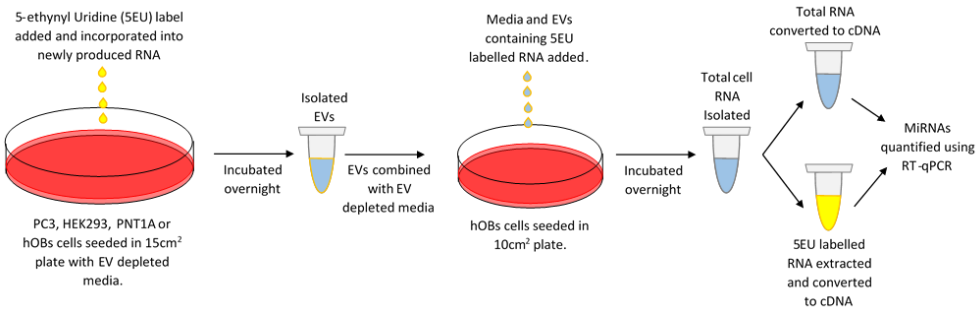


Figure 3.15 A figure to explain the stages of the experiment. For a more detailed description see materials and methods section 2.11.

In order to validate the RNA sequencing data, RNA labelling experiments were repeated and the transfer of miRNAs from prostate cancer cells to recipient osteoblasts was determined by qPCR. The addition of 5EU label to prostate cancer cells allows the identification of miRNAs produced in prostate cancer cells and then their subsequent transfer into osteoblasts via prostate cancer vesicles (Figure 6.15). PNT1A EVs were also investigated as a non-cancer prostate control and HEK EVs were included as a non-prostate comparison.

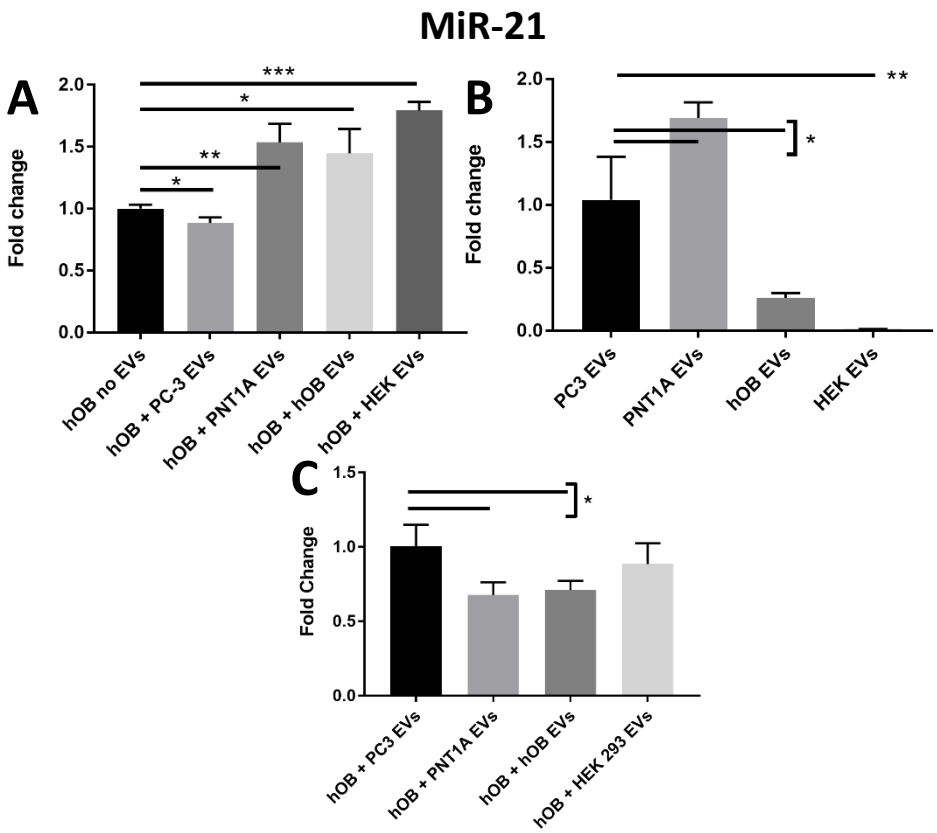


Figure 3.16 A: A graph showing the expression of total miR-21 in hOB cells treated with EVs relative to the expression in hOB cells not treated. B: A graph showing expression of miR-21 in PC3, PNT1A, hOB or HEK EVs relative to PC3 EV expression. C: A graph showing expression of 5EU-transferred miR-21 from hOB cells treated with different EVs. Bars indicate which values were compared through unpaired, non-parametric t-tests.

* $P < 0.05$, ** $P < 0.005$, *** $P < 0.0005$

N=3

Initially, we examined what happens to the total expression (endogenous osteoblast level plus any transferred miRNA for each miRNA of interest). When hOB cells were treated with PC3 EVs, it resulted in a modesty but statistically significant reduction in expression of total miR-21 (P= 0.0210) compared to hOB cells which were not treated (Figure 3.16 A). However, treatment of hOB cells with EVs from non-cancer cells (PNT1A, hOB and HEK) caused modest but statistically significant increases (PNT1A P= 0.0036, HEK P<0.0001 and hOB P= 0.0251) in the total expression of miR-21. The expression of miR-21 was significantly increased in the PNT1A EV sample (P=0.0364) but was significantly decreased in the hOB (P=0.0174) and HEK (P= 0.0066) EV samples compared to the PC3 EVs (Figure 3.16B). However, whether these differences would lead to functional changes is not certain given the low amplitude of the differences. Despite the lower level in the PC3 EVs, when we isolated and quantified only the 5-EU labelled miRNAs transferred into osteoblasts from the EVs, 5EU transferred miR-21 expression was subtly higher in osteoblasts following treatment with PC3 EVs than when osteoblasts were treated with the PNT1A EVs (P= 0.0264) (Figure 3.16C). Similarly, the expression of 5EU-transferred miR-21 was significantly decreased in osteoblasts treated with hOB EVs (P= 0.0297) but given the very low amounts of miR-21 in hOB EVs the data supports the theory that the efficiency of transfer differs depending on the origin of the vesicle. However, this requires further investigation to be conclusive.

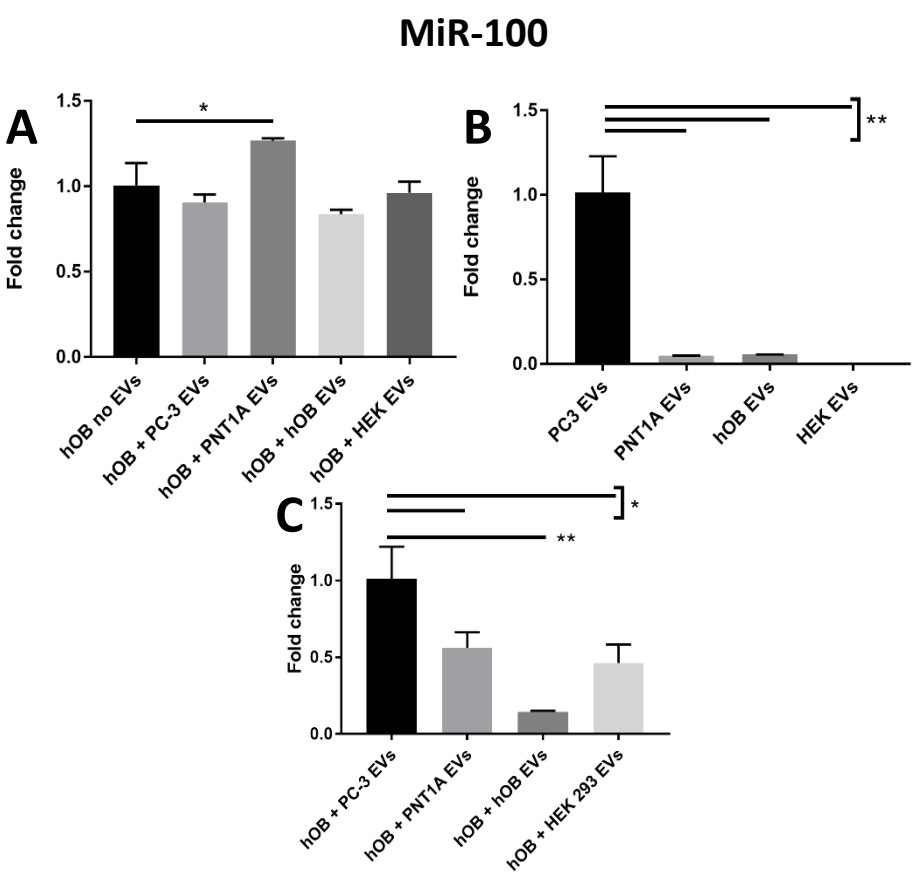


Figure 3.17 A: A graph showing the expression of total miR-100 in hOB cells treated with EVs relative to the expression in hOB cells not treated. B: A graph showing expression of miR-100 in PC3, PNT1A, hOB or HEK EVs relative to PC3 EV expression. C: A graph showing expression of 5EU-transferred miR-100 from hOB cells treated with different EVs. Bars indicate which values were compared through unpaired, non-parametric t-tests.

* $P < 0.05$, ** $P < 0.005$, *** $P < 0.0005$

N=3

The level of total miR-100 was found to be significantly slightly increased in hOB cells treated PNT1A EVs (Figure 3.17A) (P= 0.0257) but none of the other EV treatments cause a significant change in miR-100 level. The level of MiR-100 showed a statistically significant increased in PC3 EVs compared to all other EV types (PNT1A: P= 0.0014, hOB: P= 0.0014 and HEK: P= 0.0012)(Figure 3.17B) the fold change was only moderately different. Analysis of EU-transferred miR-100 (Figure 3.17C) showed similar levels as seen in the EVs as PC3 EVs transferred more miR-100 compared to all other EV types - this difference was

slight but statistically significant (PNT1A: P=0.0276, hOB: P= 0.0019 and HEK: P= 0.0164).

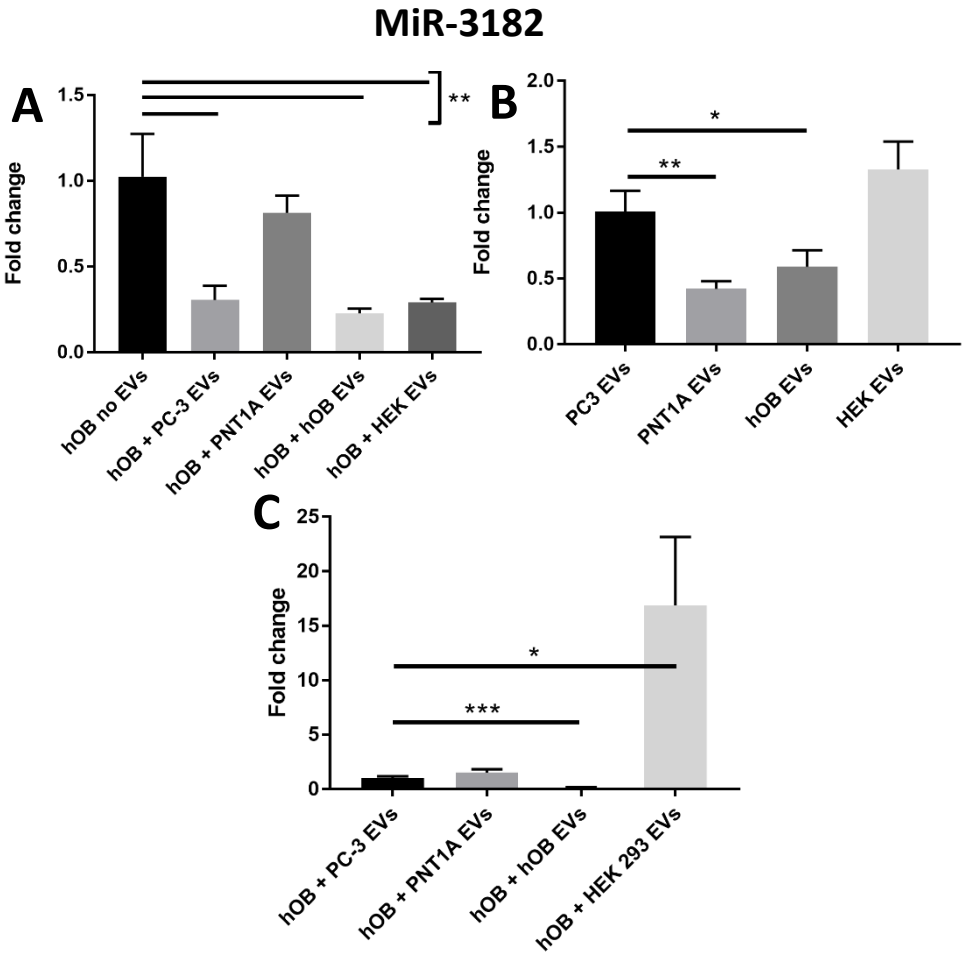


Figure 3.18. A: A graph showing the expression of total miR-3182 in hOB cells treated with EVs relative to the expression in hOB cells not treated. B: A graph showing expression of miR-3182 in PC3, PNT1A, hOB or HEK EVs relative to PC3 exosome expression. C: A graph showing expression of EU labelled, transferred miR-3182 from hOB cells treated with different EVs. Bars indicate which values were compared through unpaired, non-parametric t-tests.

* P < 0.05, ** P < 0.005, *** P < 0.0005

N=3

Total miR-3182 level was subtly but statistically significantly decreased in all cells treated with EVs (PC3: P= 0.0093, hOB: P= 0.0055 and HEK: P= 0.0073) except those treated with PNT1A EVs for which the difference was not significant (Figure 3.18A). MiR-3182 expression in PC3 EVs was significantly increased in comparison to PNT1A (P= 0.0037) and hOB (P= 0.0224) EVs (Figure 3.18B) however the fold change was minimal. There was no significant difference in expression between PC3 and HEK EVs but there was a statistically significant and marked (fold change >16) increase in the level of 5EU-transferred miR-3182 in cells treated with HEK EVs (P= 0.0119) compared to those treated with PC3 EVs (Figure 3.18C). Similarly to the pattern of vesicle levels 5EU-transferred miR-3182 was at a statistically significant but modestly lower level in cells treated with hOB EVs (P= 0.0007) compared to PC3 EVs (Figure 3.18C).

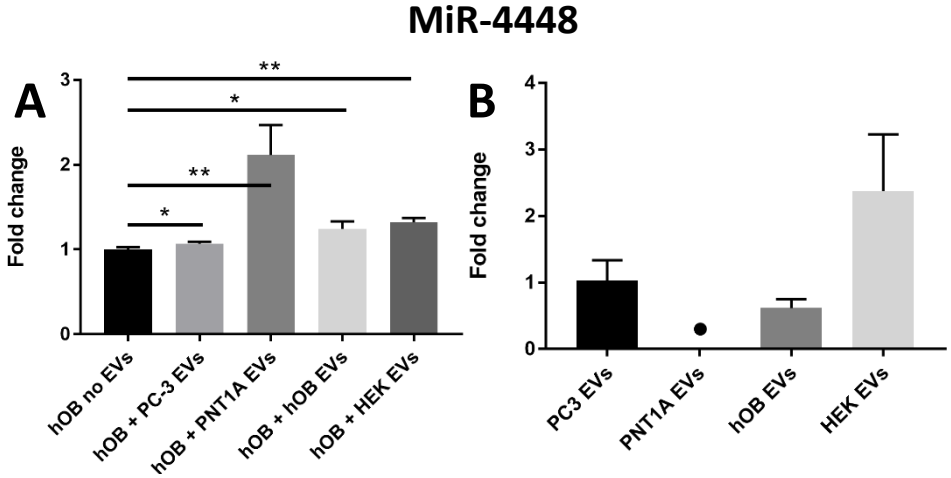


Figure 3.19 A: A graph showing the expression of total miR-4448 in hOB cells treated with EVs relative to the expression in hOB cells not treated. B: A graph showing expression of miR-4448 in PC3, PNT1A, hOB or HEK EVs relative to PC3 exosome expression. Bars indicate which values were compared through unpaired, non-parametric t-tests.
* $P < 0.05$, ** $P < 0.005$, *** $P < 0.0005$. ● Not detected under conditioned employed.
N=3

Total miR-4448 level was significantly increased in all cells treated with EVs (PC3: P= 0.0326, PNT1A: P= 0.0055, hOB: P=0.0105 and HEK: P= 0.0027. Figure 3.19A) however only cells treated with PNT1A cells had a greater than 2 fold change in the miR-4448 level. There were no significant differences in miR-4448 level between different EV types (Figure 3.19B). The levels of 5EU-transferred miR-4448 could not be detected under the conditions employed, which suggests very low transfer of this miRNA via EVs. The increase in total miR-4448 in all treated cells despite the low level of vesicle miR-4448 may indicate other factors contained within EVs are causing stimulation of endogenous miR-4448 production.

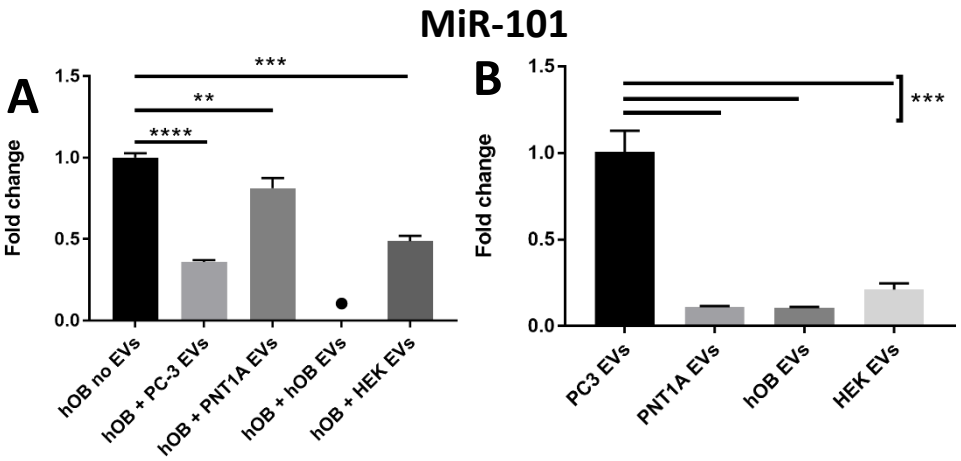


Figure 3.20 A: A graph showing the expression of total miR-101 in hOB cells treated with EVs relative to the expression in hOB cells not treated. B: A graph showing expression of miR-101 in PC3, PNT1A, hOB or HEK EVs relative to PC3 exosome expression. Bars indicate which values were compared through unpaired, non-parametric t-tests.

* $P < 0.05$, ** $P < 0.005$, *** $P < 0.0005$. ● Not detected under conditioned employed.

N=3

Total levels of miR-101 were significantly decreased in hOB cells treated with all EV types (PC3 and HEK $P<0.0001$ and PNT1A: $P= 0.0089$. Figure 3.20A) compared to the untreated cells. However, the fold change for this decrease was still minimal. The level of total miR-101 in cells treated with hOB EVs resulted in a Ct value ≥35. Both PNT1A and HEK EVs showed modest but statistically significant reductions in the level of miR-101 (PNT1A: $P= 0.0002$, HEK: $P=0.0004$) compared to PC3 EV expression (Figure 3.20B) despite the levels being subtly increased in the cells treated with these EVs. The levels of 5EU-transferred miR-101 were not detectable under the conditions employed suggesting a low level of transfer. This suggest that the increase in total miR-101 could be due to an endogenous mechanism of upregulation.

In designing this experiment we assumed that the vesicles from different cell types have similar properties, are produced from parent cells at the same rate and have similar delivery efficiency and therefore that the variation of miRNA expression in the parent cells would reflected the level transferred. This data demonstrates changes in the total osteoblast abundance of all the miRNAs investigated following treatment with vesicles. However, these changes in total abundance within the osteoblasts are not consistent with the levels of the same miRNAs present within or transferred from (5EU-transferred miRNAs) the parent cells. Therefore, indicating that other mechanisms of RNA regulation are contributing to the overall abundance of these miRNAs and their transfer from vesicles is just one factor. Despite the complexity of determining the contribution of vesicle-miRNAs to the overall abundance present in osteoblasts, the data does demonstrate differing efficiencies of miRNA transfer from vesicles that appears to be dependent on the cell origin of the vesicles, this is particularly evident for miR-21. The results from miR-21 showed increased expression of 5EU- transferred miR-21 from prostate cancer PC3 EVs relative to PNT1A EVs suggesting that PC3 EVs may be transferring this miRNA more efficiently into the recipient cells. This experiment did not consider differences in the vesicles other than their miRNA content and therefore varied membrane composition and vesicle size variation could account for this difference. The use of a synthetic miRNA would provide the opportunity to pre-load vesicles with a standardised amount of a specific miRNA, allowing the comparison of different vesicle characteristics (e.g. cell type of origin) in the transfer efficiency of that miRNA.

4 Chapter 4: Investigation of the effect of transferred miRNAs in recipient Osteoblasts

4.1 Introduction

The experiments detailed in Chapter 3 indicated that miRNAs can be isolated from EVs and that they can be transferred from these to other cell types. Though transfer into the cell has been demonstrated, it remains to be determined whether delivered miRNAs can alter gene expression in recipient cells. Therefore, we hypothesised treatment of osteoblasts with vesicles would enhance suppression of target genes when compared to untreated control cells.

To determine whether miRNAs are having a functional affect it is possible to investigate the genes that are targeted by these miRNAs. Luciferase reporter assays were designed to incorporate the 3'UTR of genes predicted to be targets of our miRNAs of interest. The ligation of a 3'UTR downstream of the Renilla-luciferase gene allows the effects of miRNAs on translation and mRNA stability to be assessed by monitoring luciferase expression. This technique was successfully used by Pegtel *et al.* (2010) where firefly luciferase reporter assay was ligated with the cDNA sequence of an Epstein Barr Virus (EBV) derived miRNA sequence. When cells were transfected with this reporter and treated with EVs derived from B-cells infected with EBV, this study reported an 80% reduction in luciferase activity compared to the control which indicated a high level of gene suppression by the miRNAs.

4.2 Results

4.2.1 Design of luciferase reporter assays

Sequences corresponding to miR-21, miR-100 and miR-101 were designed as either a perfect match to the miRNA or as a double base mis-match within the seed region of the miRNA. The creation of a perfect match to the miRNA sequence would be expected to result in the binding of the miRNA and subsequent cleavage of the RNA via Ago2. Whereas, by including a two-base mismatch following miRNA binding translational repression mediated by the RNA-Induced Silencing Complex (RISC) would ensue. The design and production of these inserts is described in methods section (2.13). Ligated constructs were sequenced to confirm the insertion of each miRNA target site. Only the perfect miR-21 target sequence was found to be correctly inserted into the PsiCHECK-2 plasmid backbone (Figure 4.1). Therefore, subsequent experiments are based on this reporter assay only.

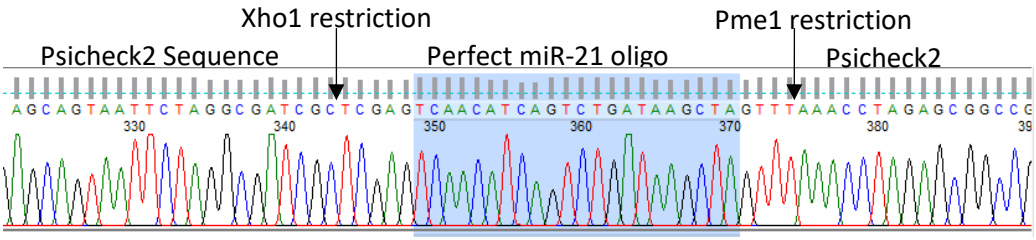


Figure 4.1 The chromatograph showing the insertion of the perfect miR-21 target oligo sequence and the restriction sites where the PsiCHECK-2 plasmid was digested in preparation for insertion.

4.2.2 Optimisation of Renilla luciferase luminescence assays

In order to test if the miR-21 luciferase assays (miR21-psiCHECK-2) could be effectively repressed within cells, we transfected miR21-psiCHECK-2 into PC3 cells and determined the expression of luciferase compared to transfection of the psiCHECK-2 plasmid only (no inserted miRNA sites). The results of the PC3 transfections confirmed the miR21-psiCHECK-2 reporter produced a lower level

of luciferase expression compared to the plasmid only control, suggesting translational repression associated with the miR-21 target site, however this would have to be confirmed by analysing resulting protein levels.

We tested our plasmids in PC3 cells due to established protocols for transfection of this cell type. However, as our experiments rely on using osteoblasts we repeated the same optimisation experiments using the hOB cell line. The results showed a similar downregulation of the luminescence in the cells transfected with miR21-psiCHECK-2 compared to the plasmid only control.

4.2.2.1 Investigation of the effect of exogenous EVs on Renilla luciferase activity in osteoblasts

HOB cells were transfected with miR21-psiCHECK-2 and 24-hours later subjected to treatment with either conditioned media or EVs isolated from prostate cancer PC3, LNCaP or C4-2 cells or non-malignant PNT1A. T-test analysis was used to determine whether there were significant differences between EV treated and non-treated cells.

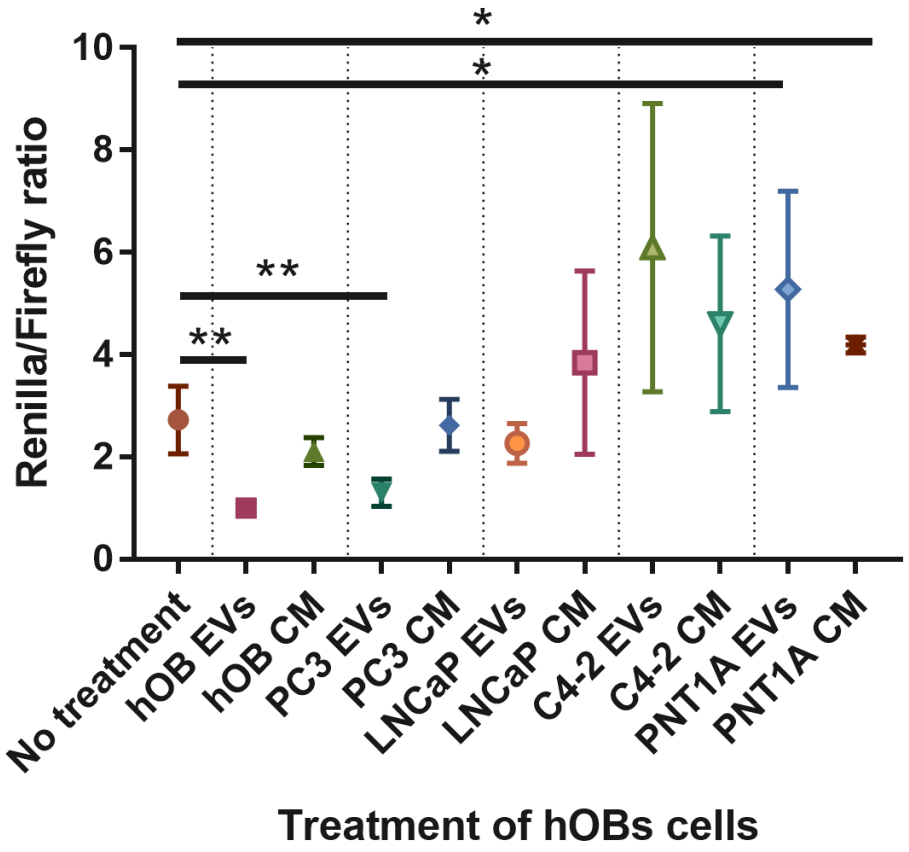


Figure 4.2 A graph to show the Renilla Firefly ratio of cells transfected with the miR21-psicheck2 reporter and then treated with isolated EVs or conditioned media (CM) from PC3, LNCaP, C4-2 or PNT1A cells.

* $P < 0.05$

** $P < 0.005$

N=4

Treatment of hOB cells with hOB EVs and PC3 EVs led to a significant reduction in Renilla luciferase expression (PC3: P= 0.0073, hOB: P= 0.0022). This decrease is consistent with the findings of Chapter 3 which showed that miR-21 is abundant in the EVs of PC3 cells. The reduced Renilla luciferase expression on

treatment with hOB EVs is unexpected considering miR-21 expression was found to be lower in hOB EVs compared to PC3 EVs (Figure 3.16B). There was no significant difference in Renilla luciferase expression for the cells treated with LNCaP or C4-2 EVs or conditioned media. There was a significant increase in the level of luminescence in cells treated with the PNT1A EVs (P= 0.0456) or conditioned media (P= 0.0143). This could be explained by these EVs causing downregulation of endogenous miR-21 or through sequestration of miR-21 by other targets within the PNT1A EVs, further investigation would be needed to determine which was occurring.

When unpaired, non-parametric t-testing was carried out to compare the difference in expression in cells treated with EVs and those treated with conditioned media from the same cell type, only osteoblasts treated with PC3 EVs or PC3 conditioned media were found to have significantly different levels of Renilla luciferase expression (P = 0.0038). This suggests that EVs and conditioned media do not have significantly different constituents.

The significant further reduction in the level of Renilla luciferase expression following treatment with vesicles indicates that the miR-21 present in the EVs is having a significant and measurable effect on post transcriptional gene expression.

Interestingly, when the isolated EVs were added the viability of the plasmid transfected cells appeared to decrease (raw data: Table 8.2), leading to much lower Renilla and firefly luminescence compared to when conditioned media was added. Further investigation of this was subsequently conducted (2.20,

4.2.3).

4.2.3 Viability experiment

This experiment investigated the viability of hOB cells transfected with miR21-psiCHECK-2, or a control, which were subsequently treated with normal media, elution buffer (from ExoEasy Maxi Kit), PC3 EVs and PNT1A EVs. The effects of transfection type and treatment type on hOB cell viability were both investigated.

To ensure the transfection complex was not the cause of altered viability a pilot study compared viability in cells which were not transfected, mock transfected or transfected with miR21-psiCHECK-2 reporter assay. There was no significant difference in viability between the control, untransfected and mock transfected cells and therefore the mock transfection was not carried out in the investigation.

For each well two counts were taken, so eight replicates were used for the statistical analysis and viable cell count was used to compare the effects of treatment.

Transfection causes a significant reduction in the number of viable cells when they had been treated with normal media (P<0.0001) or PC3 EVs (P<0.0001) (Figure 4.3). Transfection had no significant effect on cell survival when the cells had been treated with elution buffer or PNT1A EVs.

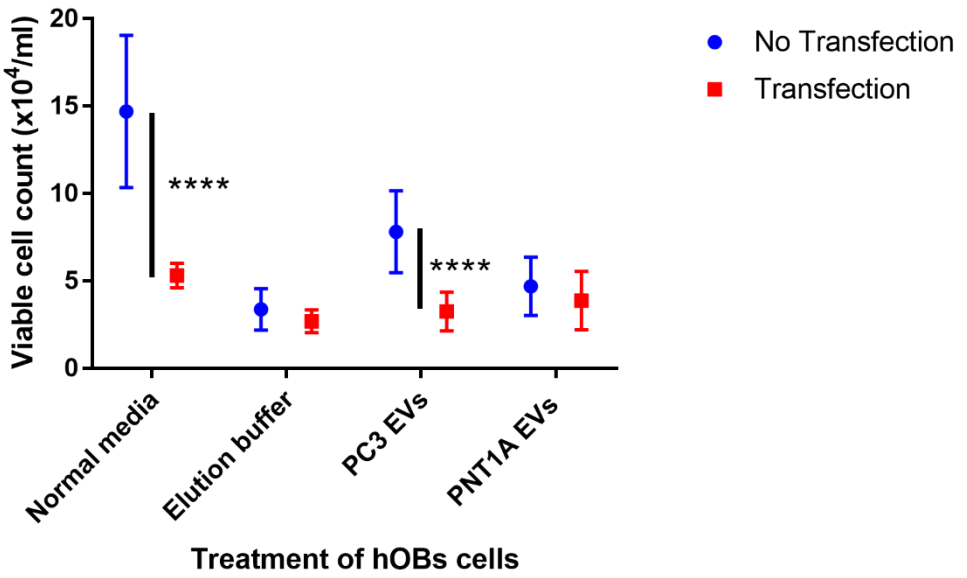


Figure 4.3 A graph comparing the number of viable cells remaining at 24hrs post transfection when cells have been transfected or not transfected and treated with normal media, elution buffer, PC3 EVs or PNT1A EVs. Bars indicate where 2-way ANOVA analysis indicated significant differences between treatment groups.
**** P < 0.0001
N=8 (All conducted on the same occasion. 2 technical replicates for each of 4 biological replicates).

In untransfected cells, treatment with elution buffer, PC3 EVs and PNT1A EVs resulted in a significant reduction in the viable cell count compared to cells treated with normal media (P<0.0001 for all) (Figure 4.4), this difference was greatest when cells were treated with elution buffer. The PC3 and PNT1A EVs are eluted within this buffer so the significant increase in viability of cells treated with PC3 EVs compared to the elution buffer (P< 0.0001) suggests that something contained within the PC3 EVs is either increasing cell proliferation or reducing apoptosis to overcome the negative effect of the elution buffer. There was a significant decrease (P=0.035) in viability of cells treated with PNT1A EVs compared to those treated with PC3 EVs which suggests that the factor increasing viability is cancer specific and not a general property of EVs.

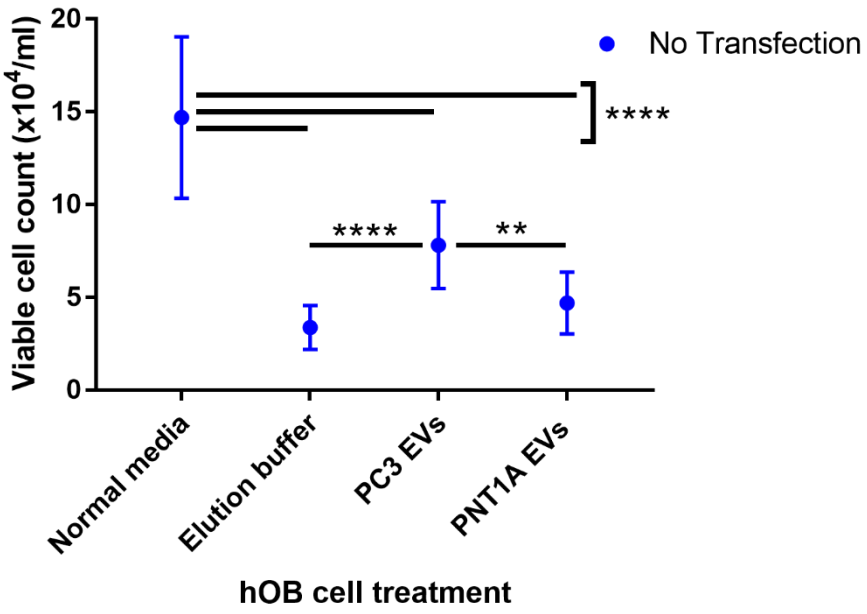


Figure 4.4 A graph showing the effect of treatment with normal media, elution buffer, PC3 EVs, or PNT1A EVs on the number of viable hOB cells remaining at 24hrs when cells had not been transfected. Bars indicate where 2-way ANOVA analysis indicated significant differences between treatment groups.

* P < 0.05

** P < 0.005

**** P < 0.0001

N=8 (All conducted on the same occasion. 2 technical replicates for each of 4 biological replicates).

Transfection with the miR21-psiCHECK-2 plasmid resulted in an overall reduction in the number of viable cells, which may make the effects of different treatment types (e.g. elution buffer versus vesicles) appear to be less significant (Figure 4.5). However significant reductions were still seen when cells were treated with elution buffer (P=0.013) and PC3 EVs (P=0.0487) compared to treatment with normal media.

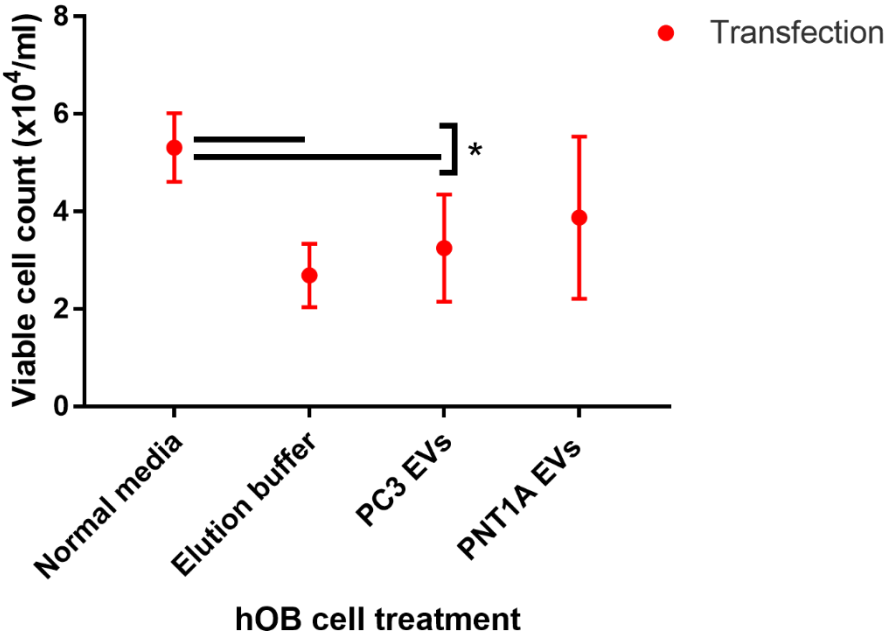


Figure 4.5 A graph showing the effect of treatment with normal media, elution buffer, PC3 EVs, or PNT1A EVs on the number of viable hOB cells remaining at 24hrs after cells were transfected. Bars indicate 2-way ANOVA analysis indicated significant differences between treatment groups.

* P < 0.05

** P < 0.005

**** P < 0.0001

N=8 (All conducted on the same occasion. 2 technical replicates for each of 4 biological replicates).

Taken together, this data indicates that treatment of osteoblasts with vesicles does result in an enhanced reduction in miR-21 target gene expression, strongly supporting a functional role for a functional role of vesicle-miR-21 function. However, this may be a miR-21 specific phenomenon and as yet we cannot rule out indirect effects. Therefore, further investigation of vesicle-

miRNA function is required to confirm this result. Our investigation of cell viability following the combination of transfection and treatment with vesicles demonstrates the complexity of these assays and that caution needs to be taken when interpreting these artificial assays, future studies should include comparisons of endogenous targets.

5 Chapter 5: Bioinformatic analysis

5.1 Introduction

The luciferase assays in chapter 4 suggested that miR-21 transferred via EVs is having a functional effect on translation in recipient cells based on the altered expression of the reporter gene. To confirm this, it would be necessary to investigate the alteration of target mRNA and protein levels. To begin to understand the potential contribution of prostate cancer vesicles in the regulation of osteoblasts, it is necessary to look at the global effects of vesicle cargos. We sought to use RNA sequencing (RNAseq) of osteoblast mRNA to determine changes in expression that result from exposure to prostate cancer and non-malignant prostate vesicles.

5.2 Results

5.2.1 Characterisation and filtration of RNAseq data

Osteoblasts were treated with vesicles isolated from either the prostate cancer cell line PC3 (H+P3), non-malignant prostate cell line PNT1A (H+P) or other osteoblasts (hOB) cells (H). Total RNA was extracted from the vesicle treated osteoblasts and subject to next-generation sequencing to determine the mRNA content (see methods sections 2.21 and 2.22).

The RNAseq analysis produced three sets of data through comparison of the treatment groups; H+P vs H+P3 (HPvsHP3), H vs H+P (HvsHP) and H vs H+P3 (HvsHP3). Due to the large amount of data produced by the RNAseq analysis it was necessary to filter the results to remove transcripts which showed low

log_2 fold change (fold change less than 2 or -2) as these are likely to be background genes which are not affected by treatment.

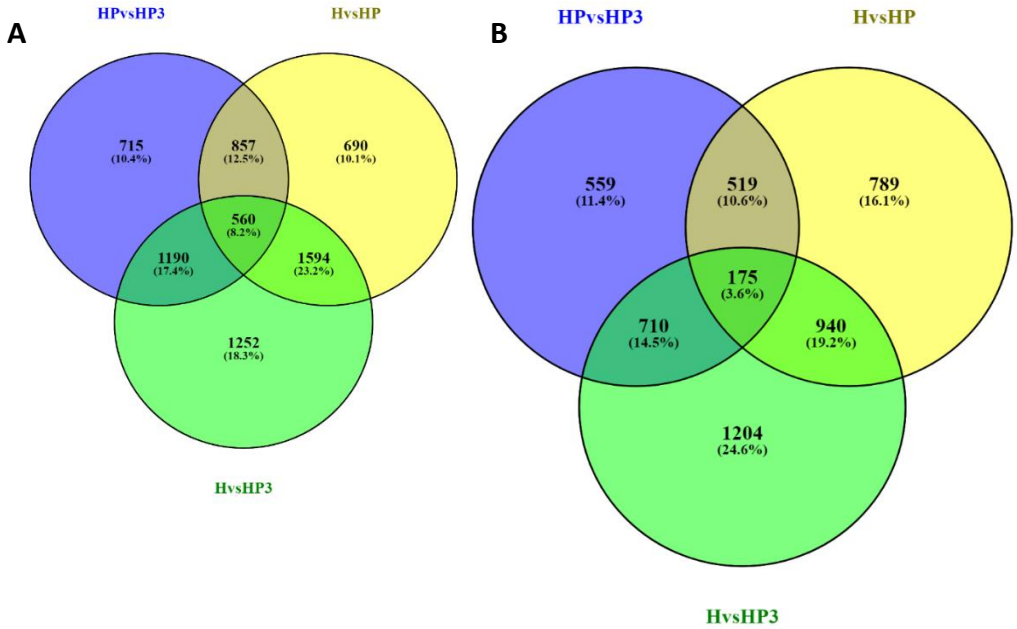


Figure 5.1 Venn diagrams comparing the genes differentially expressed between the different treatment groups. A: raw data before filtering. B: Filtered data with all transcripts with log_2 fold change between -2 and 2 removed.

Venny 2.1.0 (http://bioinfogp.cnb.csic.es/tools/venny/) was used to compare which genes commonly showed altered expression across the data groups. Figure 5.1 shows this comparison before the data with a low log_2 fold change was removed and what the overlap was once the data had been filtered. The number of genes found in only one treatment group stays consistent between these two figures, which suggests this method of filtration is effective at removing the genes whose expression is not treatment dependent whilst keeping the genes showing potentially interesting expression.

When the genes were split based on whether they were up- or downregulated the Venn diagrams showed reduced overlap between groups Figure 5.2. This suggests that the remaining genes are specifically altered in the individual data sets and are therefore less likely to be housekeeping genes. Filtering based on

whether transcripts are up or downregulated appears to be an appropriate method to identify which genes are likely to be altered due to treatment.

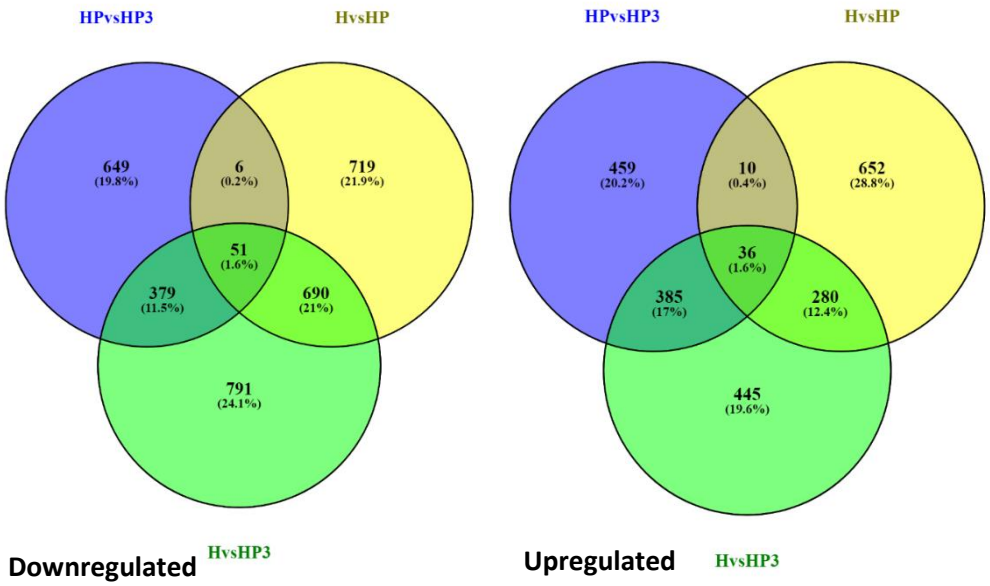


Figure 5.2 Venn diagrams showing the overlap of genes differentially expressed between treatment groups when genes are split into those that are up and downregulated.

5.2.2 Gene enrichment analysis

A large number of differentially expressed gene transcripts were found between each treatment group. Table 5.1 shows the number of gene transcripts and genes differentially expressed in each treatment group and the numbers found to be up- or downregulated.

	HPvsHP3		HvsHP		HvsHP3	
	Transcripts	Genes	Transcripts	Genes	Transcripts	Genes
Total	2392	1963	2845	2423	3739	3029
Down-regulated	1312	1084	1663	1465	2275	1910
Upregulated	1079	889	1182	977	1464	1145

Table 5.1 A table showing the number of gene transcripts found to be differentially expressed and the number of genes that these transcripts

related to. HP = hOB cells treated with PNT1A EVs. HP3 = hOB cells treated with PC3 EVs. H = hOB cells treated with hOB EVs.

The difference between the number of transcript IDs and genes is due to multiple transcripts being produced by the same gene. There was also a small proportion of transcripts the genes for which have not yet been annotated (HPvsHP3 = 0.84%, HvsHP = 0.56% and HvsHP3 = 0.88%).

For each treatment group around 35% (HPvsHP3 = 37.2%, HvsHP = 31.6% and HvsHP3 = 37.7%) of genes generated two or more transcripts. Within this percentage the maximum number of transcripts affecting one gene varied from 8 to 11 (HPvsHP3 = 8, HvsHP = 11 and HvsHP3 = 9). Of the genes which produce more than one transcript, over 7% (HPvsHP3 = 7.84%, HvsHP = 8.47% and HvsHP3 = 7.17%) have at least one transcript which was upregulated and at least one which was downregulated. Because the differential expression was calculated for the gene transcripts there is some overlap between the up or downregulated groups when the genes are compared (Figure 5.3). These data suggest that regulation at the individual transcript level is influenced by vesicles, a previously unreported finding that requires further investigation to determine how opposing regulation of transcripts of the same gene affect osteoblast function. Alternative splicing has the potential to cause alteration of the 3' target site which alters the 3' miRNA target sequence and could thereby alter miRNA gene regulation.

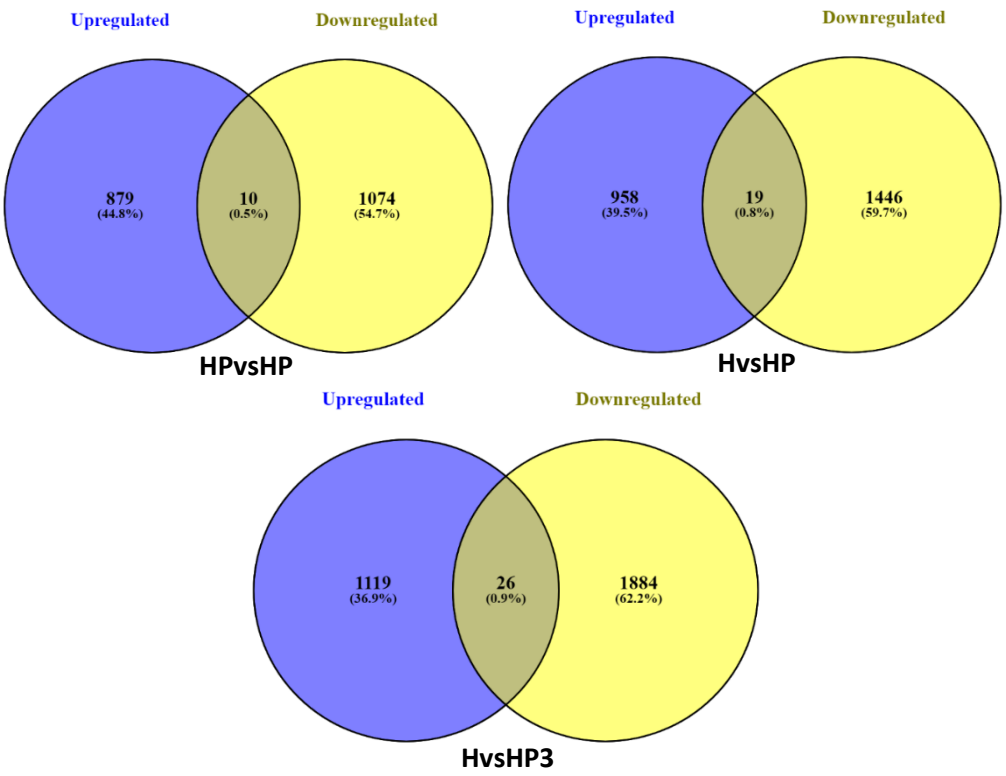


Figure 5.3 Venn diagrams showing the overlap between the up and downregulated genes for each treatment set.

5.2.3 KEGG pathway enrichment analysis

Using the human genome as the background gene list the NIPA functional analysis identified the biological pathways within which the differentially expressed genes could be found. This enables analysis of the potential effects of up- or downregulation of these genes on biological processes. The script uses multiparametric testing to determine whether pathways are significantly enriched in genes showing altered expression based on the number of genes in the pathway and the number affected; the q-value cut off was 0.05 for significance.

The number of significantly enriched pathways found by the NIPA analysis varied depending on whether data was split into up and downregulated pathways before analysis and on which treatment group was analysed (**Error!**

Reference source not found.). Although there is overlap between treatment groups this comparison does not indicate whether the same genes are commonly altered between the groups.

When the input data was split into up and downregulated genes prior to analysis the KEGG pathways found to be significantly enriched where altered. Handling the data like this results in some additional pathways being found to be significant, which are examined in the next section (5.2.3.1). These results further reinforce the previous assumption that splitting the data into those transcripts which were up- and downregulated is the most appropriate analysis pipeline.

5.2.3.1 Enriched KEGG pathways for HPvsHP3

We focussed on the comparison of hOB cells which had been treated with either PNT1A (non-malignant prostate) (HP) or PC3 (prostate cancer) (HP3) EVs. NIPA functional analysis is not a discriminative analysis technique so that although 32 (12 upregulated and 21 downregulated) pathways were found to be significantly enriched not all of these are relevant to the alterations occurring in osteoblasts. Therefore, it was necessary to focus on pathways known to be relevant to osteoblast function and bone remodelling as these are the processes affected during development of bone metastases. The selected pathways were cell cycle (Figure 5.4. q = 0.000395), Cellular senescence (Figure 5.5. q = 0.000295), cell adhesion molecules (Figure 5.7 q = 0.04622), proteoglycans in cancer (Figure 5.6. q= 0.003379) metabolic pathway map (q = $3.93x10^{-11}$), Wnt signalling pathway (Figure 5.8. q = 0.01825) and The PI3K-AKT signalling pathway (Figure 5.9 q= 0.002194).

Downregulation of p53 was common to all of these pathways and cyclins were commonly downregulated in both the cell cycle and cellular senescence pathways. All of the pathways investigated were found to contain both up and downregulated genes. Genes highlighted as both up and downregulated are due to differently expressed genes within a family (where only the family name is included on the KEGG map) or where different transcripts from the same gene are expressed in opposite directions.

The KEGG metabolic pathway map was significantly ($q = 3.93x10^{-11}$) enriched in genes which were upregulated in the hOB cells treated with PC3 EVs. 91 out of 1273 genes in the pathway were upregulated and 65 were downregulated. This suggests multiple changes to cell metabolism.

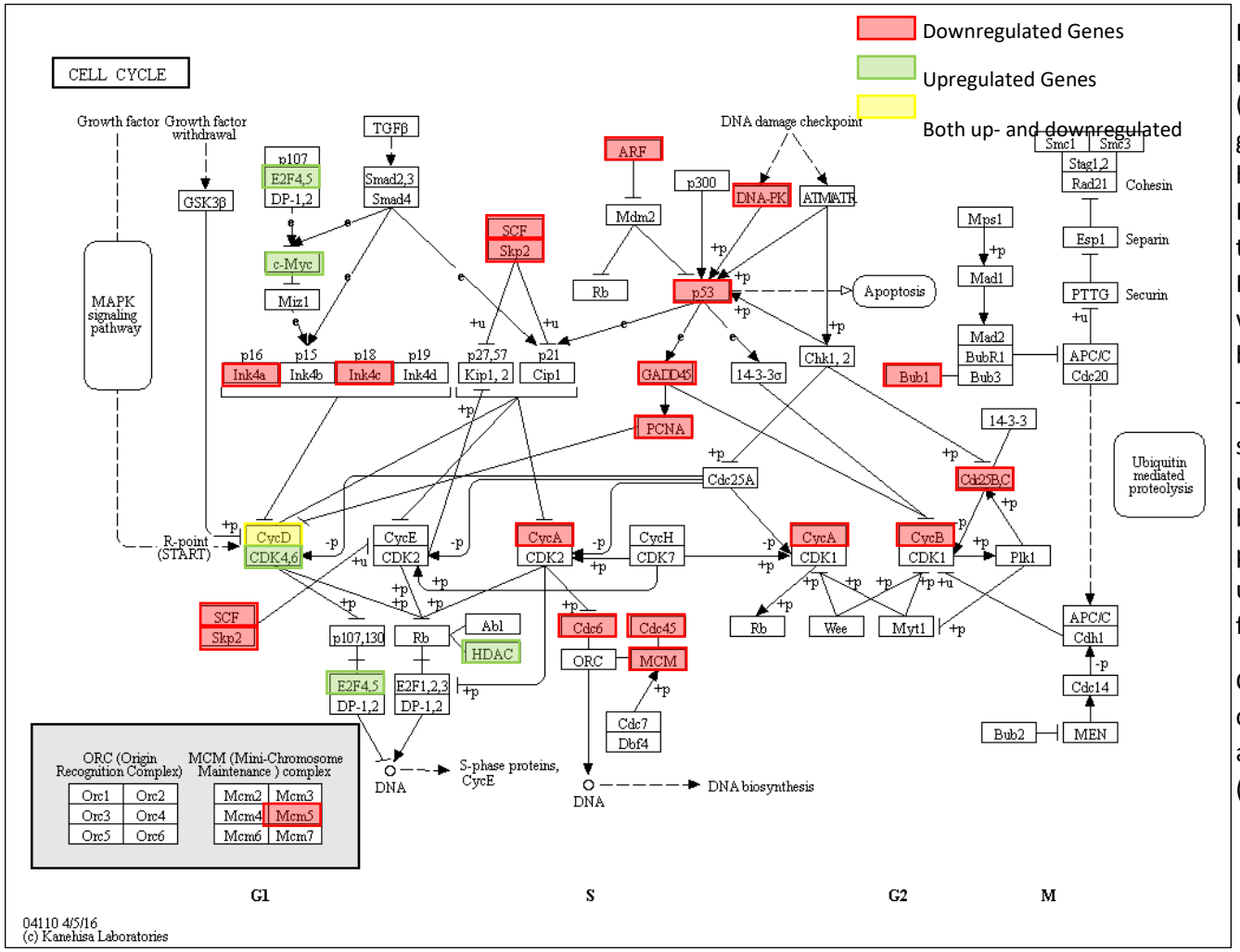


Figure 5.4 The cell cycle pathway was significantly (q= 0.000395) enriched in genes downregulated in hOB cells treated with PC3 EVs in comparison to those treated with PNT1A EVs. 17 genes out of 124 were downregulated (red) by at least two-fold.

This pathway was not significantly enriched in upregulated genes (green) but 6 genes in this pathway this were upregulated by at least 2-fold.

Cyclin D represents both cyclin D1 (upregulated) and Cyclin D3 (downregulated).

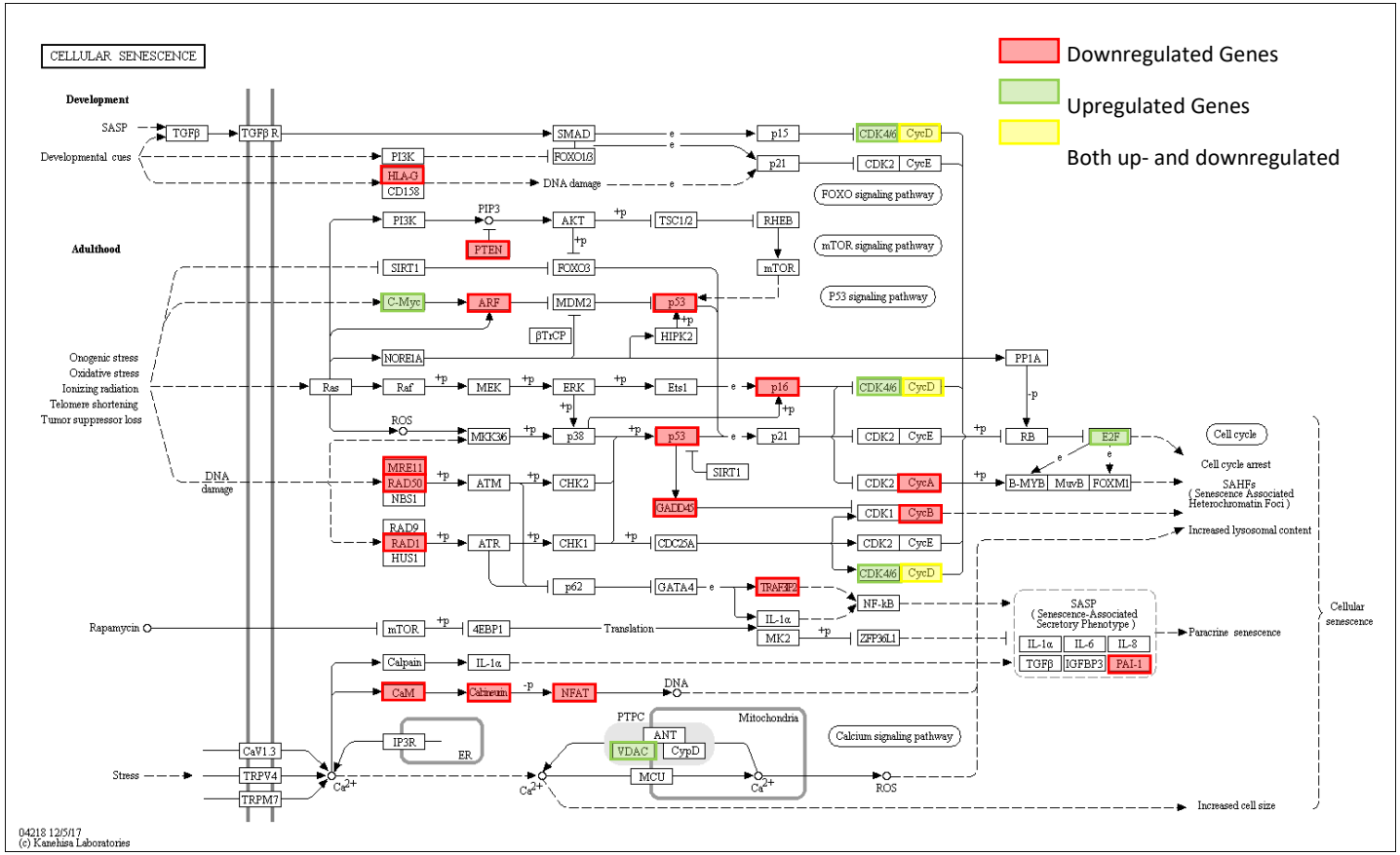
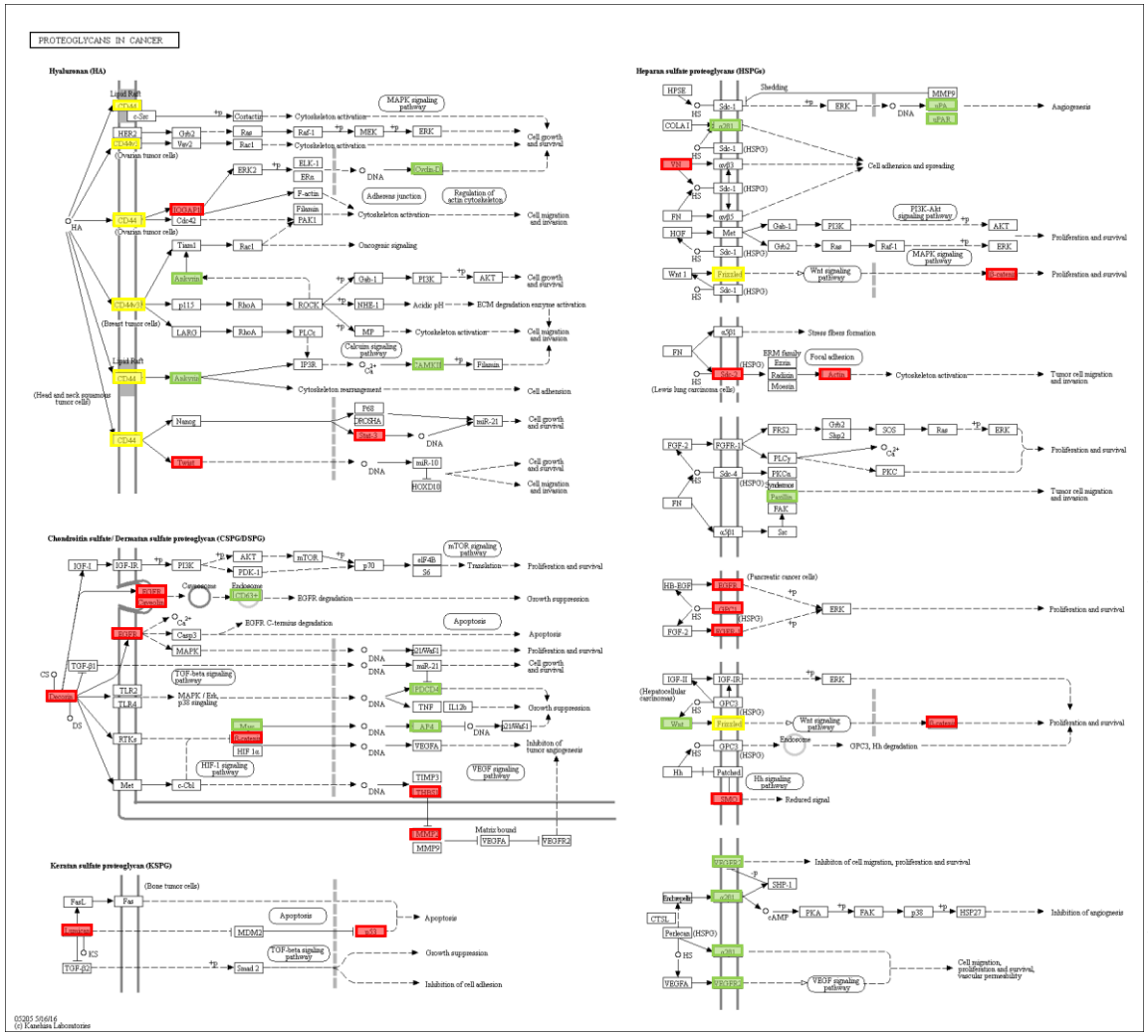


Figure 5.5 The cellular senescence pathway was significantly (q= 0.000295) enriched in genes downregulated in hOB cells treated with PC3 EVs in comparison to those treated with PNT1A EVs. 20 genes out of 160 were downregulated (red) by at least two fold. This pathway was not significantly enriched in upregulated genes (green) but 9 genes in this pathway this were upregulated by at least 2-fold.



Downregulated Genes

Upregulated Genes

Both up- and downregulated

Figure 5.6 The proteoglycans in cancer pathway was significantly (q= 0.003379) enriched in genes downregulated in hOB cells treated with PC3 EVs in comparison to those treated with PNT1A EVs. 21 genes out of 201 were downregulated (red) by at least two fold.

This pathway was not significantly enriched in upregulated genes (green) but 16 genes in this pathway this were upregulated by at least 2-fold.

Due to its splice variants CD44 has transcripts showing opposing expression.

The frizzled gene family has members showing opposing expression.

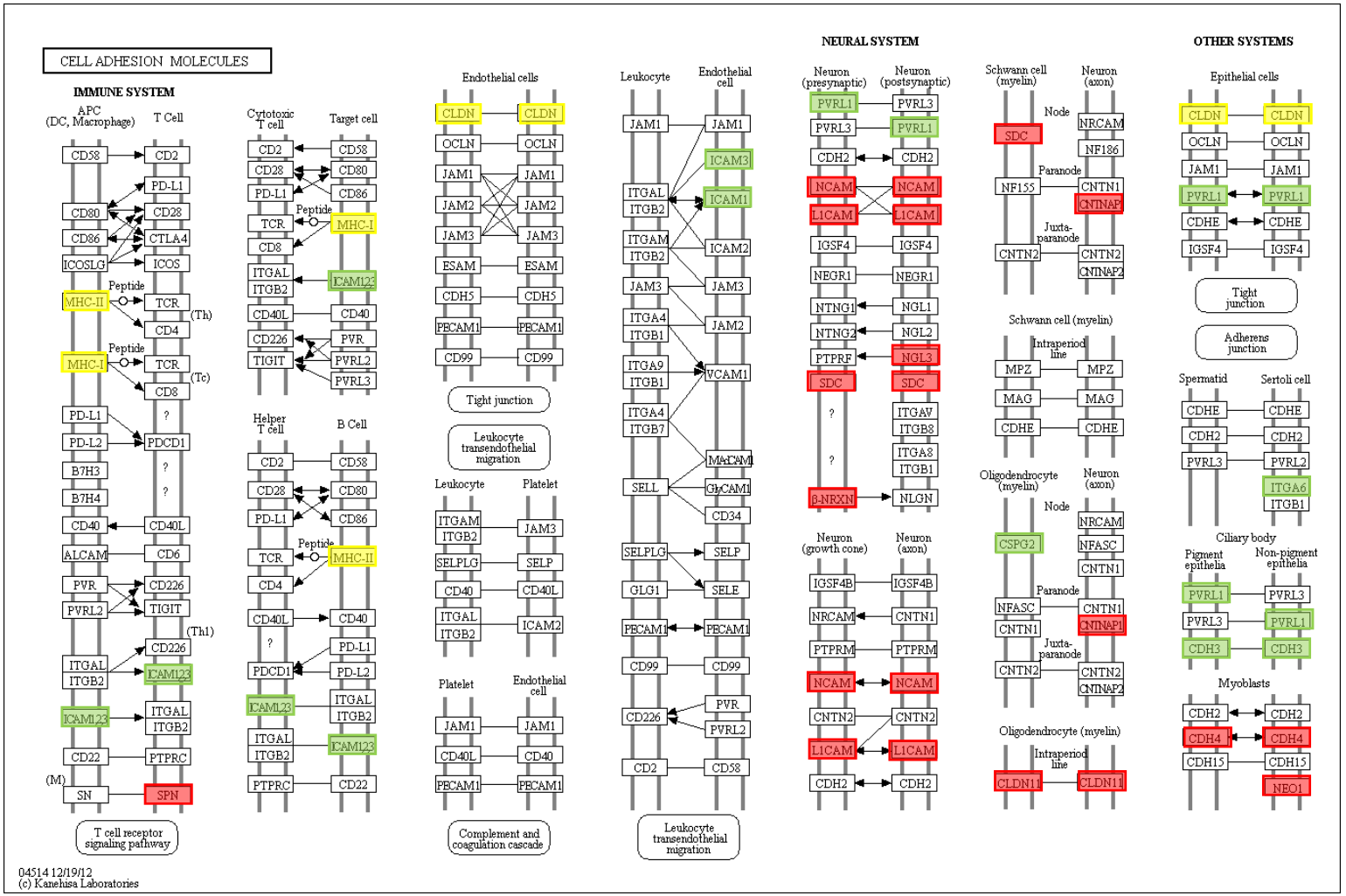


Figure 5.7 The cell adhesion molecules map was significantly (q= 0.04622) enriched in genes downregulated in hOB cells treated with PC3 EVs in comparison to those treated with PNT1A EVs. 15 genes out of 145 were downregulated (red) by at least two fold. This pathway was not significantly enriched in upregulated genes (green) but 11 genes in this pathway this were upregulated by at least 2-fold.

CLDN3 and CLDN4 (upregulated) and CLDN11 (downregulated)

MHC genes had transcripts showing opposing expression

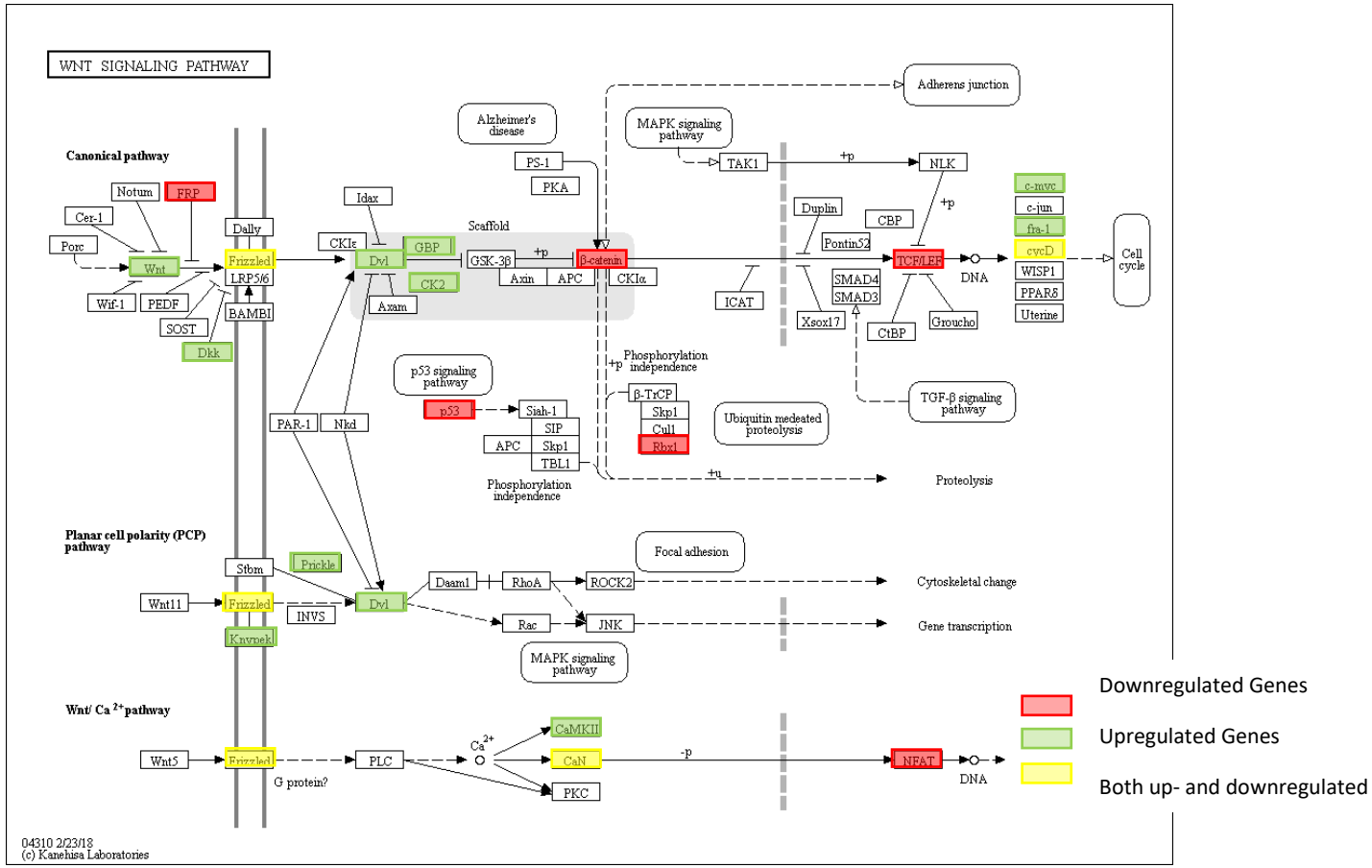


Figure 5.8 WNT signalling pathway was significantly (q= 0.01825) enriched in genes upregulated in hOB cells treated with PC3 EVs in comparison to those treated with PNT1A EVs. 14 genes out of 146 were upregulated (green) by at least two-fold. This pathway was not significantly enriched in downregulated genes (green) but 10 genes in this pathway were upregulated by at least 2-fold. CaN had had transcripts showing opposing expression.

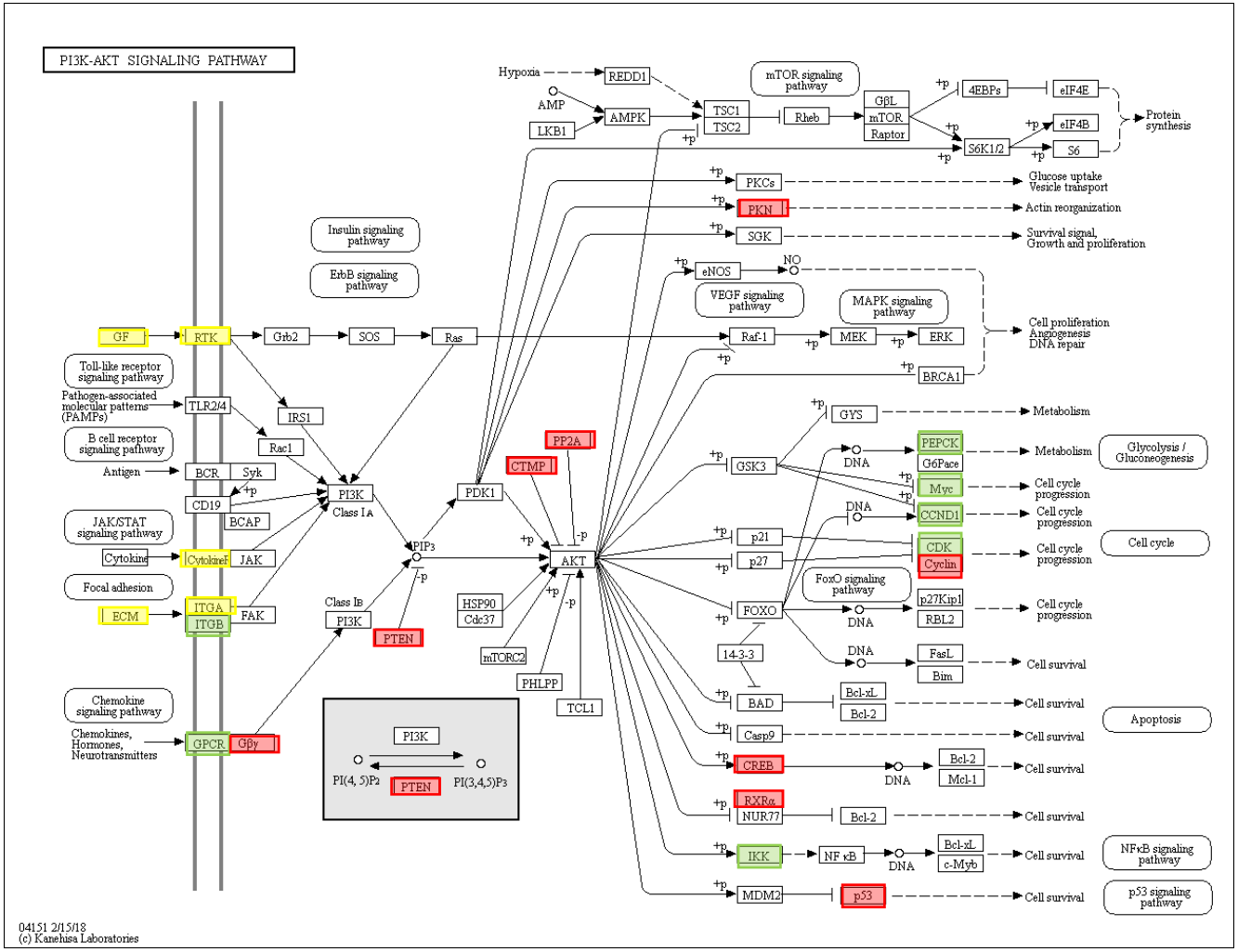


Figure 5.9 The PI3K-AKT signalling pathway was significantly (q= 0.002194) enriched in genes downregulated in hOB cells treated with PC3 EVs in comparison to those treated with PNT1A EVs. 31 genes out of 352 were downregulated (red) by at least two fold. This pathway was not significantly enriched in upregulated genes (green) but 21 genes in this pathway were upregulated by at least 2-fold.

Downregulated Genes

Upregulated Genes

Both up- and downregulated

In addition to those already discussed the NIPA functional analysis script generated a further 10 pathways which were significantly enriched in upregulated genes and 14 pathways which were significantly enriched in downregulated genes (see appendix Table 8.3). Although not obviously related to osteoblast function there is the potential that some of these pathways could be relevant to the progression of cancer. Although not relevant to osteoblast function the treatment with cancer EVs resulted in alteration of cancer specific pathways; Pathways in cancer ($q = 5.59x10^{-7}$) and Prostate cancer pathways ($q= 0.00618$) were significantly enriched in downregulated genes and the transcriptional misregulation pathway was significantly ($q = 0.007922$) enriched in upregulated genes.

These results show that the treatment of hOB cells with PC3 EVs results in significant alteration in the expression of genes on an individual and pathway level. Despite altered gene expression we cannot conclude that the same level of alteration occurs in the proteome of cells as there may be other forms of post transcriptional mRNA regulation.

6 Chapter 6: Discussion

6.1 Investigation of miRNAs contained within and transferred to recipient cells by Prostate cancer vesicles

6.1.1 Characterisation of Extracellular Vesicles

The International Society for Extracellular Vesicles has created a set of minimum criteria for the definition of extracellular vesicles (Lotvall *et al.*, 2014). They have stated that to be defined as EVs, samples should show enriched levels of at least one Transmembrane or lipid bound extracellular protein and of at least one Cytosolic protein. In addition to this samples must be shown to have low levels of an intracellular protein. Our results confirm the isolation of EVs since CD9 (a transmembrane protein) was expressed in all EV preparations, Annexin V (a cytosolic protein) was found in all preparations, apart from LNCaP EVs, and GM130 (an intracellular protein) was not found to be expressed in any preparations. The lack of expression of Annexin V in LNCaP EVs may be due to cancer specific modifications or disruptions of vesicle production pathways, which have yet to be fully elucidated (Akers *et al.*, 2013). The high level of CD9 is as would be expected given the findings of Yoshioka *et al.* (2013), who demonstrated that it is consistently present on all EVs irrespective of the levels of expression in the cells or origin. Our results also provide confirmation that the samples tested were enriched in exosomes since the results showed enrichment of proteins associated with exosome biogenesis; Annexin V and Flotillin-1.

The Brownian motion analysis showed that a proportion of the EVs isolated in this study are of a size consistent with exosomes, although given the diversity

of sizes other EV subpopulations are also present.

6.1.2 RNAseq analysis of microRNAs transferred via prostate cancer vesicles to osteoblasts

This experiment identified 13 miRNAs transferred from the prostate cancer PC3 cells to hOB cells by vesicles. Gene ontology analysis showed that the majority of the genes targeted by these 13 miRNAs had products localised to the nucleus which suggests they commonly affect RNA synthesis and processing. As expected the commonly affected molecular functions of targeted genes were transcription factor activation and translational regulation.

The similarities between the gene targets of the miRNAs identified in this experiment and the targets of miRNAs identified by Bryant *et al.* (2012) and Watahiki *et al.* (2011) were encouraging as they suggested that the miRNAs we had identified were targeting similar genes and pathways and thus were potentially important in metastasis. The similarities in molecular function also strengthen the evidence that the miRNAs we identified act similarly to those previously reported. However, the actions of miRNAs can be dependent on the tissue type and therefore they may still affect gene expression differently depending on the context (Cortez *et al.*, 2011).

6.1.3 Comparison of miRNA expression in cells and EVs

MiR-21 is widely reported to be increased in metastatic and castrate resistant prostate cancer. Ribas *et al.* (2009) linked increased miR-21 to increased growth of both androgen-dependent and independent prostate cancer cell lines and Zhang *et al.* (2011) showed that it is elevated in patients with CRPC. Surprisingly, the results presented here showed a lower expression of miR-21

in prostate cancer cells in comparison to a non-cancer control. However, despite this the level of miR-21 was significantly increased in PC3 EVs compared to the PNT1A EVs. LNCaP and C4-2 EVs showed the lowest levels of miR-21 expression suggesting that it is elevated only in the EVs from cellular models of advanced prostate cancer.

MiR-100 had consistently lower levels in the EVs compared to the cell of origin, this might suggest that the miR-100 is not as commonly transferred as other miRNAs. Despite this, when miR-100 expression in PC3 cells and EVs was compared to PNT1A cell and EV levels there was significant enrichment in the PC3 samples, this pattern was not mimicked in the other prostate cancer cell types. These findings contradict those of Porkka *et al.* (2007), who found that miR-100 was downregulated in more advanced CRPC but are consistent with the findings of Leite *et al.* (2011b) and Leite *et al.* (2011c) who showed that miR-100 is increased in high grade tumours and that increased miR-100 was correlated with increased risk of biochemical recurrence. Based on these results and the available literature it seems that miR-100 may be an important marker for advanced but not localised prostate cancer.

The results obtained here showed reduced expression of miR-101 in the cancer cells which concurs with the findings of Hudson *et al.* (2013) who described miR-101 as a tumour suppressor gene and found its expression to be reduced in localised and metastatic prostate cancer in comparison to non-malignant prostate cells. However, miR-101 was significantly increased in EVs compared to all cell types and was also increased in the cancer EVs compared to the

PNT1A EVs. Hudson *et al.* (2013) investigated miR-101 expression in tissues, and therefore did not consider the potential effects of increased circulating miR-101 due to release from prostate cancer cells.

As predicted the miRNAs investigated were shown to be selectively packaged into EVs with almost all miRNAs showing significantly (see 3.2.2) different levels across all cell types (miR-21 expression in PC3 cells and EVs and miR-101 expression in PNT1A cells and EVs were the only non-significant results for which both values were measurable). These results showed that miRNA level in the cell does not necessarily correlate to the level in EVs and therefore provides no information on the circulating level. When considering the hypothesis that a prostate cancer may adapt a pre-metastatic niche within the bone, investigating the effects of circulating miRNAs is likely to be highly important. Our data indicates the degree of selective packaging of miRNAs into EVs is cell type dependent and so no assumptions can be made about EV-miRNA expression based solely on cellular expression without investigation of EV packaging by the specific cell type. Further to this Melo *et al.* (2014) noted that miRNAs expression increased in EVs which had been cultured for 72hrs in comparison to those cultured for only 24hrs due to intra-vesicle processing of pre-miRNAs. Since the assays were conducted after 24hrs of culture and detected only mature miRNAs these results cannot indicate whether the packaging of pre-miRNAs shows the same pattern as those of mature miRNAs.

6.1.4 Validation of the transfer of characterised miRNAs from prostate cancer cell to osteoblasts via vesicles.

Changes in the total osteoblast miRNA expression, following treatment with EVs, were seen that did not relate to the proportions of EU labelled miRNAs transferred from prostate cancer EVs to osteoblasts. This suggests indirect mechanisms of regulation need to be considered when predicting the effect of EV cargos on recipient cells. Mathivanan *et al.* (2010) hypothesised that EVs could trigger the activation of signalling cascades through contact dependent binding of EV surface proteins to cell surface receptors or through cleavage of EV proteins to create ligands for these receptors. This study suggested that the process of EV-cell fusion needed to enable delivery of the miRNA cargo would also cause alteration of the cell membrane with potential downstream effects on the target cell.

The data generated demonstrates that miRNAs can be transferred into recipient cells. However, we cannot yet conclude that miRNA transfer by cancer EVs is more efficient than by EVs produced by non-cancer cells, although the results for miR-21 suggest that this might be possible. Kim *et al.* (2003) and Baran *et al.* (2010) both reported an increase in the number of circulating EVs in the plasma of patients with gastric cancer compared to healthy controls which suggests that, even though their EVs may not have innate advantages for miRNA delivery, cancer cells are likely ultimately delivering more miRNAs than other cell types.

6.2 Investigation of the effect of transferred miRNAs in recipient Osteoblasts

6.2.1 Investigation of the effect of adding EVs on renilla luciferase activity

Investigation of Renilla luciferase activity showed that miR-21 transferred by EVs is able to alter reporter gene expression in recipient osteoblast cells. Furthermore, this change in miR-21 target expression was only significant when cells were treated with cancer EVs isolated from PC3 cells, consistent with the previous finding that PC3 EVs showed the highest levels of miR-21 transfer to osteoblasts. The PC3 cell line represents the most aggressive form of prostate cancer and the type most likely to be preparing a pre-metastatic niche.

Treatment with non-malignant PNT1A EVs had no effect on reducing miR-21 target expression, suggesting the levels of miR-21 transferred were not sufficient or that alternative mechanisms of regulation controlled the action of miR-21 in this case.

6.2.2 Viability experiment

Transfection of cells with the luciferase reporters appeared to change the ability of cells to respond to EVs, resulting in a reduction in viability. It is unclear why this would be the case, but our studies clearly show the response to be different.

The finding that the addition of PC3 EVs reduced the amount of cell death in comparison to cells treated with elution buffer or other EVs suggests that components of these cancer EVs contain factors which encourage reduced cell death or increased proliferation. Both would be expected in cells undergoing

oncogenesis. Overall, the data demonstrates the need to interpret luciferase reporter assays with caution and that future studies will need to include an evaluation of endogenous targets.

Reduced cell viability is a common consequence of cell transfection. Transfection complexes are taken up via endocytosis and then need to escape the endosome to deliver their cargo to the nucleus (Juckem, 2012). This may activate stress pathways in the cell leading to altered regulation of the cell cycle and metabolism (Juckem, 2012). If an excess of DNA is added to the cells the increased number of complexes per cell can lead to further reduction in cell viability (Juckem, 2012), further investigation using variable concentrations of DNA could determine whether this was the issue in this case. Shaffer *et al.* (2011) suggested that the quality of the plasmid DNA used for transfection could also affect cell viability since it could contain a high concentration of salts or transfer endotoxins. The isolation of plasmid DNA using the PureYield Plasmid Miniprep system has a stage for endotoxin removal however confirmation that this was effective was not conducted. Elution in nuclease free water means that high salt concentrations were unlikely. Although transfection of cells with a reporter plasmid is a useful method to prove that miRNAs transferred to osteoblasts can alter translation this method does not indicate what changes are occurring and there is potential for the transfection itself to alter intercellular pathways and cell regulation.

6.3 Bioinformatic analysis

6.3.1 Gene enrichment analysis

RNAseq of the osteoblast transcriptome following treatment with EVs isolated from the prostate cancer cell line PC3 and the non-malignant prostate cell line PNT1A, highlighted the regulation of alternative transcripts as an important change as a result of EV treatment. In cancer cells canonical splicing of genes is commonly altered (Sveen *et al.*, 2015) and this is likely to drive oncogenesis through the formation of transcript isoforms (Oltean and Bates, 2013). Multiple isoforms have previously been identified in genes affecting oncogenesis, for example *Bcl-x* has two isoforms which have opposite effects (Cloutier *et al.*, 2008). *Bcl-xs* is pro-apoptotic and *Bcl-xl* is anti-apoptotic due to alternative splicing through alternative 5' prime splice selection (Cloutier *et al.*, 2008). The tumour suppressors *PTEN* and *p53* are also known to have more than one splice variant which affects their function (Oltean and Bates, 2013). There is usually tissue specificity to determine which isoform is more highly expressed (Sveen *et al.*, 2015) but in cancer cells the balance of these isoforms can be altered to favour tumour progression (Oltean and Bates, 2013). Given 7% of genes produced differentially regulated transcripts suggests a role for EVs in controlling the predominance of specific gene transcripts, how this potential promotes tumour progression remains to be determined.

6.3.2 hOB cells treated with PNT1A EVs vs hOB cells treated with PC3 EVs KEGG pathway analysis

Several of the genes were found to produce multiple transcripts, which following exposure to EVs were differentially regulated. These are represented

on the KEGG pathways as showing both up and down-regulation, as without further investigation of the function of these alternative transcripts the true effect on the molecular pathways cannot be determined. Additionally, in some cases the KEGG pathway only includes the family name and not the individual genes and so where genes in the same family showed opposing expression they are highlighted as being both up and downregulated.

Cyclin dependent kinases (CDKs) are important controls for the progression of the cell cycle and form complexes which trigger apoptosis in response to deviance from normal replication (Casimiro *et al.*, 2012). Cyclin D1 (CCND1) is produced in response to mitogenic stimuli (Balk and Knudsen, 2008) and, along with its complexes CDK4 and CDK6, was upregulated in the cell cycle and cellular senescence pathways (Figure 5.4 and Figure 5.5). This suggests increased progression through the cell cycle of hOB cells treated with PC3 EVs through activation of associated target genes (Casimiro *et al.*, 2012). CCND1 has many functions including its importance for the development of the chromosomal instability (Casimiro *et al.*, 2012) which increases alteration of the genome and has the potential to give rise to phenotypic changes (Bayani *et al.*, 2007) in hOB cells. Cyclins A (CCNA) and B (CCNB) were downregulated in both these pathways in contrast to the findings of Wegiel *et al.* (2008), who found that expression of CCNA1 increased in patients with advanced prostate cancer. However, Arsic *et al.* (2012) found that CCNA2 depletion resulted in increased cell migration, an important requirement for metastatic cells, and that CCNA2 expression was lower in metastases. This study examined cyclin expression in osteoblasts, therefore, the changes in cyclin expression may

reflect the need for osteoblast migration to remodel bone. Bone remodelling releases bone derived growth factors which encourage cancer cell growth (David Roodman and Silbermann, 2015). Cancer cells in turn release osteoblastic factors to increase differentiation and proliferation, resulting in a vicious cycle to promote bone metastasis (Roodman and Silbermann, 2015).

Dysregulation of proteoglycans would be expected in metastatic bone lesions due to their role within the bone ECM for skeletal development (Lamoureux *et al.*, 2007). Decorin is a small leucine rich repeat proteoglycan (SLRP) which was downregulated in hOB cells treated with PC3 EVs (Figure 5.6). This is likely to affect the structural organisation of the bone matrix and cause changes in collagen fibril size (Lamoureux *et al.*, 2007). There was altered expression of genes within the heparin sulphate proteoglycan pathway which has been implicated in bone cancer and metastases development through sequestration of chemokines and growth factors (Lamoureux *et al.*, 2007). FGF-2 and VEGF were downregulated in this pathway which may be due to this sequestration in response to the treatment with the PC3 EVs.

The cell adhesion molecules pathway (Figure 5.7) showed upregulation of ICAM-1, an adhesion molecule cited as being important for the adhesion of CTCs to the cells in the niche to enable metastatic colonisation (Ren *et al.*, 2015). This suggests osteoblasts are undergoing changes to increase their ability to accommodate metastatic cells. This pathway also showed altered expression of claudin (CLDN), an important protein family for the formation and function of tight junctions between cells (Hewitt *et al.*, 2006). CLDN3 and

CLDN4 were upregulated, whereas CLDN11 was downregulated. Claudins are potentially responsible for the variation in cell permeability through changes at cell-to-cell tight junctions (Tsukita and Furuse, 2000). This indicates that the osteoblasts treated with PC3 EVs may undergo changes affecting their intercellular adhesion and migration within the bone niche. Migration of osteoblasts, which are important regulators of the hematopoietic stem cell (HSC) niche (Pedersen *et al.*, 2012), is an important feature to make way for engraftment of CTCs which have been noted to compete for space in the HSC niche (Shiozawa *et al.*, 2011). Shiozawa *et al.* (2011) also reported that increased numbers of osteoblasts resulted in increased likelihood of bone metastases developing suggesting that genes promoting osteoblast proliferation ultimately aid metastasis.

The Wnt signalling pathway (Figure 5.8) regulates cell growth, differentiation and cell death (Krishnan *et al.*, 2006). This pathway is always activated by Wnt protein binding to frizzled protein family members and following this there are three different pathways through which Wnt signalling can occur (Krishnan *et al.*, 2006). Most relevant to bone is the canonical or β-catenin Wnt signalling pathway as this increases bone mass through regulation of osteoblasts (Krishnan *et al.*, 2006). The canonical pathway increases osteoblast survival and proliferation through prevention of degradation of β-catenin and alteration of its subcellular localisation (Westendorf *et al.*, 2004). Wnt was upregulated in osteoblasts treated with PC3 EVs and Frizzled 8 (FZD8) was similarly upregulated whilst Frizzled 7 was downregulated (Figure 5.8). Despite the upregulation of Wnt, the β-catenin transcript is downregulated which suggests

that the survival of these cells may not be protected. DKK, an inhibitor of the frizzled receptor in this pathway, was found to be upregulated. Since this protein is also an inhibitor of osteoblastogenesis (Westendorf *et al.*, 2004) its upregulation may have reduced osteoblast proliferation. As well as its role in the prevention of apoptosis β-catenin is important to link the actin cytoskeleton with cadherins and so plays a role in cell adhesion and migration (Westendorf *et al.*, 2004). Presumably in response to the low β-catenin expression, TCF transcription factor expression was downregulated in this pathway. Despite this there was still increased expression of the proto-oncogene c-myc suggesting that this gene may be activated through other mechanisms, highlighting the complexity of biological pathway interactions.

The PI3K-AKT signalling pathway is important for regulation of cellular growth, proliferation and survival (Vara *et al*., 2004). Changes to this signalling pathway have been previously associated with prostate cancer development (Mulholland *et al*., 2012) and our data found that it was significantly enriched in downregulated genes (Figure 5.9). Figure 5.9 show upregulation of genes associated with cell cycle progression and downregulation of *PTEN,* an important tumour suppressor (Song *et al*., 2012). The downregulation of *PTEN* leads to excessive recruitment of AKT proteins which are responsible for cell survival, proliferation and metabolism through downstream signalling (Song *et al*., 2012) so its downregulation in our results suggests that multiple changes could be occurring in the osteoblast cells. *PTEN* has also been suggested to play an important role in regulating the tumour microenvironment through inhibition of stromal fibroblasts (Trimboli *et al*., 2009). Trimboli *et al.* (2009)

found that *PTEN* deletion in fibroblast cells caused increased speed of invasion and colonisation by mammary epithelial tumour cells. Although this study looked at the fibroblasts and mammary tumour cells osteoblasts play a similarly significant role in stromal regulation (Jeong *et al*., 2016) and therefor the downregulation of *PTEN* could have a similarly pro-oncogenic effect. Metabolic reprogramming has been suggested to be an important adaption of cells prior to development of cancer characteristics (Vander Heiden *et al.*, 2009). The increased cell proliferation and cell cycle progression means that glycolysis is increased to keep up with cellular energy demands (Vander Heiden *et al.*, 2009) which may explain the upregulation of genes associated with glycolysis seen in Figure 5.9 and suggests that the osteoblasts are undergoing changes compatible with cancer development.

Downregulation of *p53*, an important tumour suppressor gene, enables proliferation and increased cell survival (Wang *et al.*, 2006). In addition to its role as a tumour suppressor, *p53* is a negative regulator of osteoblast differentiation through suppression of the osteoblast specific transcription factor, osterix (Wang *et al.*, 2006). The downregulation of *p53* in the osteoblast cells treated with PC3 EVs may increase differentiation and thereby increase osteoblast numbers (Wang *et al.*, 2006). Wang *et al.* (2006) found that mice which did not express *p53* had higher bone density that the wild-type mice, which fits with the common clinical presentation of metastatic prostate cancer bone lesions (Roudier *et al.*, 2008). Metastatic prostate cancer bone lesions commonly appear osteoblastic on radiographic imaging and yet patients are at increased risk of fractures (Roudier *et al.*, 2008). Examination of bone biopsies

from 12 patients who died of metastatic prostate cancer by Roudier *et al.* (2008) showed that within each patient there was variation of histology from osteodense to osteopenic phenotypes, sometimes within the same biopsy, indicating a complex interaction between blastic and lytic bone remodelling. Further to this, the osteodense lesions were commonly made up of woven bone without significant amounts of osteoid which weakens the resulting bone despite increased osteoblast activity.

The dysregulation of these pathways affects osteoblast regulation either directly or through links between the genes within the pathways. There is not altered expression of RANK and RANKL, important for osteoclast regulation (Naito *et al.*, 2001), but the competitive inhibitor OPG (Schoppet *et al.*, 2002) was downregulated suggesting that this pathway is likely still active.

Overall, the results suggest exposure of osteoblasts to prostate cancer EVs could potentially result in increased proliferation and altered interaction with the microenvironment promoting cell migration and altering the balance of bone resorption and production in favour of osteoblasts. Given the importance of osteoblast function in prostate cancer bone metastasis, this data supports the re-education of osteoblasts by the prostate cancer EVs to promote an environment primed towards the formation of osteoblastic bone lesions. Further investigation using *in vivo* models of prostate bone metastasis would demonstrate the feasibility of this proposed hypothesis.

6.4 Conclusions

In conclusion, the data presented within this project shows that osteoblast cells can be functionally altered by their interaction with miRNAs and other small RNAs delivered by prostate cancer EVs. The level of functionality of transferred miRNAs compared to endogenous miRNAs remains to be fully elucidated. This is an important finding given EVs may deliver these miRNAs both locally to aid primary tumour development and also in distant tissues to create a pre-metastatic niche. The RNAseq data showing alteration of the osteoblast transcriptome supports the ability of PC3 EVs to aid with pre-metastatic niche formation through alteration of gene expression potentially resulting in increased osteoblast survival, differentiation and proliferation. Treatment with PC3 EVs may also alter the osteoblasts' ability to interact with the microenvironments thereby priming the bone niche for potential metastatic colonisation. These changes have yet to be definitively linked to the EV miRNA cargo but the data supports at least a partial role for transferred miRNA activity. All experiments were conducted *in vitro* and therefore further investigation is necessary to confirm whether prostate cancer communication in the development of metastasis occurs similarly *in vivo.* Additionally the development of new tools capable of determining the specific role of miRNAs within EV cargos will be important for development of potential therapeutics to prevent EV mediated prostate cancer communication to metastatic lesions.

7 References

ADAM, B.-L., QU, Y., DAVIS, J. W., WARD, M. D., CLEMENTS, M. A., CAZARES, L. H., SEMMES, O. J., SCHELLHAMMER, P. F., YASUI, Y., FENG, Z. & WRIGHT, G. L. 2002. Serum Protein Fingerprinting Coupled with a Pattern-matching Algorithm Distinguishes Prostate Cancer from Benign Prostate Hyperplasia and Healthy Men. *Cancer Research,* 62**,** 3609-3614.

AGAOGLU, Y. F., KOVANCILAR, M., DIZDAR, Y., DARENDELILER, E., HOLDENRIEDER, S., DALAY, N. & GEZER, U. 2011. Investigation of miR-21, miR-141, and miR-221 in blood circulation of patients with prostate cancer. *Tumour Biol,* 32**,** 583-8.

AIHARA, M., TRUONG, L. D., DUNN, J. K., WHEELER, T. M., SCARDINO, P. T. & THOMPSON, T. C. 1994. Frequency of apoptotic bodies positively correlates with Gleason grade in prostate cancer. *Human Pathology,* 25**,** 797-801.

AJCC 2018. *AJCC Cancer Staging Manual*, Springer.

AKERS, J. C., GONDA, D., KIM, R., CARTER, B. S. & CHEN, C. C. 2013. Biogenesis of extracellular vesicles (EV): exosomes, microvesicles, retrovirus-like vesicles, and apoptotic bodies. *Journal of neuro-oncology,* 113**,** 1-11.

AMBS, S., PRUEITT, R. L., YI, M., HUDSON, R. S., HOWE, T. M., PETROCCA, F., WALLACE, T. A., LIU, C. G., VOLINIA, S., CALIN, G. A., YFANTIS, H. G., STEPHENS, R. M. & CROCE, C. M. 2008. Genomic profiling of microRNA and messenger RNA reveals deregulated microRNA expression in prostate cancer. *Cancer Res,* 68**,** 6162-70.

ANDERSON, S. I., DOWNES, S., PERRY, C. C. & CABALLERO, A. M. 1998. Evaluation of the osteoblast response to a silica gel in vitro. *Journal of Materials Science: Materials in Medicine,* 9**,** 731-735.

ARROYO, J. D., CHEVILLET, J. R., KROH, E. M., RUF, I. K., PRITCHARD, C. C., GIBSON, D. F., MITCHELL, P. S., BENNETT, C. F., POGOSOVA-AGADJANYAN, E. L., STIREWALT, D. L., TAIT, J. F. & TEWARI, M. 2011. Argonaute2 complexes carry a population of circulating microRNAs independent of vesicles in human plasma. *Proceedings of the National Academy of Sciences,* 108**,** 5003-5008.

ARSIC, N., BENDRIS, N., PETER, M., BEGON-PESCIA, C., REBOUISSOU, C., GADÉA, G., BOUQUIER, N., BIBEAU, F., LEMMERS, B. & BLANCHARD, J. M. 2012. A novel function for Cyclin A2: Control of cell invasion via RhoA signaling. *The Journal of Cell Biology,* 196**,** 147-162.

BALK, S. P. & KNUDSEN, K. E. 2008. AR, the cell cycle, and prostate cancer. *Nuclear Receptor Signaling,* 6**,** e001.

BALK, S. P., KO, Y. J. & BUBLEY, G. J. 2003. Biology of prostate-specific antigen. *J Clin Oncol,* 21**,** 383-91.

BARAN, J., BAJ-KRZYWORZEKA, M., WEGLARCZYK, K., SZATANEK, R., ZEMBALA, M., BARBASZ, J., CZUPRYNA, A., SZCZEPANIK, A. & ZEMBALA, M. 2010. Circulating tumour-derived microvesicles in plasma of gastric cancer patients. *Cancer Immunol Immunother,* 59**,** 841-50.

BAUS, T. B. A. O. U. S. 2014. Analyses of Prostetectomy Dataset January 1st-31st December 2013. *In:* FOWLER, S. (ed.). The British Association of Urological Surgeons.

BAYANI, J., SELVARAJAH, S., MAIRE, G., VUKOVIC, B., AL-ROMAIH, K., ZIELENSKA, M. & SQUIRE, J. A. 2007. Genomic mechanisms and measurement of structural and numerical instability in cancer cells. *Seminars in Cancer Biology,* 17**,** 5-18.

BILL-AXELSON, A., HOLMBERG, L., RUUTU, M., HÄGGMAN, M., ANDERSSON, S.-O., BRATELL, S., SPÅNGBERG, A., BUSCH, C., NORDLING, S. & GARMO, H. 2005. Radical prostatectomy versus watchful waiting in early prostate cancer. *New England journal of medicine,* 352**,** 1977-1984.

BOULAIS, P. E. & FRENETTE, P. S. 2015. Making sense of hematopoietic stem cell niches. *Blood,* 125**,** 2621-2629.

BRASE, J. C., JOHANNES, M., SCHLOMM, T., FALTH, M., HAESE, A., STEUBER, T., BEISSBARTH, T., KUNER, R. & SULTMANN, H. 2011. Circulating miRNAs are correlated with tumor progression in prostate cancer. *Int J Cancer,* 128**,** 608-16.

BRAY, N. L., PIMENTEL, H., MELSTED, P. & PACHTER, L. 2016. Near-optimal probabilistic RNA-seq quantification. *Nature Biotechnology,* 34**,** 525.

BRYANT, R. J., PAWLOWSKI, T., CATTO, J. W., MARSDEN, G., VESSELLA, R. L., RHEES, B., KUSLICH, C., VISAKORPI, T. & HAMDY, F. C. 2012. Changes in circulating microRNA levels associated with prostate cancer. *Br J Cancer,* 106**,** 768-74.

BUCHANAN, G., GREENBERG, N. M., SCHER, H. I., HARRIS, J. M., MARSHALL, V. R. & TILLEY, W. D. 2001. Collocation of androgen receptor gene mutations in prostate cancer. *Clin Cancer Res,* 7**,** 1273-81.

CALAIS DA SILVA, F. E., BONO, A. V., WHELAN, P., BRAUSI, M., MARQUES QUEIMADELOS, A., MARTIN, J. A., KIRKALI, Z., CALAIS DA SILVA, F. M. & ROBERTSON, C. 2009. Intermittent androgen deprivation for locally advanced and metastatic prostate cancer: results from a randomised phase 3 study of the South European Uroncological Group. *Eur Urol,* 55**,** 1269-77.

CALIN, G. A., SEVIGNANI, C., DUMITRU, C. D., HYSLOP, T., NOCH, E., YENDAMURI, S., SHIMIZU, M., RATTAN, S., BULLRICH, F., NEGRINI, M. & CROCE, C. M. 2004. Human microRNA genes are frequently

located at fragile sites and genomic regions involved in cancers. *Proc Natl Acad Sci U S A,* 101**,** 2999-3004.

CASIMIRO, M. C., CROSARIOL, M., LORO, E., LI, Z. & PESTELL, R. G. 2012. Cyclins and Cell Cycle Control in Cancer and Disease. *Genes Cancer,* 3**,** 649-57.

CHEN, N. & ZHOU, Q. 2016. The evolving Gleason grading system. *Chinese Journal of Cancer Research,* 28**,** 58-64.

CLOUTIER, P., TOUTANT, J., SHKRETA, L., GOEKJIAN, S., REVIL, T. & CHABOT, B. 2008. Antagonistic effects of the SRp30c protein and cryptic 5' splice sites on the alternative splicing of the apoptotic regulator Bcl-x. *J Biol Chem,* 283**,** 21315-24.

COHEN, S. J., PUNT, C. J., IANNOTTI, N., SAIDMAN, B. H., SABBATH, K. D., GABRAIL, N. Y., PICUS, J., MORSE, M., MITCHELL, E., MILLER, M. C., DOYLE, G. V., TISSING, H., TERSTAPPEN, L. W. & MEROPOL, N. J. 2008. Relationship of circulating tumor cells to tumor response, progression-free survival, and overall survival in patients with metastatic colorectal cancer. *J Clin Oncol,* 26**,** 3213-21.

CORTEZ, M. A., BUESO-RAMOS, C., FERDIN, J., LOPEZ-BERESTEIN, G., SOOD, A. K. & CALIN, G. A. 2011. MicroRNAs in body fluids--the mix of hormones and biomarkers. *Nat Rev Clin Oncol,* 8**,** 467-77.

CRAWFORD, E. D. & HOU, A. H. 2009. The role of LHRH antagonists in the treatment of prostate cancer. *Oncology (Williston Park),* 23**,** 626-30.

CRISTOFANILLI, M., BUDD, G. T., ELLIS, M. J., STOPECK, A., MATERA, J., MILLER, M. C., REUBEN, J. M., DOYLE, G. V., ALLARD, W. J., TERSTAPPEN, L. W. & HAYES, D. F. 2004. Circulating tumor cells, disease progression, and survival in metastatic breast cancer. *N Engl J Med,* 351**,** 781-91.

CROCE, C. M. 2009. Causes and consequences of microRNA dysregulation in cancer. *Nature reviews. Genetics,* 10**,** 704-714.

CROSET, M., KAN, C. & CLEZARDIN, P. 2015. Tumour-derived miRNAs and bone metastasis. *Bonekey Rep,* 4**,** 688.

CULIG, Z., HOBISCH, A., CRONAUER, M. V., RADMAYR, C., TRAPMAN, J., HITTMAIR, A., BARTSCH, G. & KLOCKER, H. 1994. Androgen Receptor Activation in Prostatic Tumor Cell Lines by Insulin-like Growth Factor-I, Keratinocyte Growth Factor, and Epidermal Growth Factor. *Cancer Research,* 54**,** 5474-5478.

DANNEMAN, D., DREVIN, L., DELAHUNT, B., SAMARATUNGA, H., ROBINSON, D., BRATT, O., LOEB, S., STATTIN, P. & EGEVAD, L. 2017. Accuracy of prostate biopsies for predicting Gleason score in radical prostatectomy specimens: nationwide trends 2000–2012. *BJU International,* 119**,** 50-56.

DAVEY, R. A. & GROSSMANN, M. 2016. Androgen Receptor Structure, Function and Biology: From Bench to Bedside. *Clin Biochem Rev,* 37**,** 3-15.

DAVID ROODMAN, G. & SILBERMANN, R. 2015. Mechanisms of osteolytic and osteoblastic skeletal lesions. *BoneKEy Rep,* 4.

DE MARZO, A. M., PLATZ, E. A., SUTCLIFFE, S., XU, J., GRÖNBERG, H., DRAKE, C. G., NAKAI, Y., ISAACS, W. B. & NELSON, W. G. 2007. Inflammation in prostate carcinogenesis. *Nature Reviews Cancer,* 7**,** 256.

DRAISMA, G., ETZIONI, R., TSODIKOV, A., MARIOTTO, A., WEVER, E., GULATI, R., FEUER, E. & DE KONING, H. 2009. Lead Time and Overdiagnosis in Prostate-Specific Antigen Screening: Importance of Methods and Context. *JNCI Journal of the National Cancer Institute,* 101**,** 374-383.

ECACC. *ECACC General Cell Collection: PC-3* [Online]. https://www.phe-culturecollections.org.uk/products/celllines/generalcell/detail.jsp?refId=90112714&collection=ecacc_gc: Public Health England, . [Accessed 03.10.17 2017].

EGEVAD, L., GRANFORS, T., KARLBERG, L., BERGH, A. & STATTIN, P. 2002. Prognostic value of the Gleason score in prostate cancer. *BJU International,* 89**,** 538-542.

EGEVAD, L., NORLEN, B. J. & NORBERG, M. 2001. The value of multiple core biopsies for predicting the Gleason score of prostate cancer. *BJU Int,* 88**,** 716-21.

ELLINGER, J., MÜLLER, S. C., STADLER, T. C., JUNG, A., VON RUECKER, A. & BASTIAN, P. J. 2011. The role of cell-free circulating DNA in the diagnosis and prognosis of prostate cancer. *Urologic Oncology: Seminars and Original Investigations,* 29**,** 124-129.

ETZIONI, R., PENSON, D. F., LEGLER, J. M., DI TOMMASO, D., BOER, R., GANN, P. H. & FEUER, E. J. 2002. Overdiagnosis Due to Prostate-Specific Antigen Screening: Lessons From U.S. Prostate Cancer Incidence Trends. *JNCI: Journal of the National Cancer Institute,* 94**,** 981-990.

FARACE, F., MASSARD, C., VIMOND, N., DRUSCH, F., JACQUES, N., BILLIOT, F., LAPLANCHE, A., CHAUCHEREAU, A., LACROIX, L., PLANCHARD, D., LE MOULEC, S., ANDRE, F., FIZAZI, K., SORIA, J. C. & VIELH, P. 2011. A direct comparison of CellSearch and ISET for circulating tumour-cell detection in patients with metastatic carcinomas. *Br J Cancer,* 105**,** 847-853.

FELDMAN, B. J. & FELDMAN, D. 2001. The development of androgen-independent prostate cancer. *Nat Rev Cancer,* 1**,** 34-45.

FIDLER, I. J. 1970. Metastasis: Quantitative Analysis of Distribution and Fate of Tumor Emboli Labeled With 125I-5-Iodo-2′ -

deoxyuridine23. *JNCI: Journal of the National Cancer Institute,* 45**,** 773-782.

FINE, S. W. & MEHRA, R. 2015. Anatomy of the Prostate Revisited: Implications for Prostate Biopsy and Zonal Origins of Prostate Cancer. *In:* MAGI-GALLUZZI, C. & PRZYBYCIN, C. G. (eds.) *Genitourinary Pathology: Practical Advances.* New York, NY: Springer New York.

FUTTER, C. E. & WHITE, I. J. 2007. Annexins and Endocytosis. *Traffic,* 8**,** 951-958.

GAO, W., BOHL, C. E. & DALTON, J. T. 2005. Chemistry and Structural Biology of Androgen Receptor. *Chem Rev,* 105**,** 3352-70.

GEOSPIZA 2016. FinchTV. 1.4 ed.: Geospiza.

GERKE, V. & MOSS, S. E. 2002. Annexins: from structure to function. *Physiol Rev,* 82**,** 331-71.

GLEASON, D. F. 1966. Classification of prostatic carcinomas. *Cancer chemotherapy reports,* 50**,** 125-128.

GOESSL, C., MULLER, M., HEICAPPELL, R., KRAUSE, H. & MILLER, K. 2001. DNA-based detection of prostate cancer in blood, urine, and ejaculates. *Ann N Y Acad Sci,* 945**,** 51-8.

GOTO, Y., KUROZUMI, A., ENOKIDA, H., ICHIKAWA, T. & SEKI, N. 2015a. Functional significance of aberrantly expressed microRNAs in prostate cancer. *International Journal of Urology* 22**,** 242-52.

GOTO, Y., KUROZUMI, A., ENOKIDA, H., ICHIKAWA, T. & SEKI, N. 2015b. Functional significance of aberrantly expressed microRNAs in prostate cancer. *International Journal of Urology,* 22**,** 242-52.

GRAPHPAD SOFTWARE 2017. GraphPad Prism 7.01. https://www.graphpad.com/scientific-software/prism/.

GREGORY, C. W., JOHNSON, R. T., JR., MOHLER, J. L., FRENCH, F. S. & WILSON, E. M. 2001. Androgen receptor stabilization in recurrent prostate cancer is associated with hypersensitivity to low androgen. *Cancer Res,* 61**,** 2892-8.

GRIFFITHS-JONES, S. 2004. The microRNA Registry. *Nucleic Acids Res,* 32**,** D109-11.

GUO, W., REN, D., CHEN, X., TU, X., HUANG, S., WANG, M., SONG, L., ZOU, X. & PENG, X. 2013. HEF1 promotes epithelial mesenchymal transition and bone invasion in prostate cancer under the regulation of microRNA-145. *J Cell Biochem,* 114**,** 1606-15.

GURURAJAN, M., JOSSON, S., CHU, G. C., LU, C. L., LU, Y. T., HAGA, C. L., ZHAU, H. E., LIU, C., LICHTERMAN, J., DUAN, P., POSADAS, E. M. & CHUNG, L. W. 2014. miR-154* and miR-379 in the DLK1-DIO3 microRNA mega-cluster regulate epithelial to mesenchymal transition and bone metastasis of prostate cancer. *Clin Cancer Res,* 20**,** 6559-69.

HEMLER, M. E. 2005. Tetraspanin functions and associated microdomains. *Nature Reviews Molecular Cell Biology,* 6**,** 801.
HENSEL, J. & THALMANN, G. N. 2016. Biology of Bone Metastases in Prostate Cancer. *Urology,* 92**,** 6-13.
HESSVIK, N. P., PHUYAL, S., BRECH, A., SANDVIG, K. & LLORENTE, A. 2012. Profiling of microRNAs in exosomes released from PC-3 prostate cancer cells. *Biochim Biophys Acta,* 1819**,** 1154-63.
HEWITT, K. J., AGARWAL, R. & MORIN, P. J. 2006. The claudin gene family: expression in normal and neoplastic tissues. *BMC Cancer,* 6**,** 186.
HIRATA, H., UENO, K., SHAHRYARI, V., DENG, G., TANAKA, Y., TABATABAI, Z. L., HINODA, Y. & DAHIYA, R. 2013. MicroRNA-182-5p promotes cell invasion and proliferation by down regulating FOXF2, RECK and MTSS1 genes in human prostate cancer. *PLoS One,* 8**,** e55502.
HOSHINO, A., COSTA-SILVA, B., SHEN, T. L., RODRIGUES, G., HASHIMOTO, A., TESIC MARK, M., MOLINA, H., KOHSAKA, S., DI GIANNATALE, A., CEDER, S., SINGH, S., WILLIAMS, C., SOPLOP, N., URYU, K., PHARMER, L., KING, T., BOJMAR, L., DAVIES, A. E., ARARSO, Y., ZHANG, T., ZHANG, H., HERNANDEZ, J., WEISS, J. M., DUMONT-COLE, V. D., KRAMER, K., WEXLER, L. H., NARENDRAN, A., SCHWARTZ, G. K., HEALEY, J. H., SANDSTROM, P., LABORI, K. J., KURE, E. H., GRANDGENETT, P. M., HOLLINGSWORTH, M. A., DE SOUSA, M., KAUR, S., JAIN, M., MALLYA, K., BATRA, S. K., JARNAGIN, W. R., BRADY, M. S., FODSTAD, O., MULLER, V., PANTEL, K., MINN, A. J., BISSELL, M. J., GARCIA, B. A., KANG, Y., RAJASEKHAR, V. K., GHAJAR, C. M., MATEI, I., PEINADO, H., BROMBERG, J. & LYDEN, D. 2015. Tumour exosome integrins determine organotropic metastasis. *Nature,* 527**,** 329-35.
HUANG, S. P., LÉVESQUE, E., GUILLEMETTE, C., YU, C. C., HUANG, C. Y., LIN, V. C., CHUNG, I. C., CHEN, L. C., LAVERDIÈRE, I., LACOMBE, L., FRADET, Y., CHANG, T. Y., LEE, H. Z., JUANG, S. H. & BAO, B. Y. 2014. Genetic variants in microRNAs and microRNA target sites predict biochemical recurrence after radical prostatectomy in localized prostate cancer. *International Journal of Cancer,* 135**,** 2661-2667.
HUDSON, R. S., YI, M., ESPOSITO, D., GLYNN, S. A., STARKS, A. M., YANG, Y., SCHETTER, A. J., WATKINS, S. K., HURWITZ, A. A., DORSEY, T. H., STEPHENS, R. M., CROCE, C. M. & AMBS, S. 2013. MicroRNA-106b-25 cluster expression is associated with early disease recurrence and targets caspase-7 and focal adhesion in human prostate cancer. *Oncogene,* 32**,** 4139-4147.
HUSSAIN, M., TANGEN, C. M., BERRY, D. L., HIGANO, C. S., CRAWFORD, E. D., LIU, G., WILDING, G., PRESCOTT, S., KANAGA SUNDARAM, S.,

SMALL, E. J., DAWSON, N. A., DONNELLY, B. J., VENNER, P. M., VAISHAMPAYAN, U. N., SCHELLHAMMER, P. F., QUINN, D. I., RAGHAVAN, D., ELY, B., MOINPOUR, C. M., VOGELZANG, N. J. & THOMPSON, I. M., JR. 2013. Intermittent versus continuous androgen deprivation in prostate cancer. *N Engl J Med,* 368**,** 1314-25.

IQWIG - INSTITUTE FOR QUALITY AND EFFICIENCY IN HEALTH CARE. 2016. *How does the prostate work?* [Online]. https://www.ncbi.nlm.nih.gov/pubmedhealth/PMH0072475/: PubMed Health. [Accessed 10.10.17 2017].

ISAACS, J. T. 1999. The biology of hormone refractory prostate cancer. Why does it develop? *Urol Clin North Am,* 26**,** 263-73.

JACOBS, S. C. 1983. Spread of prostatic cancer to bone. *Urology,* 21**,** 337-344.

JAIN, S., BHOJWANI, A. G. & MELLON, J. K. 2002. Improving the utility of prostate specific antigen (PSA) in the diagnosis of prostate cancer: the use of PSA derivatives and novel markers. *Postgraduate Medical Journal,* 78**,** 646.

JEONG, H. M., CHO, S. W. & PARK, S. I. 2016. Osteoblasts Are the Centerpiece of the Metastatic Bone Microenvironment. *Endocrinology and Metabolism,* 31**,** 485-492.

JIANG, H., LEI, R., DING, S.-W. & ZHU, S. 2014. Skewer: a fast and accurate adapter trimmer for next-generation sequencing paired-end reads. *BMC Bioinformatics,* 15**,** 182.

JOSSON, S., GURURAJAN, M., HU, P., SHAO, C., CHU, G. Y., ZHAU, H. E., LIU, C., LAO, K., LU, C. L., LU, Y. T., LICHTERMAN, J., NANDANA, S., LI, Q., ROGATKO, A., BEREL, D., POSADAS, E. M., FAZLI, L., SAREEN, D. & CHUNG, L. W. 2014. miR-409-3p/-5p promotes tumorigenesis, epithelial-to-mesenchymal transition, and bone metastasis of human prostate cancer. *Clin Cancer Res,* 20**,** 4636-46.

JUCKEM, L. 2012. *Cellular Toxicity Caused by Transfection: Why is it important?* [Online]. https://www.biocompare.com/Bench-Tips/121111-Cellular-Toxicity-Caused-by-Transfection-Why-is-it-important/: Biocompare. Available: https://www.biocompare.com/Bench-Tips/121111-Cellular-Toxicity-Caused-by-Transfection-Why-is-it-important/ [Accessed 19.03.18 2018].

KAIGHN, M. E., NARAYAN, K. S., OHNUKI, Y., LECHNER, J. F. & JONES, L. W. 1979. Establishment and characterization of a human prostatic carcinoma cell line (PC-3). *Investigative urology,* 17**,** 16-23.

KANEHISA, M., SATO, Y., KAWASHIMA, M., FURUMICHI, M. & TANABE, M. 2016. KEGG as a reference resource for gene and protein annotation. *Nucleic Acids Research,* 44**,** D457-D462.

KASHYAP, V., AHMAD, S., NILSSON, E. M., HELCZYNSKI, L., KENNA, S., PERSSON, J. L., GUDAS, L. J. & MONGAN, N. P. 2013. The lysine specific demethylase-1 (LSD1/KDM1A) regulates VEGF-A expression in prostate cancer. *Mol Oncol,* 7**,** 555-66.

KESHAVA PRASAD, T. S., GOEL, R., KANDASAMY, K., KEERTHIKUMAR, S., KUMAR, S., MATHIVANAN, S., TELIKICHERLA, D., RAJU, R., SHAFREEN, B., VENUGOPAL, A., BALAKRISHNAN, L., MARIMUTHU, A., BANERJEE, S., SOMANATHAN, D. S., SEBASTIAN, A., RANI, S., RAY, S., HARRYS KISHORE, C. J., KANTH, S., AHMED, M., KASHYAP, M. K., MOHMOOD, R., RAMACHANDRA, Y. L., KRISHNA, V., RAHIMAN, B. A., MOHAN, S., RANGANATHAN, P., RAMABADRAN, S., CHAERKADY, R. & PANDEY, A. 2009. Human Protein Reference Database—2009 update. *Nucleic Acids Research,* 37**,** D767-D772.

KIM, H. K., SONG, K. S., PARK, Y. S., KANG, Y. H., LEE, Y. J., LEE, K. R., KIM, H. K., RYU, K. W., BAE, J. M. & KIM, S. 2003. Elevated levels of circulating platelet microparticles, VEGF, IL-6 and RANTES in patients with gastric cancer: possible role of a metastasis predictor. *Eur J Cancer,* 39**,** 184-91.

KOIVISTO, P., KONONEN, J., PALMBERG, C., TAMMELA, T., HYYTINEN, E., ISOLA, J., TRAPMAN, J., CLEUTJENS, K., NOORDZIJ, A., VISAKORPI, T. & KALLIONIEMI, O. P. 1997. Androgen receptor gene amplification: a possible molecular mechanism for androgen deprivation therapy failure in prostate cancer. *Cancer Res,* 57**,** 314-9.

KOPRESKI, M. S., BENKO, F. A. & GOCKE, C. D. 2001. Circulating RNA as a Tumor Marker. *Annals of the New York Academy of Sciences,* 945**,** 172-178.

KORFAGE, I. J., ESSINK-BOT, M. L., BORSBOOM, G. J., MADALINSKA, J. B., KIRKELS, W. J., HABBEMA, J. D., SCHRODER, F. H. & DE KONING, H. J. 2005. Five-year follow-up of health-related quality of life after primary treatment of localized prostate cancer. *Int J Cancer,* 116**,** 291-6.

KOWAL, J., TKACH, M. & THÉRY, C. 2014. Biogenesis and secretion of exosomes. *Current Opinion in Cell Biology,* 29**,** 116-125.

KRISHNAN, V., BRYANT, H. U. & MACDOUGALD, O. A. 2006. Regulation of bone mass by Wnt signaling. *Journal of Clinical Investigation,* 116**,** 1202-1209.

LAMBA, V., GHODKE-PURANIK, Y., GUAN, W. & LAMBA, J. K. 2014. Identification of suitable reference genes for hepatic microRNA quantitation. *BMC Res Notes,* 7**,** 129.

LAMOUREUX, F., BAUD'HUIN, M., DUPLOMB, L., HEYMANN, D. & RÉDINI, F. 2007. Proteoglycans: key partners in bone cell biology. *BioEssays,* 29**,** 758-771.

LANGHORST, M. F., REUTER, A. & STUERMER, C. A. 2005. Scaffolding microdomains and beyond: the function of reggie/flotillin proteins. *Cell Mol Life Sci,* 62**,** 2228-40.

LE, M. T. N., TEH, C., SHYH-CHANG, N., XIE, H., ZHOU, B., KORZH, V., LODISH, H. F. & LIM, B. 2009. MicroRNA-125b is a novel negative regulator of p53. *Genes & Development,* 23**,** 862-876.

LEE, Y., EL ANDALOUSSI, S. & WOOD, M. J. A. 2012. Exosomes and microvesicles: extracellular vesicles for genetic information transfer and gene therapy. *Human Molecular Genetics,* 21**,** R125-R134.

LEITE, K. R., CANAVEZ, J. M., REIS, S. T., TOMIYAMA, A. H., PIANTINO, C. B., SANUDO, A., CAMARA-LOPES, L. H. & SROUGI, M. 2011a. miRNA analysis of prostate cancer by quantitative real time PCR: comparison between formalin-fixed paraffin embedded and fresh-frozen tissue. *Urol Oncol,* 29**,** 533-7.

LEITE, K. R., SOUSA-CANAVEZ, J. M., REIS, S. T., TOMIYAMA, A. H., CAMARA-LOPES, L. H., SANUDO, A., ANTUNES, A. A. & SROUGI, M. 2011b. Change in expression of miR-let7c, miR-100, and miR-218 from high grade localized prostate cancer to metastasis. *Urol Oncol,* 29**,** 265-9.

LEITE, K. R., TOMIYAMA, A., REIS, S. T., SOUSA-CANAVEZ, J. M., SANUDO, A., CAMARA-LOPES, L. H. & SROUGI, M. 2013. MicroRNA expression profiles in the progression of prostate cancer--from high-grade prostate intraepithelial neoplasia to metastasis. *Urol Oncol,* 31**,** 796-801.

LEITE, K. R. M., TOMIYAMA, A., REIS, S. T., SOUSA-CANAVEZ, J. M., SAÑUDO, A., DALL'OGLIO, M. F., CAMARA-LOPES, L. H. & SROUGI, M. 2011c. MicroRNA-100 Expression is Independently Related to Biochemical Recurrence of Prostate Cancer. *The Journal of Urology,* 185**,** 1118-1122.

LI, H., HANDSAKER, B., WYSOKER, A., FENNELL, T., RUAN, J., HOMER, N., MARTH, G., ABECASIS, G. & DURBIN, R. 2009. The Sequence Alignment/Map format and SAMtools. *Bioinformatics,* 25**,** 2078-9.

LI, T., LI, R.-S., LI, Y.-H., ZHONG, S., CHEN, Y.-Y., ZHANG, C.-M., HU, M.-M. & SHEN, Z.-J. 2012. miR-21 as an Independent Biochemical Recurrence Predictor and Potential Therapeutic Target for Prostate Cancer. *The Journal of Urology,* 187**,** 1466-1472.

LIOTTA, L. A., KLEINERMAN, J. & SALDEL, G. M. 1976. The Significance of Hematogenous Tumor Cell Clumps in the Metastatic Process. *Cancer Research,* 36**,** 889-894.

LIVAK, K. J. & SCHMITTGEN, T. D. 2001. Analysis of Relative Gene Expression Data Using Real-Time Quantitative PCR and the 2−ΔΔCT Method. *Methods,* 25**,** 402-408.

LOTVALL, J., HILL, A. F., HOCHBERG, F., BUZAS, E. I., DI VIZIO, D., GARDINER, C., GHO, Y. S., KUROCHKIN, I. V., MATHIVANAN, S., QUESENBERRY, P., SAHOO, S., TAHARA, H., WAUBEN, M. H., WITWER, K. W. & THERY, C. 2014. Minimal experimental requirements for definition of extracellular vesicles and their functions: a position statement from the International Society for Extracellular Vesicles. *J Extracell Vesicles,* 3**,** 26913.

LOTVALL, J. & VALADI, H. 2007. Cell to Cell Signalling via Exosomes Through esRNA. *Cell Adh Migr,* 1**,** 156-8.

MAGLOTT, D., OSTELL, J., PRUITT, K. D. & TATUSOVA, T. 2005. Entrez Gene: gene-centered information at NCBI. *Nucleic Acids Res,* 33**,** D54-8.

MAKRIDAKIS, N., ROSS, R. K., PIKE, M. C., CHANG, L., STANCZYK, F. Z., KOLONEL, L. N., SHI, C. Y., YU, M. C., HENDERSON, B. E. & REICHARDT, J. K. 1997. A prevalent missense substitution that modulates activity of prostatic steroid 5alpha-reductase. *Cancer Res,* 57**,** 1020-2.

MALIK, G., WARD, M. D., GUPTA, S. K., TROSSET, M. W., GRIZZLE, W. E., ADAM, B. L., DIAZ, J. I. & SEMMES, O. J. 2005. Serum levels of an isoform of apolipoprotein A-II as a potential marker for prostate cancer. *Clin Cancer Res,* 11**,** 1073-85.

MARIEB, E. N. & HOEHN, K. N. 2015. *Human Anatomy & Physiology, Global Edition*, Pearson Education Limited.

MARTIN, M. 2011. Cutadapt removes adapter sequences from high-throughput sequencing reads. *EMBnet.journal; Vol 17, No 1: Next Generation Sequencing Data Analysis*.

MATHIVANAN, S., JI, H. & SIMPSON, R. J. 2010. Exosomes: Extracellular organelles important in intercellular communication. *Journal of Proteomics,* 73**,** 1907-1920.

MAVROUDIS, D. 2010. Circulating cancer cells. *Annals of Oncology,* 21**,** vii95-vii100.

MAYER, M. P. & BUKAU, B. 2005. Hsp70 chaperones: Cellular functions and molecular mechanism. *Cell Mol Life Sci,* 62**,** 670-84.

MCDONNELL, T. J., TRONCOSO, P., BRISBAY, S. M., LOGOTHETIS, C., CHUNG, L. W., HSIEH, J. T., TU, S. M. & CAMPBELL, M. L. 1992. Expression of the protooncogene bcl-2 in the prostate and its association with emergence of androgen-independent prostate cancer. *Cancer Res,* 52**,** 6940-4.

MCNEAL, J. E. 1981. The zonal anatomy of the prostate. *Prostate,* 2**,** 35-49.

MEHDIANI, A., MAIER, A., PINTO, A., BARTH, M., AKHYARI, P. & LICHTENBERG, A. 2015. An Innovative Method for Exosome Quantification and Size Measurement. *Journal of Visualized Experiments : JoVE*, 50974.

MELO, S. A., SUGIMOTO, H., O'CONNELL, J. T., KATO, N., VILLANUEVA, A., VIDAL, A., QIU, L., VITKIN, E., PERELMAN, L. T., MELO, C. A., LUCCI, A., IVAN, C., CALIN, G. A. & KALLURI, R. 2014. Cancer exosomes perform cell-independent microRNA biogenesis and promote tumorigenesis. *Cancer Cell,* 26, 707-21.

MICROSOFT 2016. Excel.

MILLER, M. C., DOYLE, G. V. & TERSTAPPEN, L. W. M. M. 2010. Significance of Circulating Tumor Cells Detected by the CellSearch System in Patients with Metastatic Breast Colorectal and Prostate Cancer. *Journal of Oncology,* 2010.

MITCHELL, P. S., PARKIN, R. K., KROH, E. M., FRITZ, B. R., WYMAN, S. K., POGOSOVA-AGADJANYAN, E. L., PETERSON, A., NOTEBOOM, J., O'BRIANT, K. C., ALLEN, A., LIN, D. W., URBAN, N., DRESCHER, C. W., KNUDSEN, B. S., STIREWALT, D. L., GENTLEMAN, R., VESSELLA, R. L., NELSON, P. S., MARTIN, D. B. & TEWARI, M. 2008. Circulating microRNAs as stable blood-based markers for cancer detection. *Proc Natl Acad Sci U S A,* 105, 10513-8.

MOLTZAHN, F., OLSHEN, A. B., BAEHNER, L., PEEK, A., FONG, L., STOPPLER, H., SIMKO, J., HILTON, J. F., CARROLL, P. & BLELLOCH, R. 2011. Microfluidic-based multiplex qRT-PCR identifies diagnostic and prognostic microRNA signatures in the sera of prostate cancer patients. *Cancer Res,* 71, 550-60.

MONTANARI, M., ROSSETTI, S., CAVALIERE, C., D'ANIELLO, C., MALZONE, M. G., VANACORE, D., DI FRANCO, R., LA MANTIA, E., IOVANE, G., PISCITELLI, R., MUSCARIELLO, R., BERRETTA, M., PERDONA, S., MUTO, P., BOTTI, G., BIANCHI, A. A. M., VENEZIANI, B. M. & FACCHINI, G. 2017. Epithelial-mesenchymal transition in prostate cancer: an overview. *Oncotarget,* 8, 35376-35389.

MONTEIRO, J. & FODDE, R. 2010. Cancer stemness and metastasis: Therapeutic consequences and perspectives. *European Journal of Cancer,* 46, 1198-1203.

MOORE, K. L., DALLEY, A. F. & AGUR, A. M. R. 2018. 6: Pelvis and Perineum. *In:* FERRAN, A. (ed.) *Clinical Orientated Anatomy.* 8th ed. Philadelphia: Wolters Kluwer.

MULHOLLAND, D. J., KOBAYASHI, N., RUSCETTI, M., ZHI, A., TRAN, L. M., HUANG, J., GLEAVE, M. & WU, H. 2012. Pten Loss and RAS/MAPK Activation Cooperate to Promote EMT and Metastasis Initiated from Prostate Cancer Stem/Progenitor Cells. *Cancer Research,* 72, 1878.

MURAYAMA, Y., MIYAGAWA, J.-I., ORITANI, K., YOSHIDA, H., YAMAMOTO, K., KISHIDA, O., MIYAZAKI, T., TSUTSUI, S., KIYOHARA, T., MIYAZAKI, Y., HIGASHIYAMA, S., MATSUZAWA, Y. & SHINOMURA, Y. 2004. CD9-mediated activation of the p46 Shc isoform leads to apoptosis in cancer cells. *Journal of Cell Science,* 117**,** 3379-3388.

NAITO, A., AZUMA, S., TANAKA, S., MIYAZAKI, T., TAKAKI, S., TAKATSU, K., NAKAO, K., NAKAMURA, K., KATSUKI, M., YAMAMOTO, T. & INOUE, J. I. 2001. Severe osteopetrosis, defective interleukin-1 signalling and lymph node organogenesis in TRAF6-deficient mice. *Genes to Cells,* 4**,** 353-362.

NAM, E. J., YOON, H., KIM, S. W., KIM, H., KIM, Y. T., KIM, J. H., KIM, J. W. & KIM, S. 2008. MicroRNA Expression Profiles in Serous Ovarian Carcinoma. *Clinical Cancer Research,* 14**,** 2690-2695.

NATIONAL CANCER INSTITUTE. 2014. *Hormone Therapy for Prostate Cancer* [Online]. https://www.cancer.gov/types/prostate/prostate-hormone-therapy-fact-sheet: National Cancer Institute, . [Accessed 24.01.18 2018].

NATIONAL COLLABORATING CENTRE FOR CANCER 2014. Prostate Cancer: Diagnosis and treatment. Clinical Guideline. *In:* EXCELLENCE, N. I. F. H. A. C. (ed.). https://www.nice.org.uk/guidance/cg175/evidence/full-guideline-191710765: NICE.

NCBI. 2017. *ICAM1; intercellular adhesion molecule 1* [Online]. https://www.ncbi.nlm.nih.gov/gene/3383: NCBI. [Accessed 30.11.17 2017].

NCBI. 2018. *FLOT1 flotillin 1 - Homo sapiens* [Online]. https://www.ncbi.nlm.nih.gov/gene?Db=gene&Cmd=ShowDetailView&TermToSearch=10211: NCBI. [Accessed 06.02.18 2018].

NGUYEN, H. C., XIE, W., YANG, M., HSIEH, C. L., DROUIN, S., LEE, G. S. & KANTOFF, P. W. 2013. Expression differences of circulating microRNAs in metastatic castration resistant prostate cancer and low-risk, localized prostate cancer. *Prostate,* 73**,** 346-54.

OFFICE FOR NATIONAL STATISTICS. 2018. *Cancer registration statistics, England: 2016* [Online]. https://www.ons.gov.uk/peoplepopulationandcommunity/healthandsocialcare/conditionsanddiseases/bulletins/cancerregistrationstatisticsengland/final2016#toc: Office for National statistics. Available: https://www.ons.gov.uk/peoplepopulationandcommunity/healthandsocialcare/conditionsanddiseases/bulletins/cancerregistrationstatisticsengland/final2016#toc [Accessed 26/06/18 2018].

OLIVEROS, J. C. 2007-2015. Venny. An interactive tool for comparing lists with Venn's diagrams. 2.1 ed. http://bioinfogp.cnb.csic.es/tools/venny/index.html.

OLTEAN, S. & BATES, D. O. 2013. Hallmarks of alternative splicing in cancer. *Oncogene,* 33**,** 5311.

OZEN, M., CREIGHTON, C. J., OZDEMIR, M. & ITTMANN, M. 2008. Widespread deregulation of microRNA expression in human prostate cancer. *Oncogene,* 27**,** 1788-93.

PANG, J., LIU, W.-P., LIU, X.-P., LI, L.-Y., FANG, Y.-Q., SUN, Q.-P., LIU, S.-J., LI, M.-T., SU, Z.-L. & GAO, X. 2010. Profiling Protein Markers Associated with Lymph Node Metastasis in Prostate Cancer by DIGE-based Proteomics Analysis. *Journal of Proteome Research,* 9**,** 216-226.

PANTEL, K. & ALIX-PANABIÈRES, C. 2010. Circulating tumour cells in cancer patients: challenges and perspectives. *Trends in Molecular Medicine,* 16**,** 398-406.

PATHAN, M., KEERTHIKUMAR, S., CHISANGA, D., ALESSANDRO, R., ANG, C. S., ASKENASE, P., BATAGOV, A. O., BENITO-MARTIN, A., CAMUSSI, G., CLAYTON, A., COLLINO, F., DI VIZIO, D., FALCON-PEREZ, J. M., FONSECA, P., FONSEKA, P., FONTANA, S., GHO, Y. S., HENDRIX, A., HOEN, E. N., IRACI, N., KASTANIEGAARD, K., KISLINGER, T., KOWAL, J., KUROCHKIN, I. V., LEONARDI, T., LIANG, Y., LLORENTE, A., LUNAVAT, T. R., MAJI, S., MONTELEONE, F., OVERBYE, A., PANARETAKIS, T., PATEL, T., PEINADO, H., PLUCHINO, S., PRINCIPE, S., RONQUIST, G., ROYO, F., SAHOO, S., SPINELLI, C., STENSBALLE, A., THERY, C., VAN HERWIJNEN, M. J. C., WAUBEN, M., WELTON, J. L., ZHAO, K. & MATHIVANAN, S. 2017. A novel community driven software for functional enrichment analysis of extracellular vesicles data. *J Extracell Vesicles,* 6**,** 1321455.

PEDERSEN, E. A., SHIOZAWA, Y., PIENTA, K. J. & TAICHMAN, R. S. 2012. The prostate cancer bone marrow niche: more than just 'fertile soil'. *Asian Journal of Andrology,* 14**,** 423-427.

PEGTEL, D. M., COSMOPOULOS, K., THORLEY-LAWSON, D. A., VAN EIJNDHOVEN, M. A., HOPMANS, E. S., LINDENBERG, J. L., DE GRUIJL, T. D., WURDINGER, T. & MIDDELDORP, J. M. 2010. Functional delivery of viral miRNAs via exosomes. *Proc Natl Acad Sci U S A,* 107**,** 6328-33.

PENG, X., GUO, W., LIU, T., WANG, X., TU, X. A., XIONG, D., CHEN, S., LAI, Y., DU, H., CHEN, G., LIU, G., TANG, Y., HUANG, S. & ZOU, X. 2011. Identification of miRs-143 and -145 that Is Associated with Bone Metastasis of Prostate Cancer and Involved in the Regulation of EMT. *PLOS ONE,* 6**,** e20341.

PETRICOIN, E. F., 3RD, ORNSTEIN, D. K., PAWELETZ, C. P., ARDEKANI, A., HACKETT, P. S., HITT, B. A., VELASSCO, A., TRUCCO, C., WIEGAND, L., WOOD, K., SIMONE, C. B., LEVINE, P. J., LINEHAN, W. M., EMMERT-BUCK, M. R., STEINBERG, S. M., KOHN, E. C. & LIOTTA, L. A. 2002. Serum proteomic patterns for detection of prostate cancer. *J Natl Cancer Inst,* 94**,** 1576-8.

PIMENTEL, H., BRAY, N. L., PUENTE, S., MELSTED, P. & PACHTER, L. 2017. Differential analysis of RNA-seq incorporating quantification uncertainty. *Nature Methods,* 14**,** 687.

PORKKA, K. P., PFEIFFER, M. J., WALTERING, K. K., VESSELLA, R. L., TAMMELA, T. L. & VISAKORPI, T. 2007. MicroRNA expression profiling in prostate cancer. *Cancer Res,* 67**,** 6130-5.

POUND, C. R., PARTIN, A. W., EISENBERGER, M. A., CHAN, D. W., PEARSON, J. D. & WALSH, P. C. 1999. Natural history of progression after PSA elevation following radical prostatectomy. *Jama,* 281**,** 1591-7.

PRATT, A. J. & MACRAE, I. J. 2009. The RNA-induced Silencing Complex: A Versatile Gene-silencing Machine. *The Journal of Biological Chemistry,* 284**,** 17897-17901.

PSAILA, B. & LYDEN, D. 2009. The metastatic niche: adapting the foreign soil. *Nature Reviews Cancer,* 9**,** 285.

PUBLIC HEALTH ENGLAND. 2014. *RE: Personal Communication to RAS Working Group.* Type to RAS WORKING GROUP.

RADISKY, D. C. 2005. Epithelial-mesenchymal transition. *Journal of Cell Science,* 118**,** 4325.

RAMASWAMY, S., ROSS, K. N., LANDER, E. S. & GOLUB, T. R. 2003. A molecular signature of metastasis in primary solid tumors. *Nat Genet,* 33**,** 49-54.

RAPOSO, G. & STOORVOGEL, W. 2013. Extracellular vesicles: Exosomes, microvesicles, and friends. *The Journal of Cell Biology,* 200**,** 373-383.

RATAJCZAK, M. Z., KUCIA, M., JADCZYK, T., GRECO, N. J., WOJAKOWSKI, W., TENDERA, M. & RATAJCZAK, J. 2012. Pivotal role of paracrine effects in stem cell therapies in regenerative medicine: can we translate stem cell-secreted paracrine factors and microvesicles into better therapeutic strategies? *Leukemia,* 26**,** 1166-73.

RATERT, N., MEYER, H.-A., JUNG, M., MOLLENKOPF, H.-J., WAGNER, I., MILLER, K., KILIC, E., ERBERSDOBLER, A., WEIKERT, S. & JUNG, K. 2012. Reference miRNAs for miRNAome Analysis of Urothelial Carcinomas. *PLOS ONE,* 7**,** e39309.

REN, G., ESPOSITO, M. & KANG, Y. 2015. Bone metastasis and the metastatic niche. *Journal of molecular medicine (Berlin, Germany),* 93**,** 1203-1212.

RESCHER, U. & GERKE, V. 2004. Annexins – unique membrane binding proteins with diverse functions. *Journal of Cell Science,* 117**,** 2631-2639.

RIBAS, J., NI, X., HAFFNER, M., WENTZEL, E. A., SALMASI, A. H., CHOWDHURY, W. H., KUDROLLI, T. A., YEGNASUBRAMANIAN, S., LUO, J., RODRIGUEZ, R., MENDELL, J. T. & LUPOLD, S. E. 2009. miR-21: An androgen receptor regulated microRNA which promotes hormone dependent and independent prostate cancer growth. *Cancer research,* 69**,** 7165-7169.

RIETHDORF, S., FRITSCHE, H., MULLER, V., RAU, T., SCHINDLBECK, C., RACK, B., JANNI, W., COITH, C., BECK, K., JANICKE, F., JACKSON, S., GORNET, T., CRISTOFANILLI, M. & PANTEL, K. 2007. Detection of circulating tumor cells in peripheral blood of patients with metastatic breast cancer: a validation study of the CellSearch system. *Clin Cancer Res,* 13**,** 920-8.

ROBINSON, M. D., MCCARTHY, D. J. & SMYTH, G. K. 2010. edgeR: a Bioconductor package for differential expression analysis of digital gene expression data. *Bioinformatics,* 26**,** 139-40.

ROKHLIN, O. W. & COHEN, M. B. 1996. Soluble forms of CD44 and CD54 (ICAM-1) cellular adhesion molecules are released by human prostatic cancer cell lines. *Cancer Lett,* 107**,** 29-35.

ROODMAN, D. G. & SILBERMANN, R. 2015. Mechanisms of osteolytic and osteoblastic skeletal lesions. *BoneKEy Rep,* 4.

ROUDIER, M. P., MORRISSEY, C., TRUE, L. D., HIGANO, C. S., VESSELLA, R. L. & OTT, S. M. 2008. Histopathologic Assessment of Prostate Cancer Bone "Osteoblastic" Metastases. *The Journal of urology,* 180**,** 1154-1160.

ROVE, K. O. & CRAWFORD, E. D. 2013. Androgen annihilation as a new therapeutic paradigm in advanced prostate cancer. *Current Opinion in Urology,* 23**,** 208-213.

RUIJTER, E. T., VAN DE KAA, C. A., SCHALKEN, J. A., DEBRUYNE, F. M. & RUITER, D. J. 1996. Histological grade heterogeneity in multifocal prostate cancer. Biological and clinical implications. *J Pathol,* 180**,** 295-9.

RUMBLE, S. M., LACROUTE, P., DALCA, A. V., FIUME, M., SIDOW, A. & BRUDNO, M. 2009. SHRiMP: accurate mapping of short color-space reads. *PLoS Comput Biol,* 5**,** e1000386.

RUSSELL, P. J. & KINGSLEY, E. A. 2003. Human Prostate Cancer Cell Lines. *In:* RUSSELL, P. J., JACKSON, P. & KINGSLEY, E. A. (eds.) *Prostate Cancer Methods and Protocols.* Totowa, NJ: Springer New York.

SANDERS, I., HOLDENRIEDER, S., WALGENBACH-BRUNAGEL, G., VON RUECKER, A., KRISTIANSEN, G., MULLER, S. C. & ELLINGER, J. 2012. Evaluation of reference genes for the analysis of serum miRNA in

patients with prostate cancer, bladder cancer and renal cell carcinoma. *Int J Urol,* 19**,** 1017-25.

SAUER, E., BABION, I., MADEA, B. & COURTS, C. 2014. An evidence based strategy for normalization of quantitative PCR data from miRNA expression analysis in forensic organ tissue identification. *Forensic Sci Int Genet,* 13**,** 217-23.

SCHER, H. I., JIA, X., DE BONO, J. S., FLEISHER, M., PIENTA, K. J., RAGHAVAN, D. & HELLER, G. 2009. Circulating tumour cells as prognostic markers in progressive, castration-resistant prostate cancer: a reanalysis of IMMC38 trial data. *The Lancet Oncology,* 10**,** 233-239.

SCHOPPET, M., PREISSNER, K. T. & HOFBAUER, L. C. 2002. RANK Ligand and Osteoprotegerin. *Arteriosclerosis, Thrombosis, and Vascular Biology,* 22**,** 549.

SCHOREY, J. S. & BHATNAGAR, S. 2008. Exosome Function: From Tumor Immunology to Pathogen Biology. *Traffic,* 9**,** 871-81.

SCHWARZENBACH, H., ALIX-PANABIÈRES, C., MÜLLER, I., LETANG, N., VENDRELL, J.-P., REBILLARD, X. & PANTEL, K. 2009. Cell-free Tumor DNA in Blood Plasma As a Marker for Circulating Tumor Cells in Prostate Cancer. *Clinical Cancer Research,* 15**,** 1032-1038.

SCHWARZENBACH, H., HOON, D. S. B. & PANTEL, K. 2011. Cell-free nucleic acids as biomarkers in cancer patients. 11**,** 426.

SETHI, S., MACOSKA, J., CHEN, W. & SARKAR, F. H. 2011. Molecular signature of epithelial-mesenchymal transition (EMT) in human prostate cancer bone metastasis. *American Journal of Translational Research,* 3**,** 90-99.

SHAFFER, C. 2011. *In DNA Transfection, Efficiency and Cytotoxicity Are Two Sides of the Same Coin* [Online]. https://www.biocompare.com/Editorial-Articles/41821-In-DNA-Transfection-Efficiency-and-Cytotoxicity-Are-Two-Sides-of-the-Same-Coin/: Biocompare. Available: https://www.biocompare.com/Editorial-Articles/41821-In-DNA-Transfection-Efficiency-and-Cytotoxicity-Are-Two-Sides-of-the-Same-Coin/ [Accessed 19.03.18 2018].

SHIOZAWA, Y., PEDERSEN, E. A., HAVENS, A. M., JUNG, Y., MISHRA, A., JOSEPH, J., KIM, J. K., PATEL, L. R., YING, C., ZIEGLER, A. M., PIENTA, M. J., SONG, J., WANG, J., LOBERG, R. D., KREBSBACH, P. H., PIENTA, K. J. & TAICHMAN, R. S. 2011. Human prostate cancer metastases target the hematopoietic stem cell niche to establish footholds in mouse bone marrow. *The Journal of Clinical Investigation,* 121**,** 1298-1312.

SIKES, R. A., NICHOLSON, B. E., KOENEMAN, K. S., EDLUND, N. M., BISSONETTE, E. A., BRADLEY, M. J., THALMANN, G. N., CECCHINI,

M. G., PIENTA, K. J. & CHUNG, L. W. 2004. Cellular interactions in the tropism of prostate cancer to bone. *Int J Cancer,* 110**,** 497-503.

SIMONS, M. & RAPOSO, G. 2009. Exosomes – vesicular carriers for intercellular communication. *Current Opinion in Cell Biology,* 21**,** 575-581.

SO, A., GLEAVE, M., HURTADO-COL, A. & NELSON, C. 2005. Mechanisms of the development of androgen independence in prostate cancer. *World Journal of Urology,* 23**,** 1-9.

SOBEL, R. E. & SADAR, M. D. 2005. Cell lines used in prostate cancer research: a compendium of old and new lines--part 1. *J Urol,* 173**,** 342-59.

SOHEL, M. H. 2016. Extracellular/Circulating MicroRNAs: Release Mechanisms, Functions and Challenges. *Achievements in the Life Sciences,* 10**,** 175-186.

SONG, M. S., SALMENA, L. & PANDOLFI, P. P. 2012. The functions and regulation of the PTEN tumour suppressor. *Nat Rev Mol Cell Biol,* 13**,** 283-96.

STRICKER, H. J. 2001. Luteinizing hormone–releasing hormone antagonists in prostate cancer. *Urology,* 58**,** 24-27.

SUNAMI, E., SHINOZAKI, M., HIGANO, C. S., WOLLMAN, R., DORFF, T. B., TUCKER, S. J., MARTINEZ, S. R., MIZUNO, R., SINGER, F. R. & HOON, D. S. 2009. Multimarker circulating DNA assay for assessing blood of prostate cancer patients. *Clin Chem,* 55**,** 559-67.

SUVA, L. J., WASHAM, C., NICHOLAS, R. W. & GRIFFIN, R. J. 2011. Bone metastasis: mechanisms and therapeutic opportunities. *Nat Rev Endocrinol,* 7**,** 208-18.

SUZUKI, H. I., YAMAGATA, K., SUGIMOTO, K., IWAMOTO, T., KATO, S. & MIYAZONO, K. 2009. Modulation of microRNA processing by p53. *Nature,* 460**,** 529-533.

SVEEN, A., KILPINEN, S., RUUSULEHTO, A., LOTHE, R. A. & SKOTHEIM, R. I. 2015. Aberrant RNA splicing in cancer; expression changes and driver mutations of splicing factor genes. *Oncogene,* 35**,** 2413.

SWARUP, V. & RAJESWARI, M. R. 2007. Circulating (cell-free) nucleic acids – A promising, non-invasive tool for early detection of several human diseases. *FEBS Letters,* 581**,** 795-799.

TAKAHASHI, R. U., PRIETO-VILA, M., HIRONAKA, A. & OCHIYA, T. 2017. The role of extracellular vesicle microRNAs in cancer biology. *Clin Chem Lab Med,* 55**,** 648-656.

TAPLIN, M. E., BUBLEY, G. J., SHUSTER, T. D., FRANTZ, M. E., SPOONER, A. E., OGATA, G. K., KEER, H. N. & BALK, S. P. 1995. Mutation of the

androgen-receptor gene in metastatic androgen-independent prostate cancer. *N Engl J Med,* 332**,** 1393-8.
THE UNIPROT CONSORTIUM 2017. UniProt: the universal protein knowledgebase. *Nucleic Acids Research,* 45**,** D158-D169.
THÉRY, C., ZITVOGEL, L. & AMIGORENA, S. 2002. Exosomes: composition, biogenesis and function. *Nature Reviews Immunology,* 2**,** 569.
TORRE, L. A., BRAY, F., SIEGEL, R. L., FERLAY, J., LORTET-TIEULENT, J. & JEMAL, A. 2015. Global cancer statistics, 2012. *CA: A Cancer Journal for Clinicians,* 65**,** 87-108.
TRIMBOLI, A. J., CANTEMIR-STONE, C. Z., LI, F., WALLACE, J. A., MERCHANT, A., CREASAP, N., THOMPSON, J. C., CASERTA, E., WANG, H., CHONG, J.-L., NAIDU, S., WEI, G., SHARMA, S. M., STEPHENS, J. A., FERNANDEZ, S. A., GURCAN, M. N., WEINSTEIN, M. B., BARSKY, S. H., YEE, L., ROSOL, T. J., STROMBERG, P. C., ROBINSON, M. L., PEPIN, F., HALLETT, M., PARK, M., OSTROWSKI, M. C. & LEONE, G. 2009. Pten in Stromal Fibroblasts Suppresses Mammary Epithelial Tumors. *Nature,* 461**,** 1084-1091.
TRZPIS, M., MCLAUGHLIN, P. M. J., DE LEIJ, L. & HARMSEN, M. C. 2007. Epithelial Cell Adhesion Molecule: More than a Carcinoma Marker and Adhesion Molecule. *Am J Pathol,* 171**,** 386-95.
TSUKITA, S. & FURUSE, M. 2000. Pores in the wall: claudins constitute tight junction strands containing aqueous pores. *J Cell Biol,* 149**,** 13-6.
TURCHINOVICH, A., WEIZ, L. & BURWINKEL, B. 2012. Extracellular miRNAs: the mystery of their origin and function. *Trends in Biochemical Sciences,* 37**,** 460-465.
TURCHINOVICH, A., WEIZ, L., LANGHEINZ, A. & BURWINKEL, B. 2011. Characterization of extracellular circulating microRNA. *Nucleic Acids Research,* 39**,** 7223-7233.
UHLEN, M., ZHANG, C., LEE, S., SJOSTEDT, E., FAGERBERG, L., BIDKHORI, G., BENFEITAS, R., ARIF, M., LIU, Z., EDFORS, F., SANLI, K., VON FEILITZEN, K., OKSVOLD, P., LUNDBERG, E., HOBER, S., NILSSON, P., MATTSSON, J., SCHWENK, J. M., BRUNNSTROM, H., GLIMELIUS, B., SJOBLOM, T., EDQVIST, P. H., DJUREINOVIC, D., MICKE, P., LINDSKOG, C., MARDINOGLU, A. & PONTEN, F. 2017. A pathology atlas of the human cancer transcriptome. *Science,* 357.
UHLÉN, M., BJÖRLING, E., AGATON, C., SZIGYARTO, C. A.-K., AMINI, B., ANDERSEN, E., ANDERSSON, A.-C., ANGELIDOU, P., ASPLUND, A., ASPLUND, C., BERGLUND, L., BERGSTRÖM, K., BRUMER, H., CERJAN, D., EKSTRÖM, M., ELOBEID, A., ERIKSSON, C., FAGERBERG, L., FALK, R., FALL, J., FORSBERG, M., BJÖRKLUND, M. G., GUMBEL, K., HALIMI, A., HALLIN, I., HAMSTEN, C., HANSSON, M., HEDHAMMAR, M., HERCULES, G., KAMPF, C., LARSSON, K.,

LINDSKOG, M., LODEWYCKX, W., LUND, J., LUNDEBERG, J., MAGNUSSON, K., MALM, E., NILSSON, P., ÖDLING, J., OKSVOLD, P., OLSSON, I., ÖSTER, E., OTTOSSON, J., PAAVILAINEN, L., PERSSON, A., RIMINI, R., ROCKBERG, J., RUNESON, M., SIVERTSSON, Å., SKÖLLERMO, A., STEEN, J., STENVALL, M., STERKY, F., STRÖMBERG, S., SUNDBERG, M., TEGEL, H., TOURLE, S., WAHLUND, E., WALDÉN, A., WAN, J., WERNÉRUS, H., WESTBERG, J., WESTER, K., WRETHAGEN, U., XU, L. L., HOBER, S. & PONTÉN, F. 2005. A Human Protein Atlas for Normal and Cancer Tissues Based on Antibody Proteomics. *Molecular & Cellular Proteomics,* 4**,** 1920-1932.

UNIPROT CONSORTIUM 2010. The Universal Protein Resource (UniProt) in 2010. *Nucleic Acids Res,* 38**,** D142-8.

VALADI, H., EKSTROM, K., BOSSIOS, A., SJOSTRAND, M., LEE, J. J. & LOTVALL, J. O. 2007. Exosome-mediated transfer of mRNAs and microRNAs is a novel mechanism of genetic exchange between cells. *Nat Cell Biol,* 9**,** 654-9.

VANDER HEIDEN, M. G., CANTLEY, L. C. & THOMPSON, C. B. 2009. Understanding the Warburg effect: the metabolic requirements of cell proliferation. *Science,* 324**,** 1029-33.

VARA, J. Á. F., CASADO, E., DE CASTRO, J., CEJAS, P., BELDA-INIESTA, C. & GONZÁLEZ-BARÓN, M. 2004. PI3K/Akt signalling pathway and cancer. *Cancer Treatment Reviews,* 30**,** 193-204.

VELA, I., GREGORY, L., GARDINER, E. M., CLEMENTS, J. A. & NICOL, D. L. 2007. Bone and prostate cancer cell interactions in metastatic prostate cancer. *BJU Int,* 99**,** 735-42.

VICKERS, K. C., PALMISANO, B. T., SHOUCRI, B. M., SHAMBUREK, R. D. & REMALEY, A. T. 2011. MicroRNAs are transported in plasma and delivered to recipient cells by high-density lipoproteins. *Nature Cell Biology,* 13**,** 423.

VISAKORPI, T., HYYTINEN, E., KOIVISTO, P., TANNER, M., KEINÄNEN, R., PALMBERG, C., PALOTIE, A., TAMMELA, T., ISOLA, J. & KALLIONIEMI, O.-P. 1995. In vivo amplification of the androgen receptor gene and progression of human prostate cancer. *Nature Genetics,* 9**,** 401.

VONA, G., SABILE, A., LOUHA, M., SITRUK, V., ROMANA, S., SCHUTZE, K., CAPRON, F., FRANCO, D., PAZZAGLI, M., VEKEMANS, M., LACOUR, B., BRECHOT, C. & PATERLINI-BRECHOT, P. 2000. Isolation by size of epithelial tumor cells : a new method for the immunomorphological and molecular characterization of circulatingtumor cells. *Am J Pathol,* 156**,** 57-63.

VONDERSCHER, J. Qualifying Biomarkers. Institute of Medicine (US) Forum on Drug Discovery, developement, and translation, 2008 Washington (DC). National Academies Press (US).

WANG, X., KUA, H.-Y., HU, Y., GUO, K., ZENG, Q., WU, Q., NG, H.-H., KARSENTY, G., DE CROMBRUGGHE, B., YEH, J. & LI, B. 2006. p53 functions as a negative regulator of osteoblastogenesis, osteoblast-dependent osteoclastogenesis, and bone remodeling. *The Journal of Cell Biology,* 172**,** 115-125.

WANG, Y., XUE, H., CUTZ, J. C., BAYANI, J., MAWJI, N. R., CHEN, W. G., GOETZ, L. J., HAYWARD, S. W., SADAR, M. D., GILKS, C. B., GOUT, P. W., SQUIRE, J. A., CUNHA, G. R. & WANG, Y. Z. 2005. An orthotopic metastatic prostate cancer model in SCID mice via grafting of a transplantable human prostate tumor line. *Lab Invest,* 85**,** 1392-404.

WATAHIKI, A., MACFARLANE, R. J., GLEAVE, M. E., CREA, F., WANG, Y., HELGASON, C. D. & CHI, K. N. 2013. Plasma miRNAs as Biomarkers to Identify Patients with Castration-Resistant Metastatic Prostate Cancer. *International Journal of Molecular Sciences,* 14**,** 7757-7770.

WATAHIKI, A., WANG, Y., MORRIS, J., DENNIS, K., O'DWYER, H. M., GLEAVE, M., GOUT, P. W. & WANG, Y. 2011. MicroRNAs associated with metastatic prostate cancer. *PLoS One,* 6**,** e24950.

WEGIEL, B., BJARTELL, A., TUOMELA, J., DIZEYI, N., TINZL, M., HELCZYNSKI, L., NILSSON, E., OTTERBEIN, L. E., HÄRKÖNEN, P. & PERSSON, J. L. 2008. Multiple Cellular Mechanisms Related to Cyclin A1 in Prostate Cancer Invasion and Metastasis. *JNCI Journal of the National Cancer Institute,* 100**,** 1022-1036.

WEIGELT, B., PETERSE, J. L. & VAN'T VEER, L. J. 2005. Breast cancer metastasis: markers and models. *Nat Rev Cancer,* 5**,** 591-602.

WEILBAECHER, K. N., GUISE, T. A. & MCCAULEY, L. K. 2011. Cancer to bone: a fatal attraction. *Nature reviews. Cancer,* 11**,** 411-425.

WENT, P. T. H., LUGLI, A., MEIER, S., BUNDI, M., MIRLACHER, M., SAUTER, G. & DIRNHOFER, S. 2004. Frequent EpCam protein expression in human carcinomas. *Human Pathology,* 35**,** 122-128.

WESTENDORF, J. J., KAHLER, R. A. & SCHROEDER, T. M. 2004. Wnt signaling in osteoblasts and bone diseases. *Gene,* 341**,** 19-39.

WILLIAMS, S. C. P. 2013. Circulating tumor cells. *Proceedings of the National Academy of Sciences,* 110**,** 4861.

YOO, N. J., HUR, S. Y., KIM, M. S., LEE, J. Y. & LEE, S. H. 2010. Immunohistochemical analysis of RNA-induced silencing complex-related proteins AGO2 and TNRC6A in prostate and esophageal cancers. *APMIS,* 118**,** 271-276.

YOSHIOKA, Y., KONISHI, Y., KOSAKA, N., KATSUDA, T., KATO, T. & OCHIYA, T. 2013. Comparative marker analysis of extracellular vesicles in different human cancer types. *Journal of Extracellular Vesicles,* 2**,** 10.3402/jev.v2i0.20424.

ZERNECKE, A., BIDZHEKOV, K., NOELS, H., SHAGDARSUREN, E., GAN, L., DENECKE, B., HRISTOV, M., KOPPEL, T., JAHANTIGH, M. N., LUTGENS, E., WANG, S., OLSON, E. N., SCHOBER, A. & WEBER, C. 2009. Delivery of microRNA-126 by apoptotic bodies induces CXCL12-dependent vascular protection. *Sci Signal,* 2**,** ra81.

ZHANG, H.-G. & GRIZZLE, W. E. 2014. Exosomes: A Novel Pathway of Local and Distant Intercellular Communication that Facilitates the Growth and Metastasis of Neoplastic Lesions. *The American Journal of Pathology,* 184**,** 28-41.

ZHANG, H. L., QIN, X. J., CAO, D. L., ZHU, Y., YAO, X. D., ZHANG, S. L., DAI, B. & YE, D. W. 2013. An elevated serum miR-141 level in patients with bone-metastatic prostate cancer is correlated with more bone lesions. *Asian J Androl,* 15**,** 231-5.

ZHANG, H. L., YANG, L. F., ZHU, Y., YAO, X. D., ZHANG, S. L., DAI, B., ZHU, Y. P., SHEN, Y. J., SHI, G. H. & YE, D. W. 2011. Serum miRNA-21: elevated levels in patients with metastatic hormone-refractory prostate cancer and potential predictive factor for the efficacy of docetaxel-based chemotherapy. *Prostate,* 71**,** 326-31.

ZHAU, H. E., ODERO-MARAH, V., LUE, H.-W., NOMURA, T., WANG, R., CHU, G., LIU, Z.-R., ZHOU, B. P., HUANG, W.-C. & CHUNG, L. W. K. 2008. Epithelial to mesenchymal transition (EMT) in human prostate cancer: lessons learned from ARCaP model. *Clinical & Experimental Metastasis,* 25**,** 601.

ZÖLLER, M. 2008. Tetraspanins: push and pull in suppressing and promoting metastasis. *Nature Reviews Cancer,* 9**,** 40.

8 Appendix

8.1 Restriction digest results

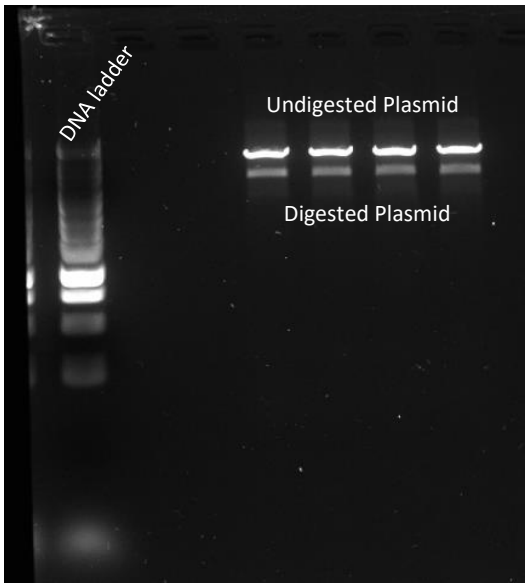


Figure 8.1 Ethidium Bromide exposure showing the two separated bands representing the Digested and undigested

8.2 Renilla luciferase luminescence assay results

8.2.1 hOB transfection optimisation results

Sample	**Firefly luminescence**	**Renilla Luminescence**	**Ratio (renilla/firefly)**
PsiCHECK-2 only plasmid	32912	1783902	54.2
PsiCHECK-2 with perfect miR-21 oligo insertion	102022	88431	0.867

Table 8.1 The results from the transfection of hOB cells with PsiCHECK-2 only and PsiCHECK-2 with miR-21 inserted plasmids.

8.2.2 Investigation of the effect of adding EVs on Renilla luciferase activity results

Treatment	Repeat	Luminescence				T-test p-value
		Firefly	Renilla	Ratio	Average	

No EVs	1	54827	107958	1.97		
	2	45908	149951	3.27		
	3	67114	159196	2.37		
	4	52165	171849	3.29	2.725	N/A
hOB EVs	1	138	126	0.91		
	2	119	110	0.92		
	3	60	65	1.08		0.0022
	4	63	70	1.11	1.008	**
hOB Conditioned media	1	33491	79440	2.37		
	2	38352	79841	2.08		
	3	30092	52492	1.74		
	4	30624	68515	2.24	2.109	0.1352
PC3 EVs	1	43	71	1.65		
	2	49	63	1.29		
	3	43	43	1.00		0.0073
	4	46	59	1.28	1.305	**
PC3 Conditioned media	1	35658	106787	2.99		
	2	29929	68923	2.30		
	3	54465	113101	2.08		
	4	29206	90860	3.11	2.621	0.8113
LNCaP EVs	1	113	321	2.84		
	2	119	236	1.98		
	3	112	241	2.15	2.270	0.2795

	4	106	223	2.10		
LNCaP Conditioned media	1	35629	87188	2.45		
	2	31308	145410	4.64		
	3	25628	153580	5.99		
	4	31253	71727	2.30	3.845	0.2851
C4-2 EVs	1	152	363	2.39		
	2	94	520	5.53		
	3	529	4052	7.66		
	4	468	4118	8.80	6.095	0.0588
C4-2 Conditioned media	1	38140	143415	3.76		
	2	28248	155451	5.50		
	3	33398	88827	2.66		
	4	24589	159579	6.49	4.603	0.0875
PNT1A EVs	1	310	1103	3.56		
	2	353	1532	4.34		
	3	341	2715	7.96		0.0456
	4	420	2206	5.25	5.278	*
PNT1A conditioned media	1	41006	176687	4.31		
	2	30269	4717	0.16		
	3	42980	172656	4.02		0.0143
	4	34454	146436	4.25	4.192	*

Table 8.2 A table showing the raw data from the luminescence assay. Represented graphically in Figure 4.2.

8.3 KEGG pathway analysis

Pathways significantly enriched in Downregulated genes		Pathways significantly enriched in Upregulated genes	
Pathway	q-value (3 s.f.)	Pathway	q-value (3 s.f.)
Phagosome	2.66×10^{-7}	Fructose and mannose metabolism	0.00191
Pathways in cancer	5.59×10^{-7}	Insulin signalling pathway	0.00210
HTLV-I infection	1.46×10^{-6}	PPAR signalling pathway	0.00443
Fluid shear stress and atherosclerosis	0.000514	Biosynthesis of amino acids	0.00578
Hippo signalling pathway	0.000626	Arginine and proline metabolism	0.00680
Herpes simplex infection	0.000877	Transcriptional misregulation in cancer	0.00792
Antigen processing and presentation	0.00213	Focal adhesion	0.0193
PI3K-Akt signalling pathway	0.00219	MAPK signalling pathway	0.0211
Focal adhesion	0.00288	Cysteine and methionine metabolism	0.0211
Prostate cancer	0.00618	Small cell lung cancer	0.0489

Pertussis	0.00953	
Complement and coagulation cascades	0.0142	
DNA replication	0.0162	
Melanoma	0.0275	
Kaposi's sarcoma-associated herpesvirus infection	0.0332	

Table 8.3 A table showing the remaining significantly upregulated pathways generated by the NIPA functional analysis.